UNIVERSITÀ POLITECNICA DELLE MARCHE

FACOLTÀ DI INGEGNERIA

Dipartimento di Ingegneria Dell'Informazione (DII)

BIOCHEMICAL ANALYSIS OF TITANIUM SCREWS COVERED WITH DECELLULARIZED HETEROLOGOUS BONE TISSUE

Advisor:

Prof. Lorenzo Scalise

Student:

Lorenzo De Massis

Co-advisor:

Prof. Paolo Fattori

Academic year 2020/2021

A papà, mamma, Giulia e Sofia,

per tutto l'amore, il supporto e l'allegria

Summary

ABSTRACT

The number of orthopedic implants used over the years is continuously increasing. In particular, titanium alloys, thanks to their characteristics, are very popular in this type of application. In the orthopedic field, a crucial aspect, in order to prevent infections and loosening, is the rapid and long-lasting fixation of the implants in the bone tissue. For this reason, researchers are placing great emphasis on the process of the direct connection between living bone tissue and the implant surface called osseointegration. One approach that is widely used and in continuous development is coating titanium implants with a substance that can rapidly promote this process. Plasma spray deposition is the most popular technique; it often uses hydroxyapatite, a bioactive ceramic that can promote the growth of bone tissue on the implant. However, the limitations of this technique have led to the need for new solutions for covering titanium implants.

The purpose of this study is to develop a procedure for coating titanium implants with heterologous bone tissue of equine origin. Tests are conducted on grade 4 titanium screws using two versions of equine bone powder. The procedure used is effective on two occurrences: diluting the powder and combining it with an alkaline solution. Using IR analysis, it is possible to verify the chemical properties of the substance deposited on the implants. The spectra obtained show that the properties of the powder used remain unchanged after treatment, demonstrating that the coating process is not deleterious to the bone powder.

1-INTRODUCTION

Estimates and research have shown that in these and coming years there will be an increasing number of interventions related to orthopedic and prosthetic surgery [1]. Titanium alloys, especially the Ti6Al4V alloy, due to their excellent biocompatibility, high corrosion resistance, and low modulus of elasticity have become very popular in this type of biomedical application [2].

Because of the increasing demand for these implants and the impact of associated complications, resources are being directed towards finding solutions that minimize their negative effects. In this regard, regenerative medicine is becoming increasingly important, as it aims to stimulate tissue growth and regeneration. In the field of orthopedic surgery, the principles of this branch of medicine are focused on increasing osseointegration, resistance to post-operative infection, and the long-term durability of modern implants [1]. One of the most promising approaches in this sense is the use of bioactive coatings with the aim of promoting the proliferation of new bone tissue around the implant in order to fix it as soon as possible in the human tissue. Osseointegration can be defined as the direct structural and functional connection between living bone and the implant surface [3]. Achieving a good and fast connection is a crucial requirement for clinical success in orthopedic and dental applications [4]. The effect and benefits of osseointegration are aspects that are becoming increasingly significant in orthopedic, orthodontic, and prosthetic surgery in recent years. As reported by numerous studies, thanks to such integration, patients in whom implants or prostheses have been placed can benefit from a better quality of life once complete healing and stability of the system have been achieved [5]. In particular, rapid osseointegration prevents the main problem associated with the implantation of a foreign device in the human body, namely the bacterial attack on the surface of the implant. This problem, in fact, in addition to being a cause of pain for the patient, prevents the fixation between the implant and the bone tissue leading to aseptic loosening and, therefore, to the failure of the implant. Consequently, as anticipated, one of the most important methods to prevent and reduce the formation of bacterial biofilm on implants and, at the same time, promote osseointegration is to coat their surface with a particular substance. Today, one of the most frequently used processes for covering orthopedic implants is Plasma Spray deposition, while a widely used substance for covering is hydroxyapatite of animal origin. This ceramic material, belonging to the class of bioactive ceramics, is the main mineral component of natural bone and, therefore, has a high affinity with it; in addition, it presents excellent biocompatibility, high affinity with hard tissue, and high ability to promote the growth of new bone without causing toxicity and inflammation [6]. The poor bond between the coating and the substrate, and the lack of uniformity of the coating produced

by the Plasma Spray Coating of the hydroxyapatite are the major disadvantages of this technique. These limitations have led to the need to seek new solutions for the coating of the titanium implants using hydroxyapatite [7].

The aim of the study described in this thesis is the development of a procedure for the coating of titanium implants, based on decellularized heterologous bone tissue of equine origin, able to promote and accelerate the process of osseointegration of orthopedic implants in human tissue.

1.1-Tissue Engineering and Regenerative Medicine

The term "Tissue Engineering" (TE) was coined in 1987 and identifies an interdisciplinary field that employs cells, biomaterials, biochemical and physical signals, as well as a combination of them to generate tissue-like structures. Therefore, the objective of this discipline is, by exploiting the principles of engineering and life sciences, to develop biological substitutes capable of maintaining, restoring, or improving the function of damaged tissues [8],[9].

Tissue engineering has received significant attention as a promising strategy in regenerative medicine that is having and will have an important impact in the medical and biomedical field. Regenerative medicine has a great potential for tissue regeneration, and this solves the problem of the shortage of organs available for transplants since, this branch of biomedicine, intends to exploit the stimulation of damaged organs so that they auto-repair. Every year millions of people suffer the loss or damage of organs, tissues, or body parts [10]. Although Tissue Engineering and Regenerative Medicine are often used interchangeably, there is a difference between the two. In the former, the tissue construction is generally performed in-vitro, while the latter refers to solutions for the stimulation of the regrowth of damaged tissues in-vivo in the patient. These two branches are complementary today and are generally conjoined in the word "TERM" [8]. In recent years, the TERM sector has increased enormously, thanks to its progress involving multiple research projects, including design and processing of biomaterials, surface characterization, and functionalization to improve interactions between cells and materials, and imaging [11]. The approach that is often used in this area is the use of a biomaterial support construct called “scaffold”, obtained using either natural or synthetic raw materials. Once the scaffold is finished, cells for growth can be implanted into it or onto it. Another approach, in the field of scaffolding, is to use a de-cellularized extracellular matrix (ECM). It is a natural scaffolding that allows cellular attachment, proliferation, and differentiation. If seeded with the right cells, the ECM can produce an autologous construct without extracting the tissues from the patient [8].

The challenge of Tissue Engineering is to develop and provide functional substitutes that can favor tissue creation and reparation of damaged tissues; there are three general strategies employed in this regard [9]:

- direct implantation of isolated cells or cell substitutes into the organism.
- administration of tissue-inducing substances (such as growth factors).
- positioning cells on or within different matrices.

1.2-Data about prostheses

According to the data collected by the ISS from 2001 to 2019, the total number of orthopedic prosthesis implants in Italy more than doubled, with 220,447 surgeries in 2019 representing one surgery every 2.4 minutes. These are the data of the Italian Arthro-prosthesis Registry (RIAP) - the system set up at the ISS that collects and analyses the data of the interventions and implanted devices. According to the study carried out by the RIAP working group, however, 2020 saw a slowdown in activity due to the Covid epidemic [12]. For about 20 years, there has been a constant growth in arthroplasty operations in Italy - on average by 4.2% per year. This trend is linked on the one hand to the increase in longevity and therefore to the number of individual candidates for surgery, on the other hand to the higher expectations of patients in terms of quality of life and the possibility of re-engaging in recreational sports activities. 2020 will represent the first exception with an anomalous decline due to the pandemic and the lockdown that led to the blocking of elective surgery and therefore the postponement of the procedures scheduled in that period. More than 12 weeks of suspension is estimated to have resulted in the postponement of the surgery for more than 50,000 patients. According to data from the 2019 RIAP Report, the number of interventions is unevenly distributed among the regions. Over 20% of the interventions are concentrated in Lombardy, followed by Emilia-Romagna, Veneto, Tuscany, Piedmont, and Lazio. In these six regions, more than 67% of the plants are carried out. In the South, the most active regions are Campania, Puglia, and Sicily which in total cover over 15% of the national volume.

In recent years, total arthroplasty, and artificial tooth replacement, considered common procedures, have become increasingly common and this trend is expected to continue in the future as evidenced by reports from the American Joint Replacement Registry. Also at the dental level, more than 5 million surgical procedures related to dental implants are performed each year and are expected to increase 12%-15% in the coming years [1]. Furthermore, according to the estimates of highly cited research, the number of people living without a limb will more than double in the year 2050 (3.6 million) compared to the year 2005 (1.6 million). These estimates are obtained from projected

population trends in mortality and age [13]. The data collected are further confirmation of the growing need for functional orthopedic implants and prostheses that can improve the quality of life of patients in need.

1.3-Prostheses

A prosthesis is a device that replaces a limb, an organ, or tissue in the human body. The most ancient forms of prostheses are dental and limb ones; currently the prostheses in use differ on the basis of the type of functionality they must cover, i.e., those purely aesthetic that reproduce the morphology of superficial organs, the acoustic ones, heart valves, and those for the reconstruction and replacement of limbs [14].

1.3.1-Exoskeletal and Endo-skeletal prostheses

Orthopedic prostheses can be categorized into two main types, endo-skeletal, and exoskeletal prostheses.

Exoskeletal prostheses, also called crustacean or conventional prostheses, are characterized by an outer supporting structure. In particular, the supporting structure is an outer shell that gives cosmetic exterior shape and weight-bearing function [15]. Typically, these kinds of prostheses are made of material such as epoxy laminating resins, wood, and expanded polyurethane that make them safe, reliable, and durable [14]. These prostheses can be worn and removed, replaced, repaired, and each patient can have a kit to use the most suitable for various needs. The advantages of the exoskeletal prostheses are that they last for a longer period, they present a higher resistance to external wear and their cost-effectiveness. On the other side, the drawbacks are several, indeed, exoskeletal prostheses are heavy and uncomfortable for patient use, their fabrication requires time, they impose limited movements, and the impossibility to apply the wide range of sophisticated components such as rotators, shock absorbers, and elastic structures (that are, instead, typic of endo-skeletal prostheses). For these reasons, with the advancement of technology the exoskeletal system has been almost completely abandoned because it is unable to meet certain patient necessities and they do not allow a good cosmetic due to their rigidity [14], [15].

Endo-skeletal prostheses, also called modular prostheses, are the most commonly used type of prostheses. They are implantable systems that are permanently placed inside the human body, where they will execute their role at direct contact with the subject tissues. Since the model of the human skeleton has a tube frame, endoprostheses use the skeleton because its structure provides the weight

support function; the central part is the tubular frame, which is called “pylon” that can be made of aluminum, stainless steel, or titanium. Then this structure is enveloped with a foam that gives the prosthesis a natural appearance [14], [15]. The assembling of individual components, called interchangeable modules, builds up the endo-skeletal prosthesis. Consequently, in this kind of prostheses is possible to intervene on the single component so that even when the prosthesis is finished it is possible to perform registration and specific correction depending on the type of activity that the subject will execute. The elements that allow the registration, with the purpose of the modular prosthesis alignment concerning the stump are the registration nucleus and adaptors. The versatility of these prostheses is determined by the possibility of separating the functionality sought from the shape of the prosthesis itself, which is not possible in exoskeletal prostheses, thus allowing the development of a great variety of modules such as joints, tubes, knee, and ankle joints useful to satisfy the functional needs of the subject. Specifically, joint prostheses, those artificial systems that completely or partially replace a joint that (due to traumatic or degenerative pathologies) no longer function adequately, can be grouped under the name of endoprostheses [14]. The several advantages presented by this kind of prostheses are the lightweight and comfortable for weight, they give the appearance of a normal limb (cosmetically acceptable), they are suitable for all levels of amputation, they give adequate adjustment and good dynamic alignment. However, they have also some disadvantages, indeed they are less resistant to external wear and the foam cover needs to be changed often [15].

1.3.2-Humerus and femur stem

One type of endo-implant used extensively in orthopedics is the stem. It is particularly used in the context of total joint replacement, such as total hip arthroplasty (THA) and total shoulder arthroplasty (TSA). The stem allows the transfer of loads from the compromised joint bone to the remaining bone and the distribution of the increased stress caused by a constrained joint [16]. For TSA, although the gold standard for implant fixation is to use cement, recent research is moving toward the use of uncemented (press-fit) humeral stems (Figure 1). Nowadays, press-fit stem designs are those with and without porous coating. In addition, the stem can have different geometries, it can have a cylindrical section, a rectangular section, or be long-stemmed, short-stemmed, and stemless [17]. The implant design for the first TSA implants was based on those of the THA with cemented humeral stem [18].

Similarly, in the case of THA, the cementless solution has become well established in orthopedic surgery due to significant long-term results [19]; the Cementless stem has become the most widely used implant in THA (Figure 1) [20].

Figure 1 *The left figure shows a humeral stem with the prosthetic humeral head while the right figure shows a femoral stem* [21] [22].

Preoperative estimation and intraoperative assessment of stem length and diameter are necessary to establish the degree of press-fit. The cortical vibration felt with a reamer at the predetermined stem length point can be relied upon to confirm the preoperative stem diameter. When there are severe bone defects and soft tissue insufficiency, a higher degree of press-fit is required. More robust support can be induced by reaming to a larger diameter and removing more endosteal bone. For the intramedullary canal filling to be optimized, the stem length and diameter must be adjusted taking into consideration the patient's anatomy, the degree of bone defect, and the constraint of the prosthesis [16]. Because of the prevalence of these devices, in which the use of cement is dispensed with, the employment of specific osteoconductive materials such as titanium and the use of surface treatments such as porous coating or hydroxyapatite coating by plasma spray that promote biological fixation of the implant is of great importance. The goal of these measures is to achieve high survival rates and long-term stability [19].

1.4-Orthopedic implants

As the body ages, the bone may lose some of its strength and elasticity, becoming more susceptible to fracture. This is due to the loss of minerals in the matrix and a reduction in the flexibility of the collagen [23]. When a bone is broken, there is no other way than to fix it by employing man-made supportive structures [24]. Beyond that, accidents, and joint diseases such as osteoarthritis force people to undergo surgeries that require implants such as total hip and knee replacements [6].

Orthopedic implants can be defined as medical devices used to either aid or substitute damaged bones and joints by providing bone fixation or by replacing damaged articulating surfaces of a joint. For the most part, implants are pressed to fit so that bone can grow into the implant in force, or, in another case, they are cemented in place. A crucial factor affecting bone healing is inter-fragmentary movement, which determines tissue strain and, consequently, the cellular reaction in the fracture healing zone. Consequently, the methods of fracture fixation are assessed by considering their ability to reduce interfragmentary motion [24]. Within this context, two main classes can be distinguished: permanent and temporary orthopedic implants. The first type is expected to serve in the human body throughout the life span of the patients (Figure 2); instead, the second one, is just necessary for locking broken or fractured bones during the healing process, so for a relatively short period (Figure 3). Permanent orthopedic implants are in general prostheses, while temporary orthopedic implants include plates, screws, pins, wires, and intramedullary rods. In this thesis the focus will be on orthopedic screws that are not used as a temporary implant but are employed to permanently stay in the bone tissue, therefore, their integration in the human body becomes a very relevant aspect.

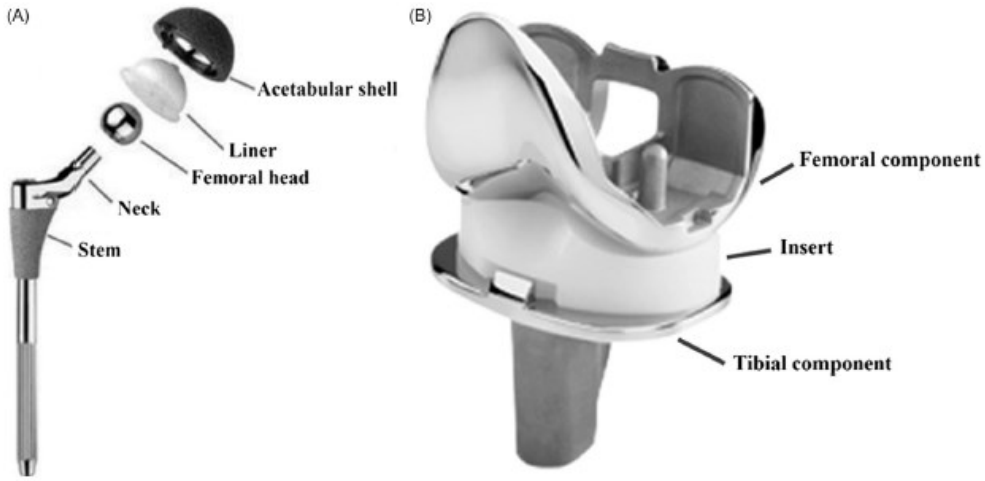

Figure 2 *(A) Total hip and (B) Knee Replacement* [6].

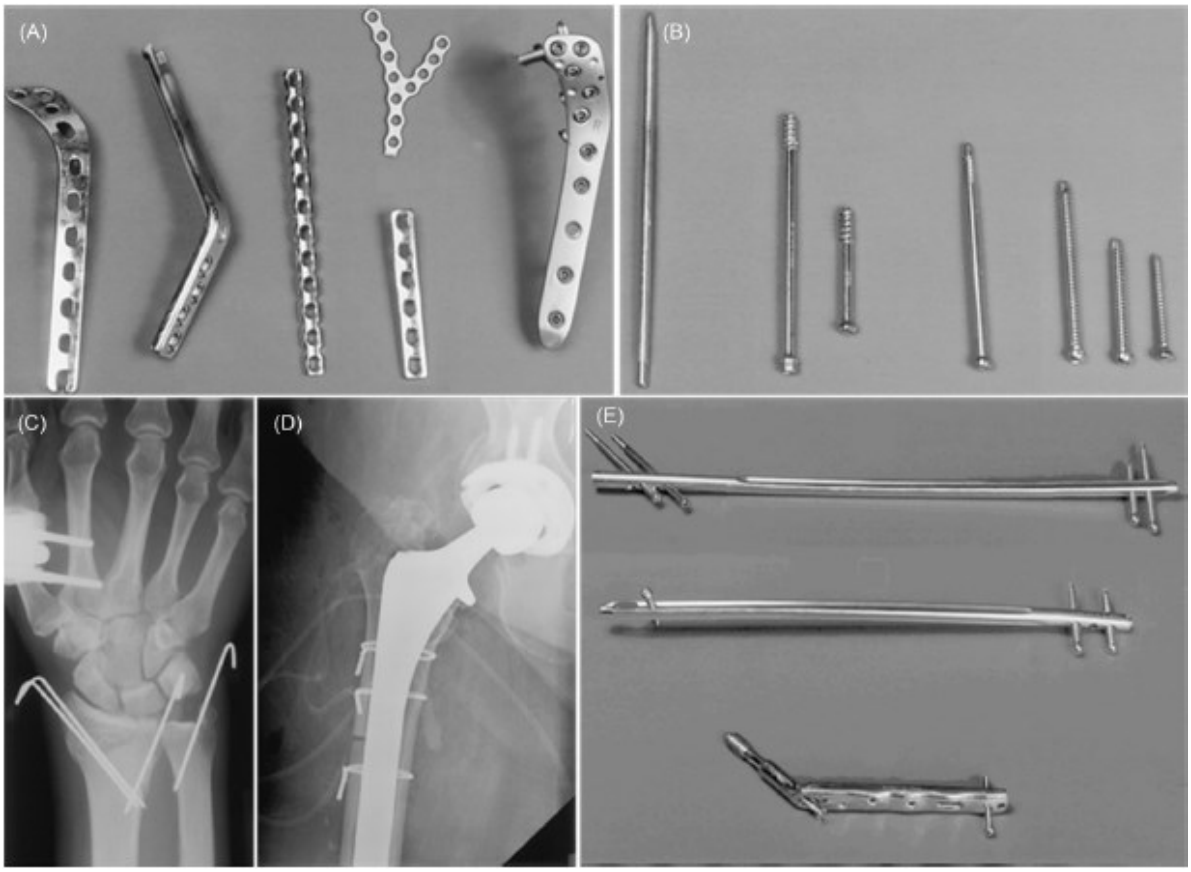

Figure 3 *(A) Plates, (B) Screws, (C) Radiographic scan of implanted pins, (D) Radiographic scan of wire, (E) Intramedullary rods* [6].

Orthopedic implants aim to restore the structural integrity and function of damaged joints and bones. To fulfill this goal, it is required to produce safe implants with a long-lasting life span that do not lead to rejection. Consequently, a crucial point is the choice of the material composing the implant, indeed from this choice can be obtained several specific characteristics of it [6].

1.4.1-Orthopedic implants materials

There are three classes of materials used in orthopedic implants: metals, ceramics, and polymers. Generally, metal materials can be used in both permanent and temporary orthopedic implants due to strength, hardness, ductility, corrosion resistance, biocompatibility, and fracture resistance, which are required for loading-bearing components such as fracture fasteners and total joint prostheses. Commonly utilized biomedical alloys can be categorized into various groups: stainless steel, Co-based alloys, titanium(Ti)-based alloys, and biodegradable alloys. The US Food and Drug Administration has approved the first three groups that, for this reason, are widely used in orthopedic implants; instead, the last group of materials is still under development and its properties are able to meet only specific clinical needs.

For what concern ceramics, there are two principal kinds of orthopedic ceramics: bioinert ceramics and bioactive ceramics. Since they undergo little physical or chemical alteration over a long time in the human body, bioinert ceramic materials provoke a minimal response from the living tissues. This kind of ceramics presents high compressive strength, excellent wear resistance, inherent chemical inertness, and biocompatibility. Bioinert ceramic materials are popularly used as joint components in total joint replacements, while due to their poor ductility they have not been applied to fracture fixation applications. The most investigated bioinert ceramics are Alumina (Al_2O_3), Zirconia (ZrO_2), and silicon nitride (Si_3N_4). Bioactive ceramic materials, instead, can establish a direct bond with surrounding living bone tissues. Because of their low mechanical strength, these materials are often used as metal bone implant liners rather than as load-bearing components.

An example of this class is hydroxyapatite, that with its porous structure is able to promote bone tissue growth inside the pores leading to better integration between the implants and adjacent tissues. Polymers generally used in orthopedics are Polymethylmethacrylate (PMMA), Ultrahigh-molecular-weight polyethylene (UHMWPE), Polyetheretherketone (PEEK), and biodegradable polymers. In particular, orthopedic polymers are used as inter-positional cementing materials between the implant surface and bone and as bearing inserts of hip and knee joint replacements. PMMA is a principal bone cement component for anchoring cemented orthopedic prostheses. In the case of polymers used as the articulating surface, the major requirements necessary are low friction and high wear resistance since the opposing articulating surface is usually made of metals. UHMWPE, instead, is adopted as a load-bearing surface in total joint replacements. The major problem of the metal-on-polymer articulating surface is the formation of wear particles such as polymer debris. For this reason, researchers are looking for new methods to improve the wear resistance of UHMWPE without impairing its other essential properties. Lastly, polyetheretherketone (PEEK) and biodegradable polymers have also emerged as constituents of joint prostheses and temporary fixation devices [6].

1.4.2-Metals

The first metals used in orthopedic implants (1926) were stainless steel. In particular, due to their good corrosion resistance 316 and its derivates, asthenic stainless steels are widely adopted in orthopedic implants [6]. They are mostly composed of iron plus nickel, chromium, and molybdenum [25]. Albeit the biocompatibility of stainless steel is good, it is still below that of other conventional metals due to faster corrosion in the physiological environment leading to the release of toxic agents (Cr3p and Ni2p). Such metal also presents poor fatigue strengths and wear resistance that can cause

failure after a while. Because of these characteristics, its application to permanent implants at load-bearing sites is limited, 316L stainless steel can be adopted only in permanent implants under small loading such as shoulders. Nevertheless, thanks to its low cost compared to other alloys, 316L stainless steel is still popular in fixation devices such as bone plates, bone screws, and intramedullary rods, which temporarily fuse two pieces of tissue together and are removed after healing [6]. Stainless steel devices are ductile enough to be modified in operative situations with simple tools and they can be polished to a relatively high smoothness [25].

The first employment of Cobalt (Co)-based alloy (1939), usually referred to as CoCr alloys, was for hip prosthetic implants. As in the case of stainless steels, Cr at a high concentration leads to the spontaneous formation of a passive Cr_2O_3 layer in the human body fluid environment, while the inclusion of Mo and Ni provides enhanced corrosion resistance. Nowadays, the alloys commonly used are those Co-Cr-Mo and Co-Ni-Cr-Mo, and the four main types are cast Co-Cr-Mo alloy (ASTM F75), wrought Co-Cr-Mo alloy (ASTM F799), wrought Co-Cr-W-Ni alloy (ASTM F90), and wrought Co-Ni-Cr-Mo alloy (ASTM F562). Good biocompatibility and a long lifetime in the human body are emerged by long-term clinical use of Co-based alloys. Nonetheless, there remain aspects of concern such as biological responsiveness to the potential release of toxic Co, Cr, and Ni ions or wear debris from implants and the stress shielding effect of the high Young's modulus (210-230 GPa) [6]. The surface of such kinds of metals can be highly polished so that a high degree of smoothness can be reached and minimal wear in metal-on-polyethylene bearing situations occur. The drawback of this material is due to the fact that is very difficult to alter or cut it in intra-operative situations [25]. The major use of Co-based alloys is in joint parts such as the femoral head in permanent orthopedic implants [6].

The majority of implantations in orthopedic surgery involving titanium are made of titanium alloys, specifically, the titanium-aluminum-vanadium alloy, Ti-6Al-4V (6% aluminum and 4% vanadium). Pure titanium implants can be used when high stresses are not expected, instead, when high strength is required titanium alloys must be used. Titanium implants are employed for hip femoral stem components, intramedullary rods, interbody devices, screws, and many other devices. A very useful aspect is related to the fact that titanium plates and other devices can be modified in the operating room and in vivo. Titanium is not capable of being polished and machined to achieve a surface smoothness competitive with other implant materials such as cobalt-chrome. A thin adherent layer of titanium oxide (TiO_2) provides corrosion resistance, making titanium significantly superior to cobalt alloys and stainless steel in this respect. In addition, the Ti oxide layer provides an excellent interface with the bone, allowing the growth to the implant surface, avoiding considerable fibrous tissue

formation which instead is visible in other metal-bone interfaces. Another significant advantage of titanium implants is their biocompatibility from the stress shielding point of view due to their lower elasticity modulus with respect to that of stainless steel and cobalt-chromium alloys. Devices made with this material also present an excellent resistance to pitting, intergranular, and crevice corrosion. It should be noted that the Ti-6Al-4V alloy is a notch-sensitive material, and without the additional surface treatment, it shows very poor wear resistance compared to stainless steel and cobalt-chromium alloys [24],[25].

Since metallic biomaterials aforementioned used for bone fixation devices must be removed by a second surgery after sufficient tissue healing and this can provoke discomfort and new damage to the patient, a new class of biodegradable metals has emerged as an alternative to traditional fixation implants. Three are the expectations about this new class: gradual corrosion in vivo, appropriate host response to released corrosion products, and complete dissolution upon fulfilling the mission to assist tissue healing with no implant residues. Mg-based alloys, Fe-based alloys, and zinc (Zn)-based alloys are the three main types of biodegradable metals and, in particular, Mg-based alloys have been most extensively studied in vitro, in vivo, and clinically [6].

1.4.3-Titanium and Ti-alloys

Since Titanium may exist in more than one crystallographic form, it is defined as an allotropic element. At room temperature, Titanium exists in the α-phase, also defined as hexagonal close-packed crystal structure (hcp) (Figure 4). When such material in the solid-state is heated to temperatures higher than 883°C or when it solidifies from a liquid it is possible a transition from the hcp to the body-centered cubic (bcc) structure, or β-phase (Figure 4) [26]. Several prior research has revealed that alloying elements can strongly impact the phase transformation temperature of pure Ti, for this reason, alloying elements are typically differentiated into α-stabilizers (such as Al, C, O) and β-stabilizers (such as Mo, Ta, Nb) [2]. Nowadays, although only 20 to 30 alloys have reached a commercial status, more than 100 titanium alloys are known. Amidst the commercial alloys, Ti-6Al-4V is the most widely used and covers more than 50% of the usage. Based on crystal structure four classes of titanium alloys can be distinguished: α-alloys, near-α-alloys, $(\alpha + \beta)$-alloys and β-alloys [27].

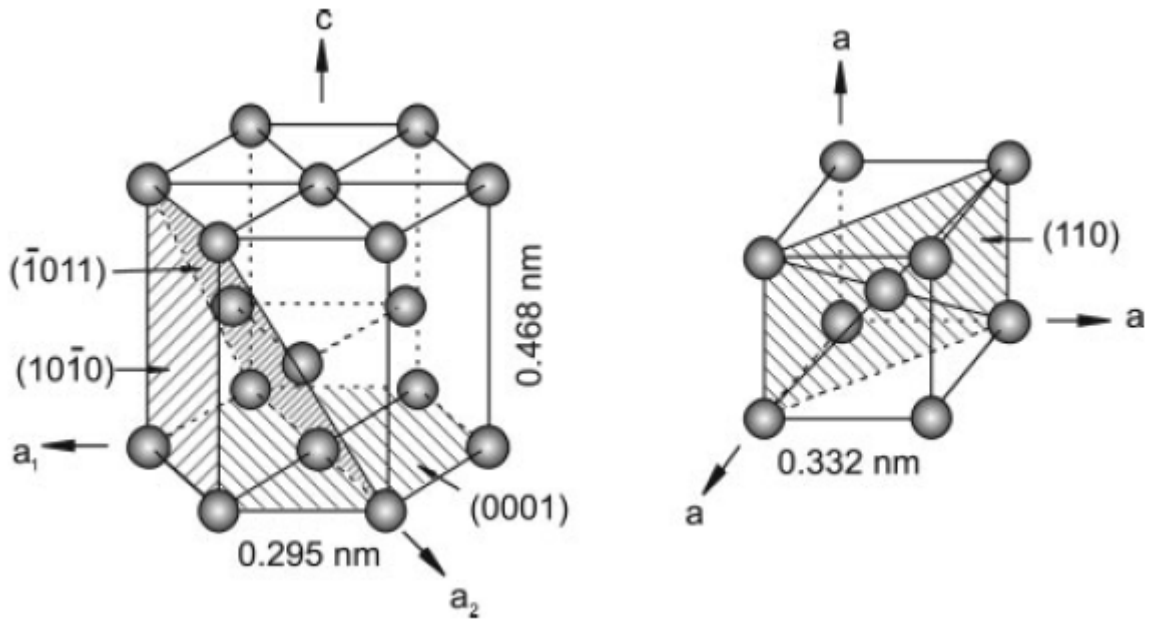

Figure 4 *Crystal structure of hcp α and bcc β phase* [28].

The α-alloys are characterized by only α-phase and include four grades of commercially pure Titanium and Ti alloys. The four grades of Ti differ for the amount of Fe (from 0.20 to 0.50 wt%) and of O (from 0.18 to 0.40). Near-α alloys, instead, are α-alloys that contain a small amount of β-stabilizers (1-2 wt%) able to stabilize 5-10% of the beta-phase in the structure at room temperature [2],[28]. These two classes show similar properties, such as good weldability, high creep resistance, and excellent corrosion resistance. On a different note, at room temperature, their strength is notably low. A higher presence of β-stabilizers compared to near-α-alloys characterizes the $(\alpha + \beta)$-alloys that indeed, possess a higher fraction of beta-phase (5-30 vol%). Contrarily to α-alloys, this class of Ti-alloys shows good fabricability, high strength at room temperature and the mechanical properties can be optimized by using heat treatment. They still exhibit excellent corrosion resistance and the capability of rapid osseointegration within the human body. Ti-6Al-4V belongs to this class and these characteristics make it the most widely employed biomedical alloy. Even higher amounts of β-stabilizers are contained in β-alloys that have a lower amount of α-stabilizers. This class of alloys shows lower elastic modulus compared to the others while they present comparable strength and better biocompatibility and higher corrosion resistance inside the human body. For that reason, many new beta-alloys with optimized properties for biomedical applications have been developed over the past two decades [2]. Thus, by varying the type and amount of alloying elements, it is possible to achieve a specific type of titanium alloy with distinct properties [28]. Since Titanium and its alloys provide an excellent combination of properties, they are the better choice for manufacturing biomedical implants [2].

1.4.4-Screws

The helical-thread screw is a significant device in mechanical engineering since is able to convert angular motion to linear motion to transmit power or to develop large forces. They are complex tools in which is possible to distinguish four-part construction: head, shaft, thread, and tip (Figure 5). The head has two functions, it serves as an attachment for the screwdriver, and it serves as the counterforce against which compression generated by the screw acts on the bone. The shaft, also called the shank, is the smooth portion of the screw between the head and the threaded region. It is possible to describe the thread by four parameters, the root (or core) diameter, the thread (or outside) diameter, the pitch (distance between adjacent threads), and the lead (distance it advances into the bone with each complete turn) [24].

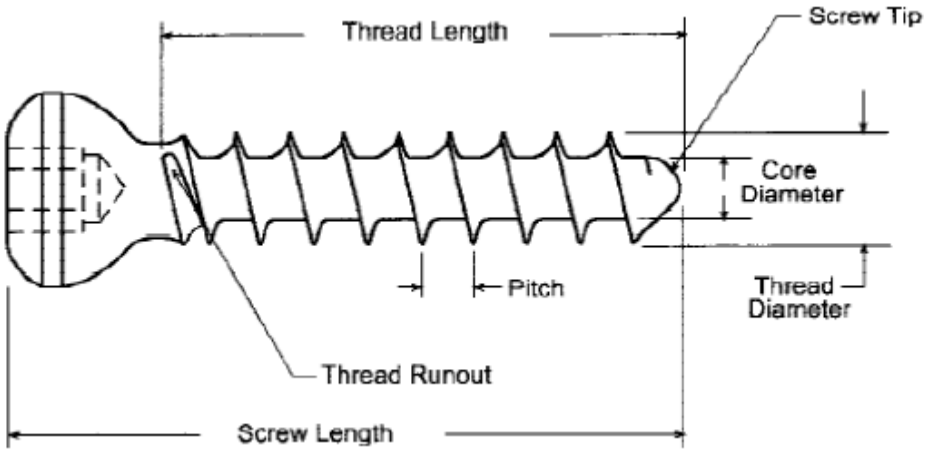

Figure 5 *Screw term definition* [24].

The screw tip can be either round or self-tapping. The resistance of the screw to pull-out forces is determined by the root area, it refers to the bone area at the thread interface and the root area of the tapped thread.

The most popular devices used for bony fracture fixation are orthopedic screws. Screws can be employed either as standalone fixators or in conjunction with other orthopedic devices, primarily plates. Principally responsible for retaining the stability of plated-bone constructs, and for providing necessary interfragmentary compression, screw-hold in bone is very crucial (Figure 6). The sealing force of screws in bone is predominantly affected by the outer diameter of the screw and the insertion length, while the shear strength of the bone is chiefly driven by the density of the host material [24] [29]. Reasoning in clinical terms, when the screw pull-out is a concern because of the soft bone, a larger thread diameter may be preferred, while when the bone is strong and the fatigue is an issue, a screw with a wider root diameter will have a higher resistance to fatigue failure.

The employment of a screw is a valuable technique as it permits the conversion of torque forces into forced compression through a fracture. Accomplishing a satisfactory fixation requires a special application of the screw, it must be positioned to enable the proximal portion of the screw to slide into the neighboring bone and gain threads in the opposite cortex, in this way the screw head will be exerting the load and will be forcing the fracture together. The screw angle respective to the fracture plays a key role in bone fixation, therefore, is necessary a meticulous selection of this angle to thwart sliding of the fracture fragments as they are compressed.

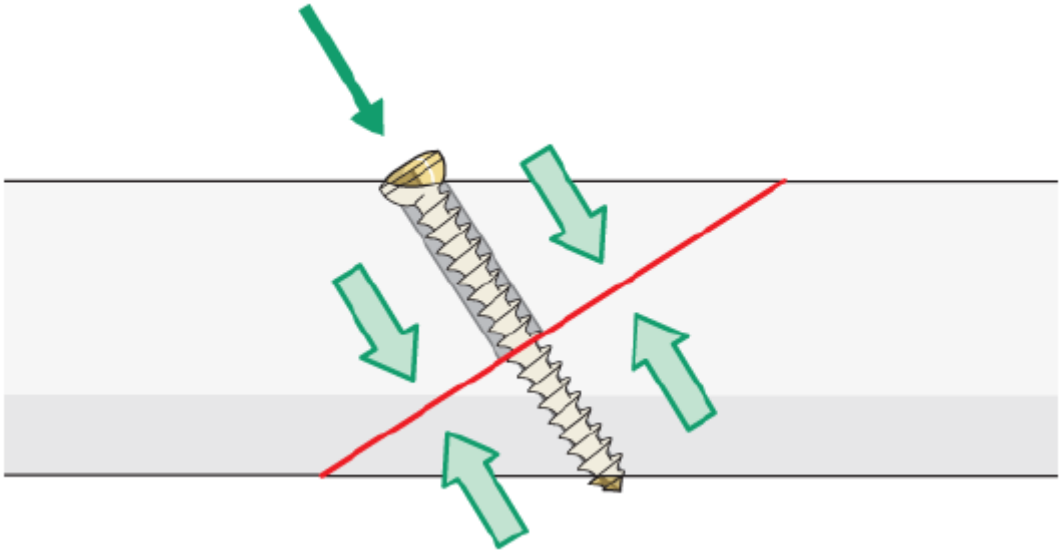

Figure 6 *Interfragmentary compression orthopedic screw* [24].

For purpose of inducing higher screw tension, the screw should be inserted at the highest possible torque, and this is because there is an approximately linear relationship between the loading torque induced on the screw and the resulting tension. A higher screw tension is desirable because a higher frictional force must be overcome for loosening to occur; it will also likely result in a greater amount of mechanical stimulus transfer to the bone, which will diminish the stress shielding. After the healing of the bony tissue, since the screw remains inserted into the bone, a decreased bone's strength and stiffness may be observed. Indeed, the significantly stiffer metallic screw (elastic modulus of 100-200 GPa) transfers most of the shared load, provoking the adjacent bone (elastic modulus of 1 to 20 GPa for cancellous and cortical bones) to be atrophied in response to the diminished load it is carrying, in accordance with Wolff's law of functional adaption [24],[30].

1.4.5-Causes of implants and prostheses failure

Several are the complications that follow the insertion of implants and prostheses within the human body that may lead to their failure; first of all, wear and the debris produced, indeed this is one of the

main issues in adult reconstructive orthopedic surgeons [31]. Wear is a surface damage phenomenon in which material is detached from the body as small debris particles, mainly by mechanical activity [32],[33]. Macrophages, fibroblasts, and osteoblasts engulf micro-sized debris activating the release of several pro-inflammatory factors and chemical mediators. Then inflammatory mediators act in concert with appropriate enzymes causing a diminishing of bone stock in the periprosthetic region, leading to localized bone loss and aseptic loosening that compromise the implant fixation causing implant failure [31].

On the flip side, another cause of implant failure is stress shielding, a phenomenon that is experienced when a prosthesis or implant takes some of the load while preventing it from reaching the bone. Since bone, based on Wolff's law, adapts its structure to the received loads, when the loads decrease, the bone reacts by reducing its mass, the so-called bone resorption. As a reaction to this bone resorption, loosening or implant failure is possible and may occur [34].

Every time that an implant is placed inside the human body surgical actions are required and, in turn, damage to the target tissues is produced. As soon as these damages occur, processes to restore tissue homeostasis around the implant begin. Nevertheless, the immune system undergoes long-term overstimulation due to the constant presence of the implant that provokes poor wound healing and chronic inflammation. Foreign body response (FBR) is the name of this unbalanced reaction that may be the cause of reduced functionality of implant in the patient and can conduce to implant failure [35].

Although, often joint arthroplasties and implant insertion provide pain-free function, in some cases infection may occur due to the deposition and proliferation of bacteria and biofilm at the implant surface. The Infection affecting the joint prosthesis and adjacent tissue is called peri-prosthetic joint infection (PJI) [36]. PJI is difficult to face because requires complex treatment strategies involving long-term antimicrobial treatment and multiple surgical revisions [37]. The persistence of such infection leads to implant failure, in particular, PJI may provoke loosening, periprosthetic fracture, wear, implant malposition, dislocation-instability, and fracture of the prosthetic material itself [36].

In further, what has transpired from clinical observations is that implants and fixation devices are often subjected to high stress, which ultimately leads to fracture either by surcharge or cyclic fatigue failure. Several undesirable consequences may be provoked by this kind of failure of implants and prostheses, with further damage to the supported bone and surrounding tissues leading to additional injury and surgical interventions [38].

1.4.6-Screw loosening

A controversial issue is the one related to screw loosening. Some have been not able to define screw loosening as a problem while others ignore it, or they combine screw fracture with screw loosening in their results. Instead, this is an important issue to face because it is a complication that can cause discomfort for the patient, can affect finances if it occurs frequently, and can be a sign of impending failure of the implant and other components. For this reason, if the screw loosening can be reduced or avoided by adopting some strategies, there will be a benefit from several points of view. Naert et al's research report 5% screw loosening while, in his study, Jamt stated that only 69.3% of prostheses had stable gold screws at the first post-insertion examination [39][40]. The incidence of loose occlusal screws is particularly examined in a study that looked at a population of patients whose use had lasted at least 5 years [40]. This study reported that in the case of slotted-head occlusal screws, 40% of them were loose, whereas in the case of screws with an internal hexagon only 10% of them were loose [40]. Consequently, the author proposes that the screw tightness has to be checked much more frequently than every 5 years, and also the replacement should be done after a shorter period of time if loosening repeats as a regular occurrence [40]. From these considerations, it is easier to understand how important the choice of the screw material is not only but also the incorporation of the implant inside the human body in such a way as to reduce and avoid all potential complications.

1.5-Bones

Bones are the elements that make up an essential apparatus of the human body, the skeletal system; this system contributes to the overall shape of the body and also has several crucial functions, including [23]:

- Protection
- Support and movement
- Blood-cell formation
- Mineral homeostasis
- Triglyceride storage

The cells that constitute the bone tissue are embedded in a matrix of ground substance and fibers [41]. Three are the main components of the bone matrix: 25% organic matrix, 25% water, and 50% inorganic mineral salts (calcium carbonate and calcium phosphate). The presence of these salts provides a higher rigidity to the bones compared to other tissues. The flexibility and the strength of the bone tissue, instead, are given by a collagenous network. In particular, the framework for the

bones is formed by the organic matrix which is, in turn, composed of approximately 90% type-I collagen fibers and 10% other proteins (such as glycoprotein, osteocalcin). Once the gaps in the collagen layer have been filled, the collagen fibers are surrounded with mineral salts and the following crystallization of these salts causes the tissue to harden concluding the action course of ossification. The main mineral found in bone is hydroxyapatite and depending on the amount and type of minerals available to the body, bone can gain a certain degree of hardness.

Another aspect derived by the collagen fibers is the flexibility of the bone, which is essential to prevent its breaking, and the tensile strength which is important to provide resistance to the daily force at which the bones undergo. Bone fragility and brittleness may be increased by altered collagen production or over-mineralization [23].

1.5.1-Bone cells

The cells contained in bone tissue can be classified into four types: osteoblasts, osteocytes, osteoclasts, and bone-lining cells. A differentiation based on origin is possible for these kinds of cells, in particular, osteoblasts, osteocytes, and bone-lining cells are derived from mesenchymal stem cells known as osteoprogenitors; instead, the precursors of osteoclasts are hemopoietic stem cells. Different are also the location of these bone cells, indeed, osteoblasts, osteoclasts, and bone-lining cells are found along the bone surface, whereas the osteocytes are located in the bone interior (Figure 7) [42].

1. Osteoblasts: located in the growing portion of the bone, they are capable of producing and releasing non-mineralized ground substances and act as calcium-phosphate pumps to move ions in and out of bone tissue. They can follow one of these three pathways: (1) remain active osteoblasts, (2) become surrounded by matrix and become osteocytes, or (3) become relatively inactive and form bone lining cells [41],[42].
2. Osteocytes: it is estimated to make up more than 90% of the bone cells in an adult skeleton, their cell body occupies a lacuna, and they constitute the main cells of fully developed bones. They along with osteoclasts play a significant role in homeostasis by helping and promoting calcium release [41],[42].
3. Osteoclasts: they are derived from white blood cells called monocytes and are multinuclear giant cells, which are known to be very mobile and are located where the bone is resorbed during its normal growth [41],[42].

4. Bone–lining cells are thin, elongated cells, that cover the surface of most bones in the adult, so mature, skeleton. They are also thought to be derived from osteoblast that ceases their physiological activity. Their function is still not well understood, some researchers hypothesize and reported that bone-lining cells may regulate the crystal growth in bone or function as a barrier between the extracellular fluid and bone [41],[42].

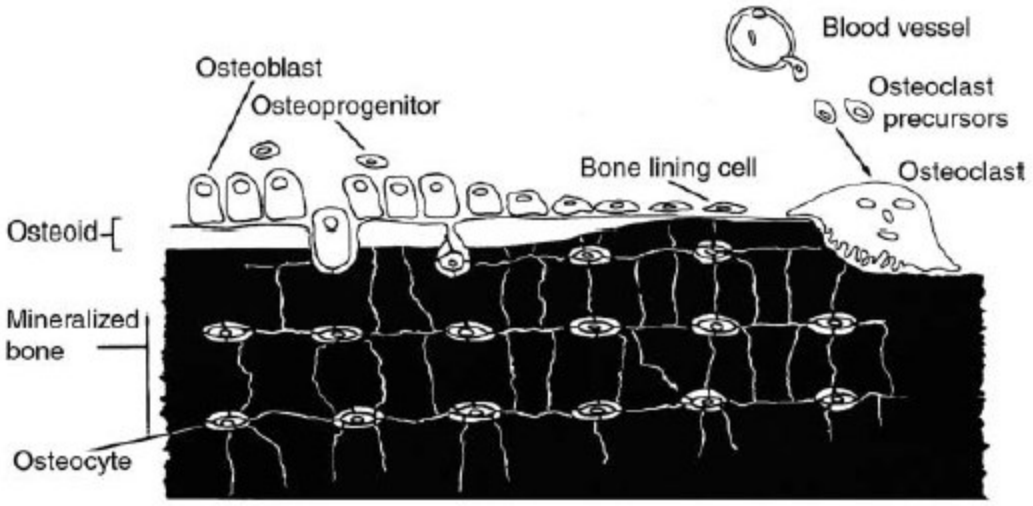

Figure 7 *The origins and locations of bone cells* [42].

Furthermore, an additional class of cells is reported, osteogenic cells. They are small spindle-shaped cells found mostly in the deepest layer of the periosteum and endosteum. Such cells are notable for their high mitotic potential and ability to be transformed into bone-forming cells [41].

1.5.2-Bone structure

Bone tissue can be distinguished in cortical (compact or Haversian) bone and cancellous (spongy or trabecular) bone [24]. These two types differ at the microscopic level and in the degree of porosities, indeed, the porosity of cortical bone varies from 5% to 30%, while cancellous bone's porosities range from 30% to more than 90% [24]. Cortical bone is a dense and hard outer sheet of the bone surrounding the inner cancellous structure, supporting, and protecting it [23],[41]. Calcified bone cylinders known as osteons are contained in the compact bone tissue; these cylinders are composed of concentric layers called lamellae. Nerves, lymphatic, and blood vessels run along the central canals of osteons (Haversian canal). In each lamella, there are little spaces called lacunae that houses bone cells. Cortical bone involves three elements: periosteum, intracortical area, and endosteum. Cancellous bone tissue is organized in lamellae arranged in an irregular lattice structure of trabeculae, which gives a honeycomb appearance. Trabeculae are the little spine of bone tissue surrounded by a bone matrix that has calcified. Thanks to the large holes between the trabeculae the bone structure is

lighter and easier to mobilize. Specifically, trabeculae are characteristically oriented along the lines of stress to help withstand forces and reduce the fracture risk (Figure 8) [23],[41].

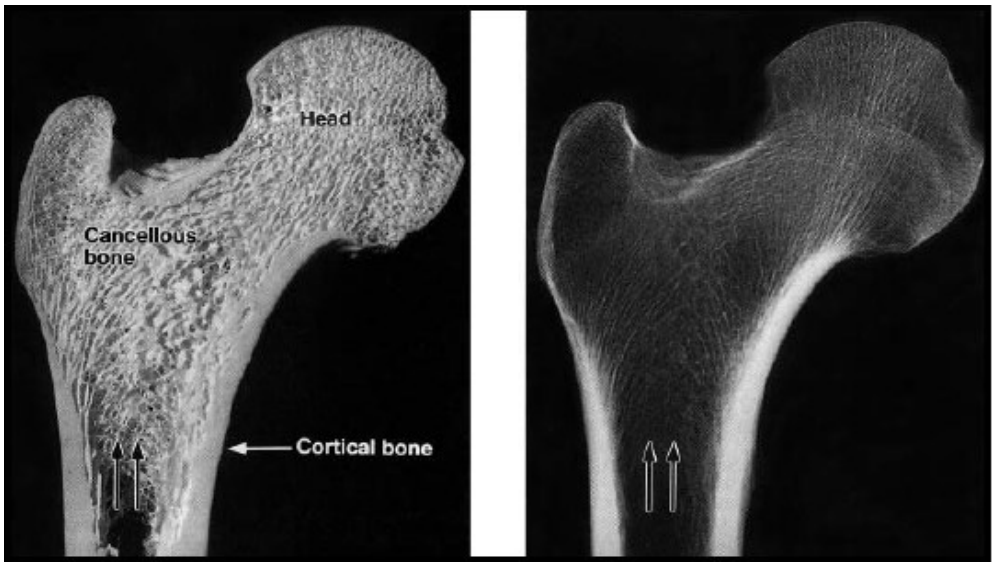

Figure 8 *Bone section (left) and radiograph (right) of the proximal femur in the frontal plane illustrating cortical and cancellous bone* [42].

1.5.3-Bone typologies and growth

Bones begin to take shape in utero in the first eight weeks following fertilization. Specifically, there are two ways in which the skeletal template, a primitive skeleton structure made of mesenchyme, develops in an embryo: Intramembranous ossification and Endochondral ossification [23],[41]. These two different processes, produce five types of bones in the skeletal system: long, short, flat, irregular, and sesamoid.

The Intra-membranous ossification involves the direct conversion of the mesenchyme structure into bone, in which fibrous tissue evolves into ossified tissue when mesenchymal stem cells differentiate into osteoblasts. The bone matrix is, then, laid down by osteoblasts and becomes ossified to build new bone. Flat and sesamoid bones are derived by intra-membranous ossification of membrane and tendon, respectively [23].

The endochondral ossification, instead, is marked by the gradual replacement of the cartilage with the bone matrix. The mineralization process begins in the center site of the cartilage structure which is called the primary ossification center. Specifically, short, long, and irregular bones develop from an initial template of hyaline cartilage.

Bones continue to shape until skeletal maturity is reached, which occurs around age 20-25. However, this can vary depending on socio-economic and geographical conditions [23].

1.5.4-Bone remodeling

After its formation and maturation, the bone goes through a phase of constant remodeling, thanks to the action of osteoblasts and osteoclasts, in which a new bone tissue replaces the old tissue [23]. Since different kinds of bone cells continuously act promoting constant processes of bone resorption and formation, bone can achieve maximum strength with minimum mass which is the main purpose of the bone remodeling process [24].

The main functions of bone remodeling are several, repairing the damaged bone, helping the body to adapt to different loads, forces, and stress applied to the skeleton, and mobilization of calcium and other minerals to maintain serum homeostasis (Figure 9). Typically, osteoclasts are found at sites where there is active bone growth, remodeling, or repair. These cells are able to decompose the bone tissue by releasing lysosomal enzymes and acids into the space between the ruffled membrane; both the minerals and part of the bone matrix are dissolved by these enzymes. Bone matrix releases minerals into the extracellular space, while the rest of the matrix is phagocytosed and metabolized in the cytoplasm of the osteoclasts. Once the area of bone has been resorbed, the osteoclasts move on, while the osteoblasts intervene to reconstruct the bone matrix [23].

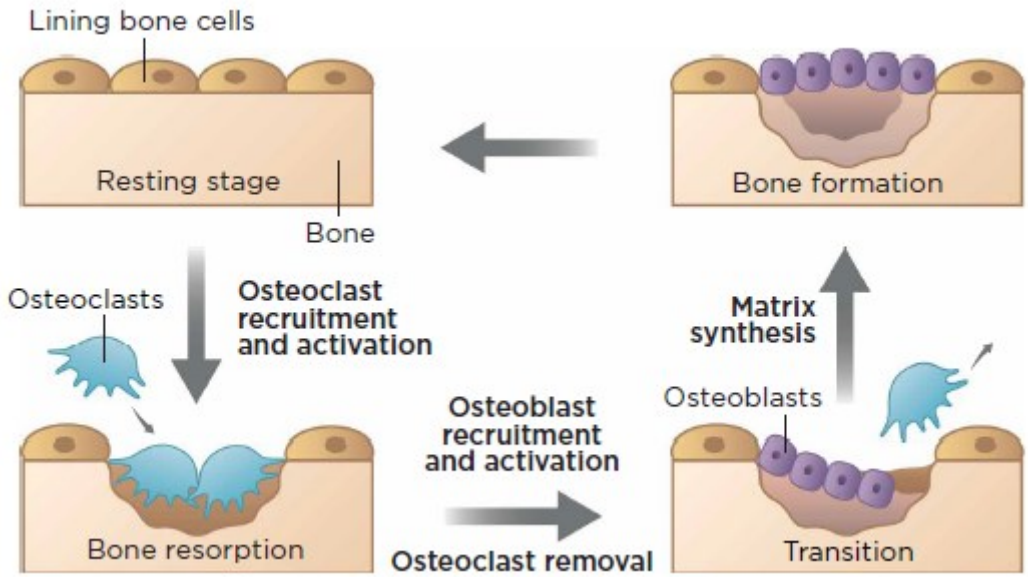

Figure 9 *Bone remodeling process* [23].

Collagen fibers and other organic elements that constitute the bone matrix are synthesized by osteoblasts. Such kind of cells also secretes a particular enzyme, alkaline phosphatase, which begins calcification through the deposit of calcium and other minerals around the matrix. When osteoblasts settle new bone tissue around them, they become trapped in the hollows of bone, called lacunae. Once this occurs, the cells differentiate into osteocytes, mature bone cells, that are no longer capable to secrete bone matrix. The balanced activity of osteoclasts and osteoblasts allows a correct bone

remodeling process; without the appropriate equilibrium between these two activities, problems may occur [23].

1.6-Osseointegration

In Dorland's Illustrated Medical Dictionary, the term osseointegration is referred to the direct anchorage of an implant, by the formation of bony tissue around it, without the growth of fibrous tissue at the bone-implant interface [43]. The first who, accidentally, observed and described this reaction was Per-Ingvar Brånemark in the early 1950s during his studies in blood flow in rabbit femurs consisting in the placement of titanium chambers in their bone. He saw that rabbit bone became strongly and inextricably linked with the titanium implants [44],[45]. Then in 1965, Brånemark used pure titanium screws in his patients for dental implants realizing the first well-documented and most well-maintained dental implants [44]. The first osseointegration surgical treatment was performed in Sweden on May 15, 1990, on an amputee woman of 25 years old. On that date, the woman had a first-stage titanium implant anchored to her right residual femur, and then, six months later, a titanium abutment was connected to the well-osseointegrated implant (Figure 10) [45],[46].

Figure 10 *Radiographic image of the right femur related to the first extremity osseointegration patient who was operated on in 1990* [46].

Osseointegration is a technique that has gradually received wider acceptance since the first successfully performed surgical procedure [45]; indeed, in amputee patients, a percutaneous osseointegrated device enables a continuous structural connection with an external prosthesis. There are several advantages to this procedure, first of all, it avoids the problems associated with socket design, reduces energy consumption, provides the walking ability, enhances range of motion, seating comfort coupled with indirect sensory feedback called Osseoproprioception [5]. This latter is an exciting phenomenon able to improve the patient experience with an osseointegrated prosthesis, Osseoproprioception is defined as the mechanical stimulation of a bone-anchored prosthesis that is transformed by mechanoreceptors probably located in skin, muscles, joints, and other bone-adjacent tissues that proceed to the central nervous system to provoke a passive awareness of patient's own sensorimotor position and function [45].

The osseointegration success is related to multiple patient factors, being skeletally mature, being in good overall health, and being able to follow the rehabilitation protocol. When the risk of superficial and deep infection increases or there is the possibility of inhibition of bone ingrowth, osseointegration is highly contraindicated. Specifically, one potential risk of osseointegration is a periprosthetic fracture that may provoke a more proximal amputation or further impairment.

In many conditions is not possible to perform osseointegration: diabetes mellitus, skeletal immaturity, peripheral arterial disease, osteoporosis, metabolic bone disease, or untreated skin disease of the residual limb [47],[48].

1.6.1-Osseointegration mechanism

The key aspect for osseointegration is the incorporation of a non-biologic implant to the host bone to establish both structural and functional direct bound between the musculoskeletal system and the implant, thus allowing load bearing [5]. The osseointegration mechanism starts with the activation of an osteogenic process. When the implant is placed, the implant-blood cell interaction causes a hematoma to form at the bone interface, which in turn leads to the development of clots on its surface. Inside this clot, platelets undergo a number of morphological and biochemical changes to stimulate the production of a fibrin matrix serving as a scaffold for osteoprogenitor cells to differentiate from osteogenic cells. A Woven bone formation develops from a calcified matrix on the surface of the device and then it transforms into the lamellar bone. This peri-implant trabecular bone corresponds to the first biological fixation. Like native host bone, the bone in direct contact with the implant undergoes adaptation, morphological reshaping, and mechanical loading [49].

Implant design, including composition and surface treatments, device fit, quality of the host bone, and pharmacologic agents are all involved in the success and failure of osseointegration. In particular, the biocompatibility is of the implant material is essential to successful osseointegration. Since its high biocompatibility, corrosion resistance and its unique ability for the development of a surface oxide layer allowing for damage resistance, titanium has come into light as an ideal material for osseointegration [50]. The roughness of the implant surface has a relevant influence on osseointegration because it enhances the platelet and monocyte adhesion with respect to a smooth surface.

Furthermore, crucial factors for successful osseointegration are early implant stability and fixation to the host bone; as a matter of fact, uncontrolled micro- and macro-motion at the bone-implant interface promotes the growth of a fibrous membrane instead of peri-implant bone, consequently leading to aseptic loosening and ultimate failure [51].

1.6.2-Surgery procedure

Despite different ways of performing osseointegration according to the surgical center and implant system, it is possible to establish some similarities between approaches. Meticulous preoperative planning is the first step; it consists of an accurate check of the soft tissues of the stump in terms of quality, integrity, and morphology is very important. In the same way, also the adequacy of bone stock must be verified, the length and quality of bone may be checked by radiologic imaging; by using CT scans, instead, endosteal diameter and cortical thickness [5],[52].

Commonly, osseointegration surgery is performed in a single stage, but it can be divided into two stages by a period ranging from 6 weeks to 6 months that allows for adequate skin and soft-tissue recovery along with the development of solid osseointegration [53]. The surgery procedure starts with the preparation of the medullary canal for implant insertion, then the intramedullary component is positioned into the distal aspect of the bone. Immediate stability of the fixture with respect to the endosteal surface of the distal osteotomy surface is necessary to prevent micro-motion. When a single-stage surgery is performed a skin preparation is required so that the device is brought through the skin and subsequently loaded according to a supervised rehabilitation schedule. Differently, in two-stage surgery, once the soft tissues have healed after the initial surgery, socket use without end-bearing is sometimes allowed [54]. The second surgery consists of the connection of the osseointegrated fixture to a percutaneous abutment, with careful management of the surrounding

flaps, muscles, and skin-implant interface to form a stabilized soft tissue that diminishes the likelihood of infection.

1.6.3-Current osseointegrated systems

Of the various osseointegrated implants under development, six are the most frequently used: Osseo-anchored prostheses for amputee rehabilitation (OPRA), integral leg prostheses (ILP), osseointegrated prosthetic limb (OPL), transcutaneous compression implant (CTI), the percutaneous osseointegrated prosthesis (POP), and transcutaneous intraosseous amputation prosthesis (ITAP). Their main features are condensed in the table below (Table 1).

The OPRA system was introduced in 1998 and is composed of a fixture, an externally threaded intramedullary implant that allows for osseointegration; an abutment, a percutaneous implant that is inserted in the distal aspect of the fixture and serves as an attachment for an external prosthesis; and an abutment screw that threads into the distal aspect of the abutment securing it to the fixture (Figure 11). The system is made of commercially pure titanium and the surface of the fixture is treated so that a nano-porous structure is obtained. OPRA is implanted in two stages, during stage I the implant is positioned inside the intramedullary canal and an autologous bone graft from the iliac crest is used to increase the distal bone to provide a smooth surface; after about 3 months, during stage II a thin cutaneous flap is fashioned over the bone grafted portion of the bone, after which the transdermal abutment is attached to the underlying fixture [46],[55]. The FDA approved the transfemoral OPRA system through a Humanitarian Device Exemption pathway, while Institutional Review Board-approved clinical trials for both upper and lower extremity implants are underway at the Walter Reed National Military Medical Center and the University of California.

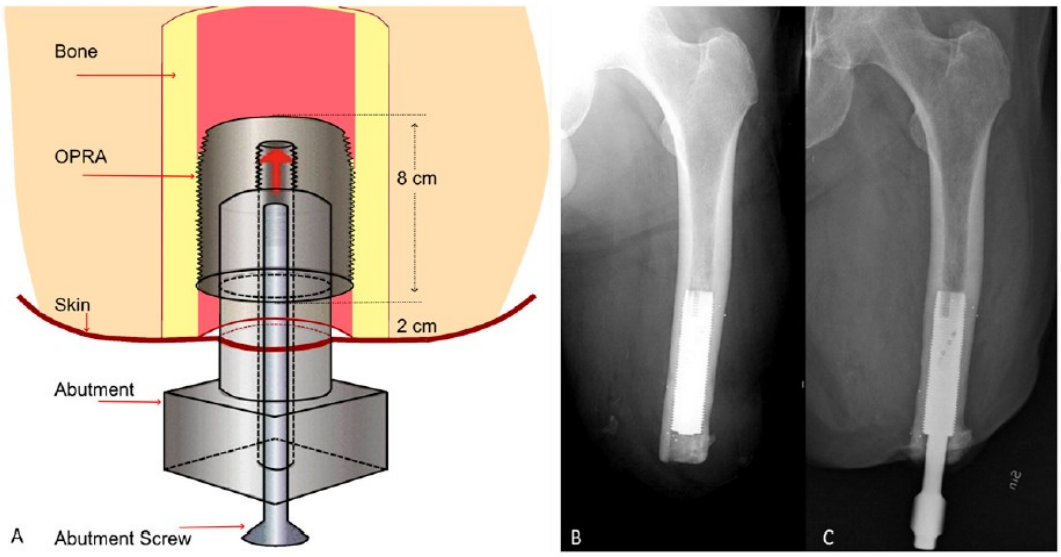

Figure 11 *(A) Schematic representation of OPRA system. (B) Radiographic depiction during stage-1 implantation. (C) Radiographic depiction after placement of the transcutaneous abutment* [45].

The ILP was introduced in 1999 in Germany, was initially designed for transfemoral amputees, however humeral and tibial applications have been described. Two major components build the ILP, an intramedullary endo-module, and a transcutaneous bridging connector. A macro-porous surface coating is contained in the endo-module, to facilitate osseointegration and is based on a press-fit into the residual bone. Furthermore, the endo-module contains a slight bow to provide rotational stability (Figure 12). The implant has a cast stem of cobalt-chrome-molybdenum, recently the stomal interface is designed with a smooth surface in an attempt to address the high rates of soft tissue irritation [52],[56]. ILP is beginning to be used primarily in Germany and the Netherlands, while its usage in the United States has not been approved by the FDA.

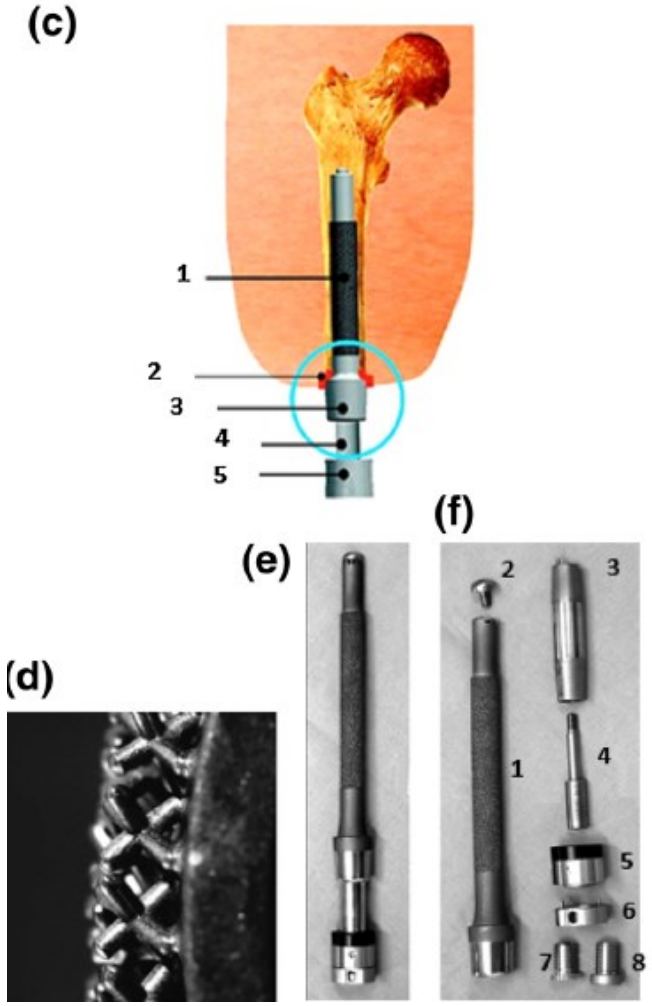

Figure 12 *(c) Schematic image of the ILP implant system: (1) Porous coated portion of the intramedullary component of the implant system, (2) inner lining, (3) Morse taper, (4) dual-cone adapter, (5) knee connecting adapter. (d) Close-up of the spongiosa metal surface to enhance osseointegration and ingrowth;*
(e) ILP implant system assembled;
(f) Exploded view of ILP implant system assembly [56].

The OPL was introduced in Australia in 2013 and then in the Netherlands in 2015. The system is used for transfemoral, transtibial, and trans-humeral amputation patients. In particular, standardized

implants are used for transfemoral amputees with almost 160 mm stump length, while custom-made implants are available for transtibial and transfemoral amputees with very short stumps [56]. OPL system is composed of an intramedullary device that is secured to a dual-cone transcutaneous implant with a locking screw (Figure 13). The composition material of the system is Ti-6Al-4V, osseointegration is promoted with a plasma-sprayed surface coating on the intramedullary implant. Two standardized designs are possible for the distal femoral OPL system: type A, with an extramedullary head, and a type B, with a flared intramedullary head for distal transfemoral amputations. The OPL is being used in Australia and the Netherlands, while it has not been approved by FDA for use in the United States [5].

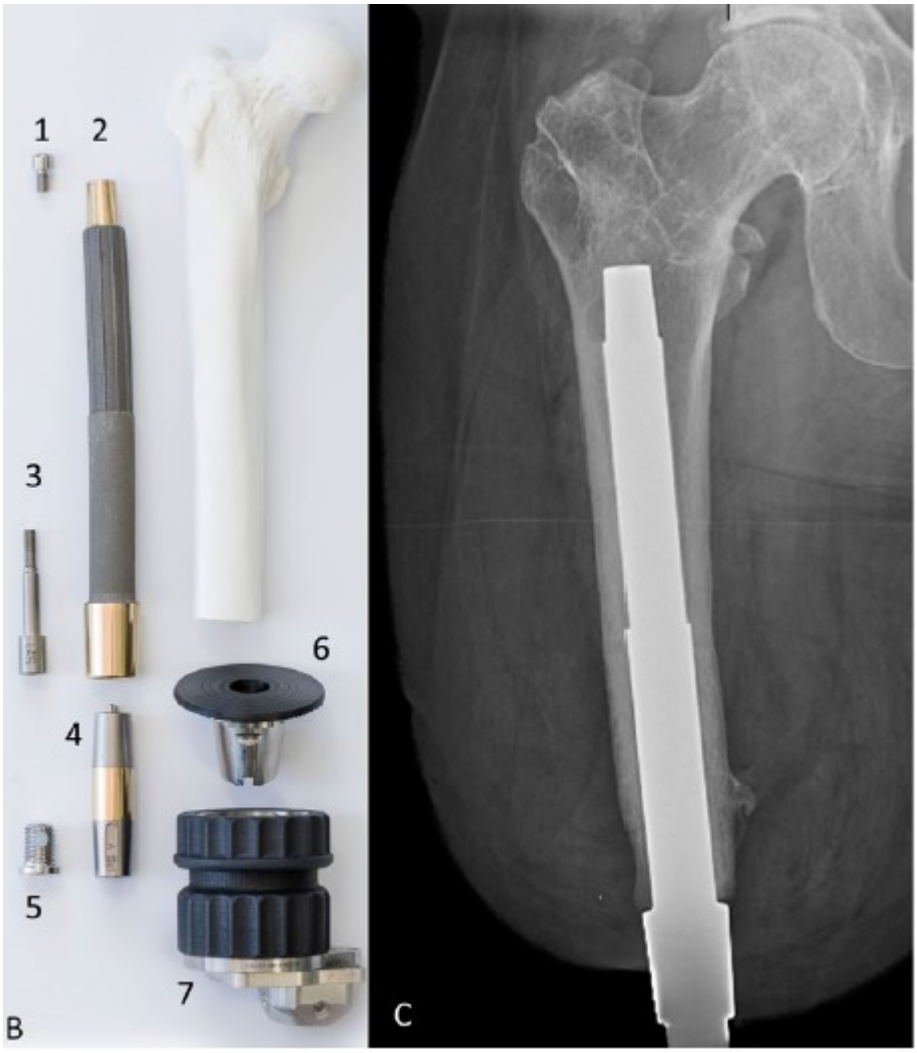

Figure 13 *(B) Exploded view of a Type-A implant: 1, proximal cap screw; 2, OPL body; 3, safety screw; 4, dual cone abutment adapter; 5, permanent locking propeller screw; 6, proximal connector; and 7, prosthetic connector. (C) Radiograph of OPL Type A in a patient who had undergone a femoral amputation* [45].

The COMPRESS was first developed as an endo-prosthetic system for oncologic limb salvage reconstruction by Biomet Corporation. The implant intramedullary part is fixed to the bone by

transverse pins in a bone-anchor plug. A porous-coated collar covers the distal interface of the amputated bone so that the process of osseointegration is promoted and enhanced. The bone collar interface is exposed to a compressive force so that osseointegration is enhanced and stress-shielding of the bone is prevented (Figure 14). Following the FDA custom device regulations, individual COMPRESS spindles were created with a transcutaneous taper, allowing implantation in both one and two-stage techniques [56],[57].

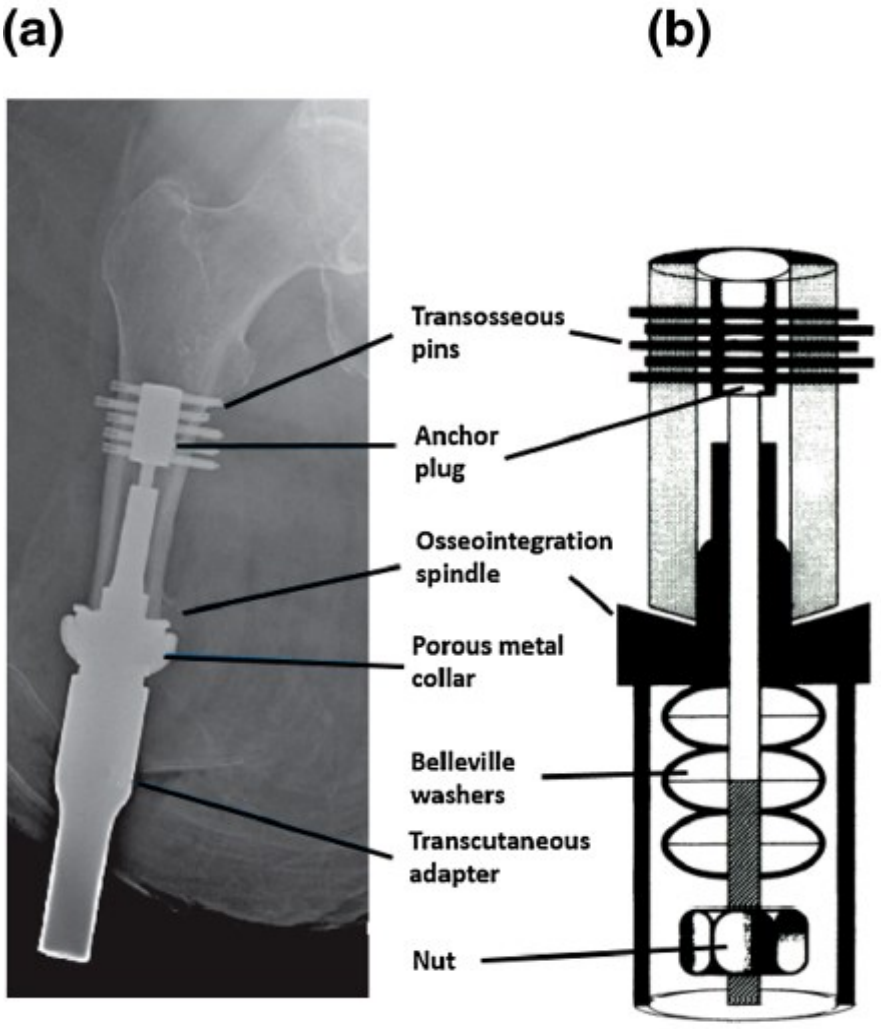

Figure 14 *(a) Compress percutaneous device radiograph; (b) Schematic diagram of the Compress endo-prosthetic implant* [56].

The POP system, designed for transfemoral application and developed at the University of Utah, is currently being evaluated as part of an initial FDA feasibility study involving 10 transfemoral amputees. The prosthesis involves an intramedullary bone region coupled to a subcutaneous collar to which the percutaneous post attaches. A ribbed region is encased in the intramedullary portion of the prosthesis, while a porous-coated region is present distally in the intramedullary implant to aid and promote osseointegration. Via a titanium adapter, the external prosthesis attaches to the percutaneous

post (Figure 15) [5],[56]. Reports show that a notable functional improvement can be obtained in transfemoral amputation patients.

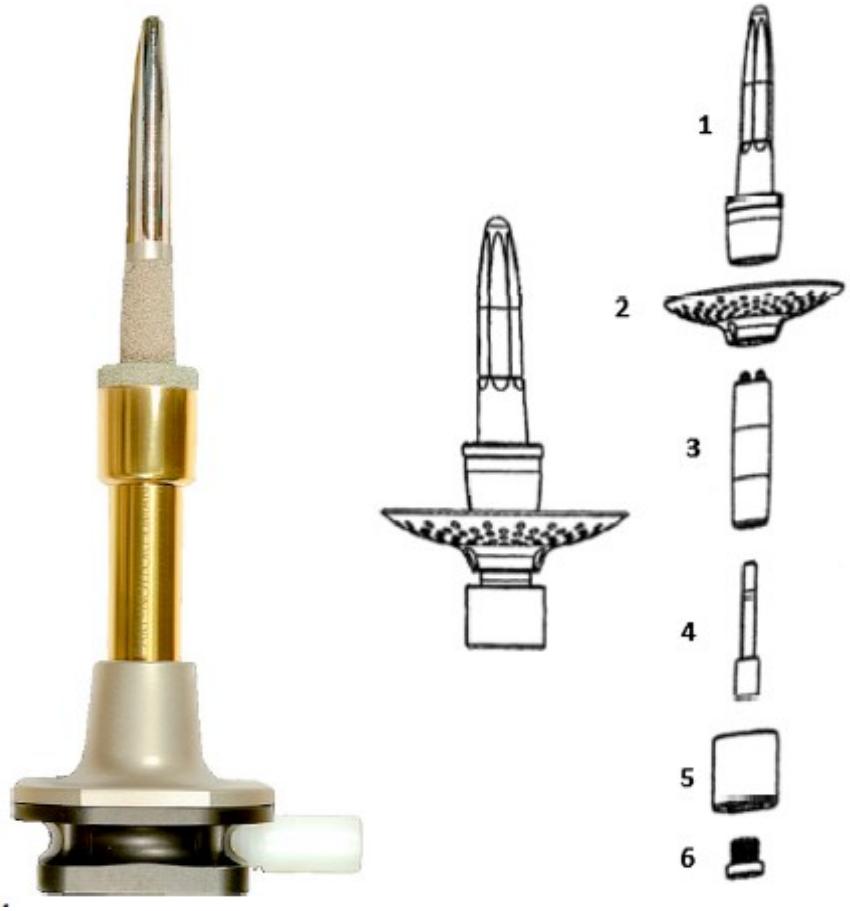

Figure 15 *The left figure shows a photograph of a POP, while the right figure shows POP implant system assembly for humans: (1) implant stem, (2) stoma shield, (3) percutaneous post, (4) assembly bolt, (5) adapter, (6) adapter bolt* [45],[56].

The ITAP implant system is under development in the United Kingdom, it is a single-component system made of the titanium alloys Ti-6Al-4V and is implanted in a single surgery. Longitudinal cutting flutes with the purpose of improving rotational stability are present in the proximal region of the intramedullary part of the ITAP. Soft tissue ingrowth and bone anchorage are promoted by means of the hydroxyapatite coating that covers the subdermal and distal regions of the implant intramedullary part. Since there are no publications available from the clinical study, it is unclear if the bone anchorage is obtained with or without bone cement (Figure 16). Furthermore, the ITAP system is characterized by a subdermal porous flange towards the distal end of the residual stump to serve as a platform for soft tissue ingrowth and skin attachment to minimize the relative movement at the percutaneous interface [56],[58].

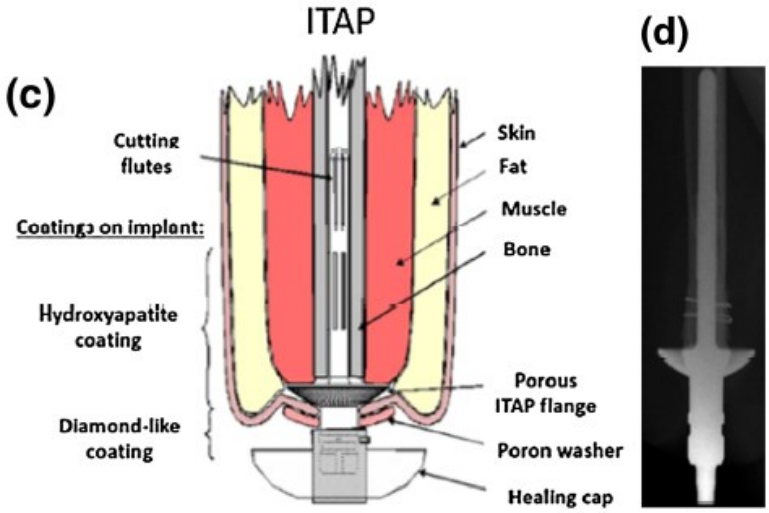

Figure 16 *(c) Schematic view of the ITAP implant; (d) Radiograph of ITAP implant in a trans-humeral amputee* [56].

Table 1 *Main features of osseointegrated devices.*

	OPRA	ILP	OPL	COMPRESS	POP	ITAP
Material	Titanium	Cobalt-chromium-molybdenum	Titanium	Titanium	Titanium	Titanium
Retention	Threaded	Press-fit	Press-fit	Cross-pin	Press-fit	Press-fit
Anatomic Suitability	Long bones, digits	Long bones	Long bones, pelvis	Humerus, femur	Femur	Humerus, femur
Skin-implant interface	Polished	Polished	Polished	Polished	Polished	Hydroxyapatite
Surgical stages	2	2	1	1	2	1
Months for implantation to full weight	3 to 18	2 to 3	2 to 3	Unspecified	Unspecified	Unspecified

1.7-Implant coating

Surface treatments are used to selectively modify the properties of biomaterials and therefore, to improve devices' multifunctionality, their tribological and mechanical properties. In this way, it is possible the enhancement of device performances that are often finalized in the achievement of better integration of the implant within the biological tissue [59]. The major problems with medical devices, specifically, orthopedic implants and prostheses are the lack of fixation and infection.

Once an orthopedic implant has been implanted, there is the occurrence of a competition between the tissue integration and the bacterial colonization to occupy the implant surface giving origin to a phenomenon called “race for the surface” [60]. As a consequence of infection, a local bone resorption results, leading to bone loss and implant loosening. Accordingly, treatment and prevention of infection are crucial to avoid tremendous damage to the bone. Coating the implant surface is the main countermeasure to lower the rate of implant infection and prevent implant loosening. Since the principle of the “race for the surface” determine that early tissue integration may also reduce the infection risk, a coating promoting tissue integration may also be regarded as an indirect method to reduce the number of infections [60]. In particular, the coating of the implant surface is an additive method, which means that other materials/agents of various thicknesses are superficially added to the surface of the core material [61]. There are different types of coating, in particular, referring to osseointegration we can discern:

- Osteoconductive coatings, drive bone formation to grow or attach to the surface of the coating (a passive coating) [60].
- Osteo-inductive coatings, induce the bone formation of undifferentiated cells in the surrounding tissue to ultimately promote osseointegration of bone to the coating (active coatings) [60].

Besides, several reports prove that the surface roughness of titanium implants also plays an impact on the rate of osseointegration and biomechanical fixation [62],[63]. Three are the levels of roughness that are significant, macro-, micro-, and nano-sized. The macro-level is directly related to implant geometry and several studies have highlighted a relationship between this kind of roughness profile, the early fixation, and long-term mechanical stability of the implant/prostheses with respect to the smooth implant surface. The micro-level of roughness has been seen as being able to maximize the interlocking between the mineralized bone and the surface of the implant. Surface roughness in this range resulted in greater bone-to-implant contact and higher resistance to torque removal than other types of surface topography, for this reason, it is mainly adopted in case of poor quality or volume of the host bone. The ideal surface roughness in micro-scale should present hemispherical pits 1.5 μm in depth and 4 μm in diameter. Roughness profiles in the nanometer range have a key role in the selective adsorption of proteins which leads to the adhesion of osteoblastic cells and thus the rate of osseointegration. However, the reproducibility of this kind of surface roughness is difficult with chemical treatments and the optimal surface roughness is unknown [62],[63].

Although are numerous methods have been developed to modify the surface of implants and prostheses in order to enhance their properties and to create a rough surface leading to better osseointegration, the most commonly used technique is the plasma spray. Because of its excellent deposition rate and compact coating formation when compared to other methods, the plasma spray technique is the only one that has been clinically approved [64].

1.7.1-Plasma spray technique

Plasma spray processes exploit the energy contained in a thermally ionized gas to melt partially and propel fine powder particles of metallic or non-metallic materials onto a surface so that they adhere and agglomerate to produce coatings [65]. Consequently, plasma coatings result from the agglomeration of splats formed by the impact, spread, and solidification of individual particles. The process may be at atmospheric pressure or under vacuum and the heat source for melting and accelerating the powders can be direct current plasma (DC-P) or radio frequency inductively coupled plasma (rf-ICP) (Figure 17) [66].

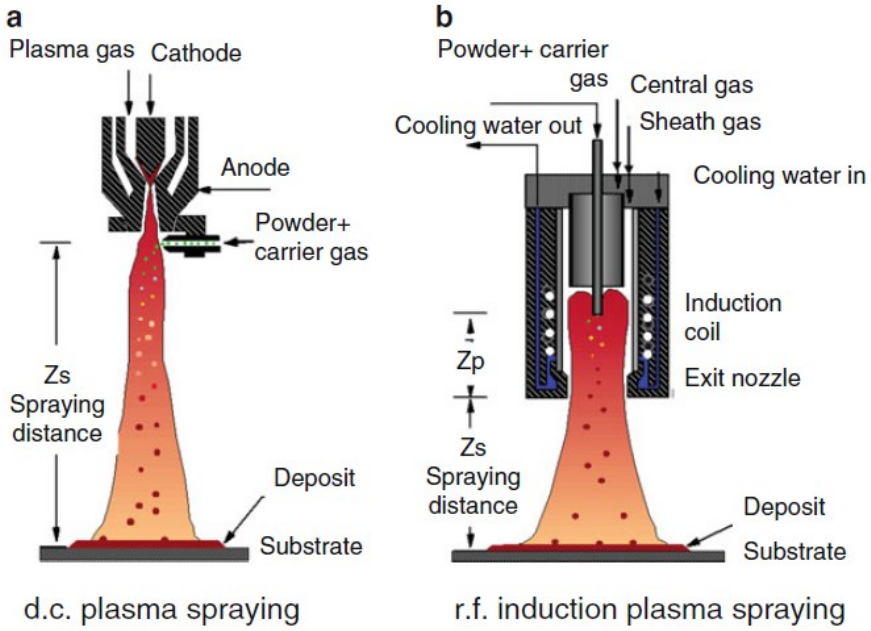

Figure 17 *(a) Schematic representations of d.c. plasma spraying techniques; (b) Schematic representations of r.f. induction plasma spraying techniques* [67].

Since the splat shape is dependent on several factors such as powder material properties, impact conditions, impact velocity, temperature, etc., to obtain a good quality coating the spray parameters must be selected carefully [66]. Several are the kinds of the plasma source, but the more common are the metallic, gaseous, and laser-based plasma sources [59]. The plasma spray torch is the device that produces and sustains a high-temperature confined region so that powder molecules injected into that region can be heated and accelerated onto a workpiece. The concentration of the power of an electric

arc in an extremely small volume allows the achievement of high temperature, while the appropriate design of the spraying nozzle provides acceleration [65].

The Plasma spray technique has become very popular in the past 30 years for its two principal advantages, complex geometry specimens can be suitably treated; the wide spectrum of materials that can be used with this technique has stimulated applications in the area of high-temperature, corrosion-resistant, and ablation resistant coatings as well as biocompatible films. On the other hand, an important drawback is poor adhesion between the substrate and coating, but numerous measures can be adopted to improve it. Often, moreover, the plasma spray process is performed on the outer coating surface to make it better not only in its performance but also from an aesthetic point of view [61].

Bioactive ceramics, such as hydroxyapatite, are widely used in the plasma spray process as interfacing osteoconductive layers in metallic surgical implants [59]. Despite plasma spray coating of Hydroxyapatite showing very good biocompatibility and osteo-conductivity, it has also some disadvantages (Figure 18). Specifically, it presents poor coating-substrate adherence (that makes necessary pre-treatment able to guarantee a minimum adhesion of coating) and dis-uniformity of the coating from two points of view: morphological and crystallinity [7].

Figure 18 *The left implant is a Plasma spray Ti and HA dual proximal coating stem; the right implant is a Plasma spray Ha coating stem at both proximal and distal portions* [68].

In general, the advantages of Plasma Spray coating are the higher deposition rate, the lower cost, and the bulk production, which allow its employment in the industry for orthopedic applications [69].

1.7.2-Hydroxyapatite and Titanium coating

In spite of great biocompatibility and mechanical properties, Ti-based implants do not effectively comply with osseointegration criteria involving efficient tissue and bone binding. The reason for this

is the poor active nature and low surface energy of the surface implant. An excellent solution has been found in the deposition of a thick layer of hydroxyapatite (HA) or Titanium (Ti) through plasma spray technique [61],[64].

Because of its compositional likeness to bone minerals, HA demonstrates excellent biocompatibility, making it widely employed as a lining material in load-bearing implants. Additionally, HA is distinguished by superior stability and a lower dissolution rate than other calcium phosphate materials [69]. The bond strength at the coating/plant interface can be increased by using a gradient HA layer that is able to reduce thermally induced stresses between HA and Ti6Al4V and decrease crack formation at the interface. HA coating doped with silver is able to improve osteo-conductivity and reduce bacterial infection; indeed, silver is effective against a wide range of bacterial infections and has been accepted for use in various medical devices for 20 years. Notably, the Ag contained in HA coatings, unlike other antimicrobial agents, provides long-term protection from infection and does not decompose during implant sterilization techniques [62],[69]. In comparison with uncoated implants, as reported in the study by Fouda et al, HA-coated titanium implant could extend the healing period [70]. On top of that, the study by Xie et al. found the improved promotion of cell proliferation by HA coatings [71]. This kind of coating makes biological fixation quicker because, following implantation of the coated titanium implant, a layer of biological apatite precipitates on the implant surface and serves as a matrix for osteogenic cell attachment and proliferation. Although loosening of the coated implants has been reported, especially about insertion in dense bone, HA-coated prostheses are still highly successful in orthopedics [62].

In the case of Titanium plasma spray coating, Ti particles are projected onto the implant surface resulting in a coating with an average roughness of about 7 μm which increases the surface area of the implant. Tensile strength is enhanced at the bone/implant interface thanks to the 3D topography produced by the plasma spray procedure [62]. Pre-clinical studies highlight a faster formation of bone/implant interface due to the minipigs present onto the Titanium Plasma Sprayed implant compared to the smooth surface implant presenting an average roughness of 0.2 μm [72]. One side effect found on this type of coating is the presence of metal wear in the bone adjacent to the TPS implants; as a matter of fact, metal particles released from the implants may be a cause of dissolution, fretting, and wear, and could be a source of concern for their potentially dangerous local and systemic carcinogenic effect. However, the local and systemic adverse effects have not been universally recognized. The histo-morphometric evaluation, which is present in the studies conducted by J.L. Ong et al, indicates a significantly higher bone-implant contact length for HA implants ($77.8 \pm 1.6\%$)

after 12 weeks of implantation with respect to TPS implants (58.6 ± 5.1%). However, TPS implants showed similar pull-out strength with respect to HA implants [73].

1.7.3-Chimera coating

Such coating process is employed for the coverage of screws, implants, and prostheses made of titanium and its alloys and it has the peculiarity to be based on decellularized bone tissue (autologous, homologous, or heterologous) containing native extracellular matrices. Despite several pros of titanium implants like high resistance to corrosion, low specific weight, sufficient durability, and excellent biocompatibility the greatest disadvantage of these materials result being their incapacity to establish a chemical bond with the bone tissue. In the long term, this drawback can provoke the implant loosening or the bone slipping leading to damage of the adjacent tissue to the area involved. For this reason, coating of the surface is continuously adopted and developed. However, the most used current techniques as plasma spray provide poor binding, are complex and expensive. Furthermore, it is not possible the use of organic materials such as bone tissue that would improve the osseointegration thanks to the presence of an extracellular matrix. Chimera coating is characterized by the activation of decellularized and de-antigenated mammalian bone tissue whose extracellular matrix is present in its native form, as it is not de-naturated by the process itself.

The process for coating the titanium implants and prostheses with the de-antigenated and decellularized entails the preparation of the bone tissue to obtain a powder that is suspended in an aqueous solution at 10-35% by volume of hydrogen peroxide, at a temperature ranging from 10 to 30 °C for a contact time ranging from 10 minutes to 4 hours, in a ratio of 1:1 by weight and characterized in that the titanium metal substrate is subsequently introduced into this solution for a maximum time of 5 minutes. Since in literature have been not found any documents reporting for the simultaneous presence of bone powder and the metal implant in the hydrogen peroxide aqueous solution. Probably, but without any scientific theory reference is this the crucial passage for the formation of the covalent bond, thus more durable, bonds that allow the titanium implant to consolidate to the suitably prepared bone tissue and therefore solve the issue cited above. The information regarding this coating procedure is set forth in the patent published by Tiss'you SRL Regenerative Company on the online platform "Patentscope" on 11.02.2021; the publication, corresponding to publication number WO/2021/024197, is entitled "Process for coating implants, plates, screws or prostheses made of titanium and its alloys with decellularized bone tissue (autologous, homologous or heterologous) containing native extracellular matrices".

1.8-Bone substitutes

Successful bone substitutions have been reported starting from the late 19th century and, nowadays, millions of procedures involving them are performed every year with the purpose of compensating the issue of bone loss [74],[75]. A bone substitute can be described as a synthetic, inorganic, or biologically compound which can be placed for the treatment of a bone defect instead of autogenous or allogenous bone [76]. Ideally, a bone substitute should present several characteristics, firstly biocompatibility, therefore no adverse effect has to be manifested. The other important properties are that it should be osteo-inductive, osteoconductive, resorbable, traceable in vivo (radiolucency), thermally nonconductive, sterilizable, readily available at a reasonable cost, easily molded into the bone defect within a short setting time [77].

Two main classes group the bone substitutes: bone substitutes derived from biologic products and synthetic bone substitutes [74]. The first category includes demineralized bone matrix (DBM), platelet-rich plasma (PRP), bone morphogenetic proteins (BMPs), hydroxyapatite (HA), coral, and bone grafts; instead, the second group consists of calcium sulfate, HA, calcium phosphate cement, beta-tri-calcium phosphate ceramics, biphasic calcium phosphates, bioactive glasses, poly-methyl-methacrylate (PMMA) and polymer-based bone substitutes [74],[78]. However, PRP and BMPs are always used in combination with other substances and not as a stand-alone substitute.

The applications of bone substitutes are numerous and are summarized in the table below (Table 2) [74].

Table 2 *Bone Substitutes applications.*

Spine fusion	It is mainly promoted by the use of autograft and allograft, despite other materials seems to fit this specific use (DBM, calcium sulphate HA, TCP) but there is not enough evidence.
Open wedge tibial osteotomy (OWTO)	The optimal biocompatibility, resorption characteristics, and bone conduction properties of Beta tricalcium phosphate ceramics are exploited for this kind of application.
Contained bone defects (benign tumors and cysts)	A wide range of substitutes has already been clinically used and validated in a specific area since this kind of defect can occur in many types. Calcium sulphate, DBM-based allografts and beta-tricalcium phosphate have obtained the better results in their specific area.
Hand enchondroma and metacarpal fractures	Beta-TCP ceramics appear suitable in this case, good functional and radiological outcomes compared with autologous bone. Also, a combination of calcium sulphate and HA (60% - 40%) provides good results as well in terms of limited complications.
Long bone fracture	Calcium phosphate cement provide similar and better mechanical support than autogenous iliac bone graft while Beta-TCP ceramics have been used as well for many decades.

Fracture non-union	The common bone substitute which is used is DBM thanks to the good result in terms of consolidation (up to 80% success) with decrement in the adverse effects. Calcium sulphate demonstrates a healing rate of 88% and is another substitute suitable in this condition.
Periodontal defects	Granules of beta-TCP and HA ceramics can be employed with relevant pocket depth reduction and clinical attachment gain. Good clinical indications have been provided also by bio-glasses.
Sinus augmentation	Significant outcomes are given by the use of DBM as injectable formulation or powder form showing no differences regarding dental implant stability and survival rate in a long term follow up. Furthermore, suitable results have been shown by a compound of beta-TPC with autologous bone.
Osteonecrosis of the jaw	An enhanced wound healing and consequently, an effective treatment is reported in some studies involving PRP.
Bone infections	Beta-TCP granules, porous HA blocks, CPC, calcium sulphate pellets and bio-glasses have been used with this purpose but clinical data in well controlled trials are very limited, for this reason the gold standard is the employment of antibiotic-loaded PMMA granules.
Cranioplasty	HA, CPC and DBM are safely used for this purpose, even if PMMA is the most extensively material used although there is no consensus on which material is better.
Vertebroplasty/Kyphoplasty	Good clinical results have been reported with PMMA but also CPCs show relevant characteristics for their use as fillers in this application.

1.8.1-Natural bone Substitutes

Nowadays, the autograft is still considered the "gold standard" in terms of bone substitution; it consists in the harvesting of osseous tissue from an anatomic site and transplantation to another anatomic site of the same subject [76],[78],[79]. The tissue for the transplantation is available in different forms such as cortical bone, cancellous bone, and bone chips depending on the requirements posed against the transplant [76]. Osteo-conductivity, osteo-inductivity, and the presence of growth factors without immune or infectious factors are the most important properties for bone formation that characterize autografts. The drawbacks of autologous grafts are related to inherent morbidity: post-operative pain and complications due to the requirement of a surgical donor site, a probability of blood loss or infection, hematomas, fracture, neurovascular injury, along with cosmetic deformity, at the explant site and longer operative time. In addition, a relevant limit of this type of graft is the availability of bone in a patient, especially in pediatric and elderly patients [75].

Allografts are considered a valid alternative to autografts, in this case, the bone tissue is gathered from one individual, dead or alive, and transplanted to a genetically different individual of the same species [75],[78],[79]. These kinds of grafts have been employed effectively in many clinical

circumstances, particularly for those patients with established non-union, poor healing potential, and extensive comminution after fractures [78]. Allogenous bone grafts can be processed and personalized, therefore it is available in different forms (Cortical and cancellous bone) that must be conserved in bone tissue bank [75]. The major advantage consists in the virtually unlimited availability of the material while the disadvantages, in the comparison with autogenous bone, refer, basically, to three points. First of all, the danger to generate an immunological reaction with the receiver, then a biological reduction, or a decrement of the material osteo-genetic power, and eventually, the danger of infection due to transplant of foreign material [76]. Other limits are the costs, the laborious procedures, and the mechanical resistance of such bone substitutes [75].

Xenogenous (or heterologous) bone graft, consists of the harvesting of bone tissue from a subject and the transplantation to another subject of different species [79]. Typically, bovine, or porcine bone is used, it can be frozen, dried, demineralized, and deproteinized; usually, xenogenous bone grafts are only distributed as a calcified matrix. They are considered an optimal possibility since they present similarities to human bone in structural and morphological properties [80]. This kind of graft presents different advantages, osteo-conductivity, good mechanical properties, easy availability, and low costs (Figure 19) [75]. Good results are obtained in dentistry while scarce validation is registered in orthopedics.

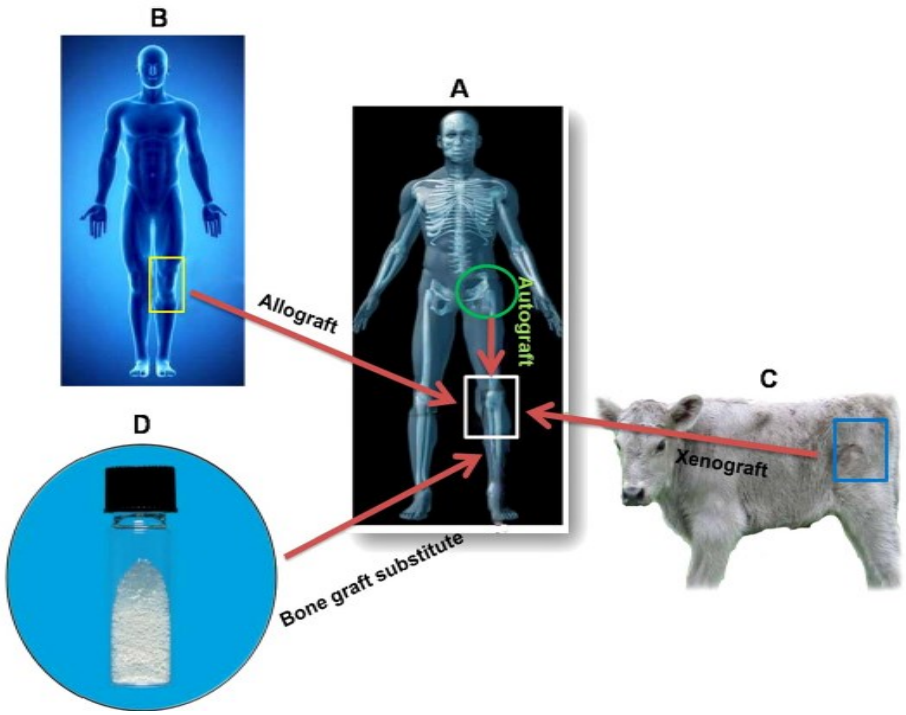

Figure 19 *(A) Autograft, (B, C) Allograft and xenograft, (D) Synthetic bone graft substitute* [81].

Demineralized bone matrix is a type of highly processed allograft derivative that is treated with mild acid, so that the mineral component is removed while the organic matrix and the growth factors are

maintained (insulin growth factor, fibroblast growth factor, transforming growth factor, and bone morphogenetic protein)[74],[78]. All these factors are able to stimulate the activity of the osteogenic cell, resulting in a good osteo-conductivity and osteo-inductivity thanks also, to the presence of a collagen structure [75]. DBM does not have great mechanical strength, so it is used exclusively for replenishing purposes and is used in combination with other substances as a bone substitute [74],[75].

1.8.2-Synthetic bone substitutes

Hydroxyapatite (HA) is one of the families of the apatite, in particular, it is a calcium apatite with formula $Ca_{10}[PO_4]_6[OH]_2$. This substance is featured by hexagonal crystal lattice and is the primary mineral component of teeth and bones [74],[78]. This kind of substance is characterized by high biocompatibility that prevents inflammatory response [82]. In addition, HA demonstrates excellent osteoconductive and osseointegration abilities [78]. It is possible to have HA both in natural and synthetic forms, but usually, a combination of HA and Tricalcium Phosphate ceramics is preferred to HA alone [74]. Often HA alone is employed as a coating on implants or in sites with low mechanical stress [78].

Beta-tricalcium phosphate ($Ca_3(PO_4)_2$) is a bioresorbable and biocompatible material that due to its porosity and composition shows also a good osteo-conductivity [74],[83]. Similarly, as can be seen for Hydroxyapatite, also beta TCP present poor mechanical properties due to interconnected porous structures that, on the other hand, may provide gain in terms of fibrovascular invasion and bone replacement [78]. Beta-TCP is resorbed after 6-24 months, and this makes it useful for filling bone defects caused by benign tumors and trauma [78],[84]. The combination of beta-TCP and HA produces a substance showing a faster resorption rate compared to HA, and better mechanical properties than beta-TCP alone [74].

Calcium sulfate (CS) is a synthetic ceramic composed of $CaSO_4$, it presents a structure similar to bone and it has many advantages; indeed, CS is inexpensive, osteoconductive, biodegradable, and available in different forms [74],[78]. Since 1892 it is used in filling void defects, it has weak internal strength, consequently, it may only be used as a small bone defects filler [78]. CS does not initiate allergic reactions; its crystalline structure gives osteo-conductivity that allows bone capillary invasion [74],[85]. Quick resorption of CS (1-3 months) produces porosity while encouraging bone regrowth [86].

Bio-glasses are synthetic silicate-based ceramics resulting from the combination of silicon dioxide, sodium oxide, calcium oxide, phosphorus pentoxide, potassium oxide, magnesium oxide, and boric

oxide. Silicate is the key component that constitutes 45-52% of the bio-glass weight, whose overall constitution is stable and provides a strong physical bonding with the host bone [78]. The use of this ceramic does not provoke an inflammatory response; indeed, it has good biocompatibility, it presents osteo-conductivity whereas the porous structure allows complete resorption in 6 months and promotes bone ingrowth [74],[87]. Bio-glasses are primarily employed in the reconstruction of facial defects in combination with growth factors. Two are the most recognized commercially available bio-glasses used as bone graft substitutes in the market: bio-glass 45S5 and bio-glass S53P4 [78].

1.8.3-Deproteinization of xenografts

The main limitations of autogenous bone grafts have been overcome by xenogenous bone grafts. However, the dangers in case of such bone grafts are of inducing an immune response and transmitting infectious diseases in patients [88]. Therefore, eliminating the antigenicity of xenograft bones is a significant prerequisite for the good result of the graft. Several studies have demonstrated that bones lacking proteins not only lose their immune reactivity but also retain their osteo-induction and osteo-conduction properties [89],[90]. Of the various current chemical and physical methods used to deproteinize bovine bone scaffolds, a strong oxidizer such as sodium hypochlorite and hydrogen peroxide represent the most popular methods [90],[91]. Researchers report that the best deproteinization effects may be achieved by using chemical deproteinization procedures of bovine cancellous bone specimens consisting in their treatment with 2.6 wt% NaOCl solutions and 7% wt H_2O_2 solution. In particular, such processes have demonstrated 90% of bone proteins were removed from the specimens [92]. The bovine bone tissue undergoes pre-treatment before the deproteinization consisting of cut and de-hydration. The process protocols involve the immersion of the bone tissue pieces in 2.6 wt% sodium hypochlorite (NaOCl; 14 days), 7 wt% hydrogen peroxides (H_2O_2; 14 days). Solvents are refreshed daily. Specimens are constantly mixed using a rocking platform, and the temperature is kept constant at 37°C using a water bath. After that, the bone specimens are dried in an oven at 60°C overnight [92]. Despite chemical deproteinization processes requiring a longer time with respect to thermal processes, they provide biomaterials with better mechano-structural properties and that are more suitable for bone tissue replacement [92].

1.8.4-Heterologous equine tissue

In the current thesis, the heterologous material used is of equine origin. This material is subjected to a treatment called "decellularization" which aims to break and eliminate cells and cell residues of the

extracellular matrix (ECM) preserving the three-dimensional structure and biochemical/biomechanical properties of the latter, in order to produce biological scaffolding that is compatible with the human immune system and can therefore be used in regenerative medicine. The most frequently used agents in these processes are chemical and physical. Using different reagents, temperatures, pressures, and/or mechanical forces in parallel and/or sequence, decellularization processes vary considerably from a practical point of view. In particular, a chemical process involving primary R-OH alcohol (in which R is a C1-C4 linear alkyl group), alkaline or alkaline earth-metal hydroxide and a water scavenger agent has been identified as a method to transform, quickly and at low cost, the lipids present in the tissues in appropriate derivatives esters of the fatty acids composing the lipids. These derivatives can be easily removed by washing or evaporation. Once these reagents have been combined, the solution is added to the tissue and the reaction can take place under certain physical conditions: a temperature ranging from 40° to 60°C, a pH between 8.0 and 10.0, and at a pressure ranging from 50 to 150 mbar. The reaction is considered finished when the total lipid concentration is less than 0.05% of the total tissue weight (dry). Finally, to eliminate the water from the product, the tissue is freeze-dried.

Employing the process, it is possible to eliminate the free lipids, phospholipids of the cell membranes, and lipoproteins bringing them to a solution or gaseous phase, given their volatility, leaving the proteins in their native structure (quaternary structure) and the polysaccharides intact. The differences of this process with respect to those currently in use are the following:

1. it exploits a reaction able to transform some tissue components into reaction products that can be easily eliminated, without damaging the proteins and the polysaccharides of the ECM;
2. it can be applied on all connective tissues (including musculoskeletal tissues, derma, and peritoneum);
3. it is the fastest method compared to the technologies currently in use;
4. it is an economically advantageous method compared to the processes commonly used today.

For the experiments conducted in this thesis, the process was carried out on horse bone. The final product, in this case, maintains the mineral composition and ECM proteins compared to the non-treated product, while cell proteins are completely absent. The information regarding this procedure is reported in the patent published by Tiss'you SRL Regenerative Company on the online platform "Patentscope" on 26/03/2020; the publication, corresponding to the publication number WO/2020/058813, is entitled "Process for the treatment of connective tissues of a mammal".

1.9-Analytic technique

1.9.1-IR Spectroscopy

Spectroscopy is the field of study that seeks to define what specific energies and amounts of incident light are absorbed by specific substances, and what specific energies and amounts are subsequently re-emitted. The spectrometers are the optical instruments that reveal the light energies absorbed and emitted by producing as a result, spectra, a series of specific wavelengths or frequencies. Such spectra give important information relating to the atomic and molecular structure of the substances on which the electromagnetic energy is focused; hence, the "fingerprints" are uniquely linked to different compounds [93].

One of the most common spectroscopic techniques is the Infrared (IR) spectroscopy (the 1940s) which is an important analytical method at disposal of today's chemists [94],[95]. It is a method, that relied on the atom vibrations of a molecule, whose spectrum is obtained by firing infrared radiation through a sample and by determining what portion of the incident radiation is absorbed in particular energy. Any peak appearing in the absorption spectrum is characterized by energy that corresponds to the frequency of vibration of a part of a sample molecule [96]. This analysis aims to define the chemical functional groups in the sample [94]. A specific aspect must be the owner of a molecule to show absorption at IR-radiation, namely an electric dipole moment of the molecule must change during the vibration [95],[96]. Vibrations entail variations either in bond length (stretching) or bond angle (bending) in molecular dipoles. Incoming infrared radiation can be absorbed by a molecule only if its frequency is equal to one of the fundamental modes of vibration of the molecule. This signifies that the vibrational motion of a small portion of the molecule is enhanced while the rest of the molecule is left unaffected. Furthermore, the larger the change in the dipole moment of the molecule the more intense will be the absorption band [95]. Generally, the total number of observed absorption bands differs from the total number of fundamental vibrations, in particular, it is lower due to the fact that some vibration modes are not IR active, and more than one motion mode can be provoked by a single tone. On the other hand, the appearance of integral multiples of the fundamental absorption frequencies, combinations of fundamental frequencies, coupling interactions of two fundamental absorption frequencies, and coupling interactions between fundamental vibrations generate additional bands with intensities lower than those of the fundamental bands. However, a unique IR spectrum for each compound is produced by the combination of all the previous factors [94].

Thereby, IR absorption information is given in the form of a spectrum in which the wavelength is assigned to the x-axis and the absorption intensity or percent transmittance is assigned to the y-axis. The transmittance, T, is defined as the ratio of radiant power transmitted by the specimen (I) to the

radiant power incident on the specimen (I_0). The base-10 logarithm of the reciprocal of the transmittance on the other hand defines the absorbance (A).

$$A = \log_{10}\left(\frac{1}{T}\right) = -\log_{10} T = -\log_{10}\frac{I}{I_0}$$

Since the Transmittance range is [0-100%], its spectra give better contrast between strong and weak bands intensities [94].

The Infrared spectral region ranges from 0.78 μm to about 1000 μm, specifically is possible to distinguish the near-infrared region from 780 nm to 2.5 μm, the mid-infrared region from 2.5 μm to 50 μm and the far-infrared region from 50 μm to 1000 μm. IR spectroscopy is a common methodology to investigate the structure of small molecules on account of its sensitivity to the chemical composition and architecture of molecules [96]. A key advantage of this technique is associated with the fact that it can be employed to virtually study any sample in any state with a reasonable choice of sampling technique [95]. Additionally, other advantages of infrared spectroscopy are a high time resolution (down to 1 μs with moderate effort), the low amount of sample required (typically 10–100 μg), a short measuring time, and the relatively low costs [97]. There are also some drawbacks: several materials do not have measurable mid-IR spectra; the more complex is the composition of the specimen, the more complex will be its spectrum and so the determination of what peaks belong to what substance; liquid water presents intense peaks that may mask the spectra of solutes dissolved in it [98].

At present, commercially available infrared spectrometers are principally Dispersive spectrometers and Fourier transform spectrometers. In particular, the latter devices are able to examine simultaneously all the frequencies and may be applied in many areas that cannot be analyzed by dispersive spectrometers, for this reason, FT-IR spectrometry has recently taken the place of Dispersive IR spectrometers [94].

1.9.2-FT-IR Spectroscopy

The modern Infrared Spectrometers are the Fourier Transform IR spectrometers whose name is due to the fact that the measured spectrum and the detector signal are related by a well-established mathematical procedure, the Fourier transformation. Such devices rely on the idea of radiation interference between two beams to produce an interferogram, which is a signal obtained as a function of the path length variation between the two beams; indeed, the key element of the FT-IR spectrometer is the Michelson interferometer (Figure 20) [96],[97].

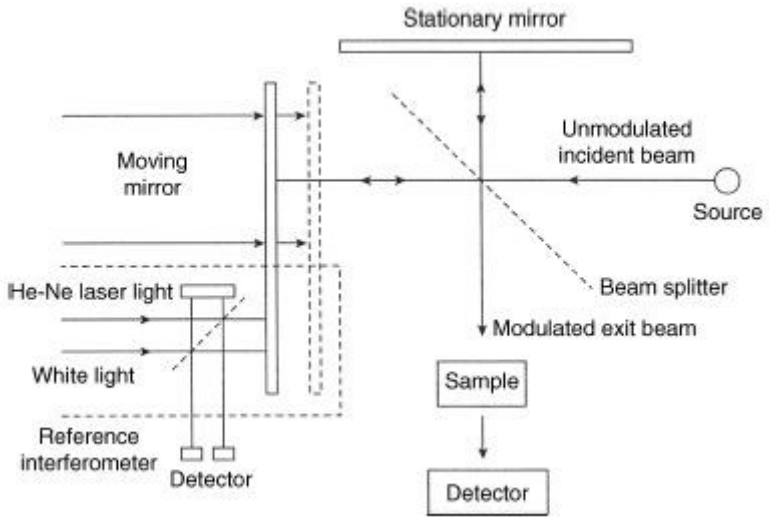

Figure 20 *Schematic representation of Michelson interferometer* [96].

Three are the basic components in an FT-IR system: radiation source, interferometer, and detector. Better power and stability are achieved by water-cooling the source in FT-IR instruments. In this type of device, the interferometer takes the role of the monochromator; it splits the radiating beams, produces an optical path difference between the beams, and then merges them again to produce repetitive interference signals measured as a function of the optical path difference by a detector. The Michelson interferometer has three active components: a moving mirror, a fixed-mirror, and a beam-splitter. The former are perpendicular to each other, the latter is a semi-reflective device that is often accomplished by the deposition of a thin film of germanium on a flat substrate of KBr [94].

Starting from the IR source, the radiations are collimated and directed on the interferometer, and they impact on the beam-splitter. Once arrived on the beam-splitter, half of the IR beam is directed to the fixed mirror while the other half is reflected in the moving mirror. The variations in the relative position of the moving mirror with respect to the fixed one produce an interference pattern. Then such a resulting beam crosses the sample and is eventually focused on the detector. For a good understanding, a single frequency component of the IR source can be considered. In this situation, where the position of the moving mirror is called the point of zero path difference (ZPD), if the two interferometer arms have the same length the two split beams are completely in phase with each other. Therefore, constructive interference occurs leading to a maximum detector response. Instead, the optical path (beam-splitter–mirror–beam-splitter), when the moving mirror is moved in either direction by the distance l/4, is variated by 2 (l/4), or l/2. In this case, the two split beams are out of phase of 180° with each other, and hence the interference is destructive. Displacing the moving mirror another l/4, the optical path difference changes again becoming 2 (l/2), or l, and results in another constructive interference [94]. The radiation intensity reaching the detector evolves in a sinusoidal

fashion if the mirror is moved at a constant velocity resulting in registration of the interference signal (interferogram) as output. The spectrum is in the time domain and collects the detector response variations versus time within the mirror scan. A more complex interferogram is obtained if the same process is extended to three-component frequencies; it is the sum of three individual modulated waves. Such interferogram shows extensive interference pattern and is a complex summation of superimposed sinusoidal waves, each wave correlating to a single frequency. When the Infrared beam with this feature is fired across the sample, the amplitudes of a set of waves are decreased by absorption if the frequency of this set of waves is equal to one of the characteristic frequencies of the sample. The information contained in the interferogram is related to the entire IR region to which the detector is responsive. At this point, a mathematical operation, the Fourier transformation, converts the interferogram in the time domain to the final IR spectrum being the frequency domain spectrum displaying intensity against frequency [94].

The fundamental equations for a Fourier-transformation associating the intensity falling on the detector, I(δ), to the spectral power density at a specific wavenumber, $\bar{\upsilon}$, provided by B($\bar{\upsilon}$) are the following:

$$I(\delta) = \int_0^{+\infty} B(\bar{\upsilon}) \cos(2\pi\bar{\upsilon}\delta)\, d\bar{\upsilon}$$

which is one half of a cosine Fourier Transform pair, the other being

$$B(\bar{\upsilon}) = \int_{-\infty}^{+\infty} I(\bar{\delta}) \cos(2\pi\bar{\upsilon}\delta)\, d\delta$$

Such equations are interconvertible and are known as a Fourier transform pair. The former illustrates the change in power density as a function of the difference in path length which is an interference pattern. The latter, instead, illustrates the change in intensity as a function of wavenumber [96]. During the mirror scan, small and precise intervals are used to sample the detector signal while the sampling rate is managed by an internal, independent reference, a Helium-Neon laser-focused on a separate detector.

The deuterated triglycine sulfate (DTGS) and mercury cadmium telluride (MCT) are the most common detector for FT-IR spectrometers in the mid-infrared region. Since it measures the variations in temperature rather than the value of temperature, DTGS, which is a pyroelectric detector, provides quick responses and is employed usually in routine experiments. For more sensitive work, instead, MCT detectors are employed, they show faster responses, and they are photon detectors. For what concern near-infrared region and far-infrared region, detectors employed are sulfide photoconductors and germanium or indium-antimony detectors, respectively [94],[96]. In the same manner, different kinds of sources are used in FT-IR spectrometers depending on the infrared region, for the near-

infrared region are tungsten–halogen lamps, for the mid-infrared region are silicon carbide or oxide mixture and for the far-infrared region are high-pressure mercury lamp [96]. Several advantageous features characterize FT-IR spectrometers, first of all, the high data collection rate, and the ability to achieve improved signal-to-noise ratio via signal averaging, leading to an enhancement of the signal-to-noise ratio proportional to the square root of time. Furthermore, it presents a precise wavenumber measurement that indicates good reproducibility of the device, good sensitivity, and simple mechanical design [96],[97],[98]. Nevertheless, there is also a relevant drawback which is due to artifacts that can be occurred in the procedure because of the presence of gas in the sample [98].

So, FT-IR spectroscopy is a fast, non-destructive, and sensitive physical technique for the analysis of organic compounds with minimum sample preparation. An interesting aspect is the association of FT-IR spectroscopy with "green analytical chemistry" due to the fact that such a technique reduces the use of chemical reagents hazardous to human health and the environment [99].

2-MATERIALS AND METHODS

All the tests reported below have been performed in the laboratories of Tiss'you SRL Regenerative Company, operating in the field of regenerative medicine. The company is located in Domagnano a fraction of the Republic of San Marino and, specifically, deals with the development and production of biomaterials and medical devices to improve the natural ability of human tissues to regenerate.

The horse bone powder employed to coat titanium implants is used in two versions. The first version is the one resulting from the de-cellularization process in which are still present ECM proteins that give the powder a yellowish color (Matrix); the second version, instead, is subjected to a calcination process (Hydroxyapatite) (Figure 21). This process consists of the heating of a substance at a temperature that is often very elevated with the aim of eliminating volatile substances, impurities, and other substances such as carbonates [100]. The granules still impregnated with hydrogen peroxide are loaded into the calcination cell which is then inserted into the Nabertherm calciner (Figure 22). The calcination process starts by starting the P01 program. It is divided into 3 steps: the first 15 minutes the temperature arrives at 100°C followed by an hour at 400°C and 24 hours at 580°C respectively. Specifically, between 300°C and 400°C respectively the product undergoes oxidation while between 400°C and 580°C the product is calcified. At the end of the process, a de-organic white powder is obtained, highly pure calcium hydroxyapatite.

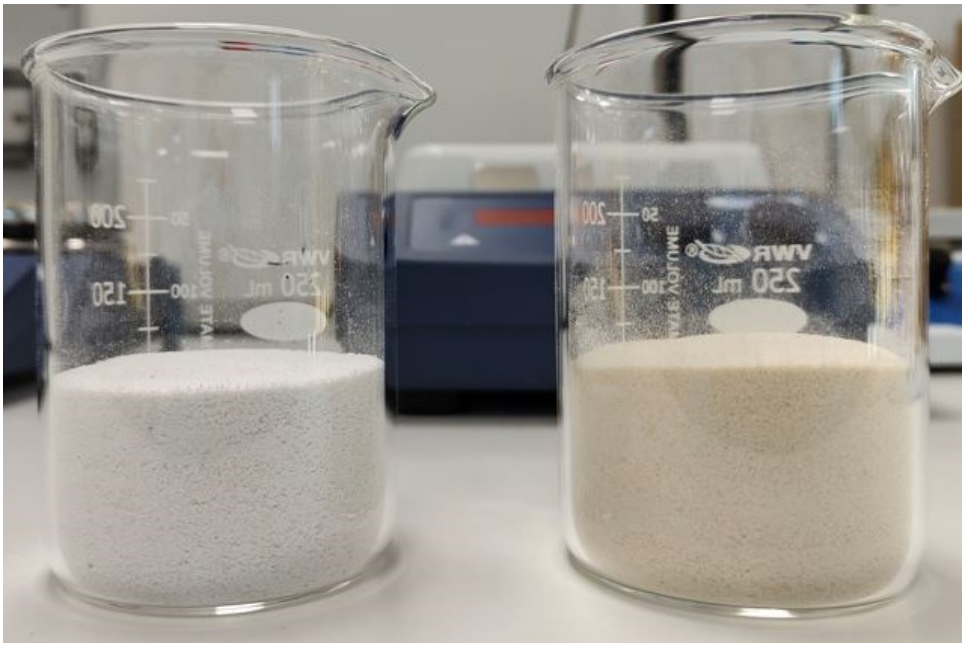

Figure 21 *The beaker on the right contains decellularized non-calcinated bone powder (Matrix) while the beaker on the left contains calcined bone powder (Hydroxyapatite).*

Figure 22 *Nabertherm calciner loaded with the cell of calcination filled with decellularized bone powder.*

2.1-Reagents and devices

For the experiments conducted, the reagents that have been used (Figure 23-24) are the following:

- Calcium Hydroxyapatite powder (calcined powder - particle size ≤ 0,5 μm);
- Matrix powder (non-calcinated powder - particle size ≤ 0,5 μm);
- "Acros Organics" Hydrogen peroxide (H_2O_2 - 35 wt% - code:202460010);
- "Titolchimica spa" ammonium hydroxide (NH_4OH - 24% - code: TC2002755);
- "Valentis srl" sodium hydroxide (NaOH - code: 34130152);
- "Honeywell Riedel-de Haën" Acetonitrile (C_2H_3N- code: 10193144);
- Deionized water;
- Grade 6 titanium bars (Zapp precision metals GmbH);
- Grade 4 titanium screws (Clover Orthopedics SRL);

Figure 23 *Solvents used in various tests.*

Figure 24 *Grade 6 titanium bar (on top), Grade 4 titanium screw (on bottom).*

The devices that have been employed (Figure 25-26-27-28), instead, are:

- "Ohaus" Scout™ STX1202;
- "Ohaus" Adventurer™ Analytical AX124;
- "ARGO LAB" M3-D Magnetic stirrer with ceramic heating plate;
- "DK SONIC" Ultrasonic cleaner DK-80;
- "ELGA Veolia" PURELAB® Flex 3 water dispenser and deionization system;
- "memmert" stove UF series;
- "Carl ZEISS microscopy GmbH" ZEISS Stemi 508 and Axiocam ERc 5s;

Figure 25 *Scout™ STX1202 (left); Adventurer™ Analytical AX124 (right).*

Figure 26 *M3-D Magnetic stirrer with ceramic heating plate (left); Ultrasonic cleaner DK-80 (right).*

Figure 27 *PURELAB® Flex 3 water dispenser and deionization system (left); stove UF series (right).*

Figure 28 *ZEISS Stemi 508 (left) and Axiocam ERc 5s (right).*

2.2-Proceedings

All tests were repeated three times. First, the titanium implants are dipped in Acetonitrile, in a 100 ml beaker, and subjected to an ultrasonic bath, by using DK-80, for 3 minutes so that all surface impurities are removed (Figure 29).

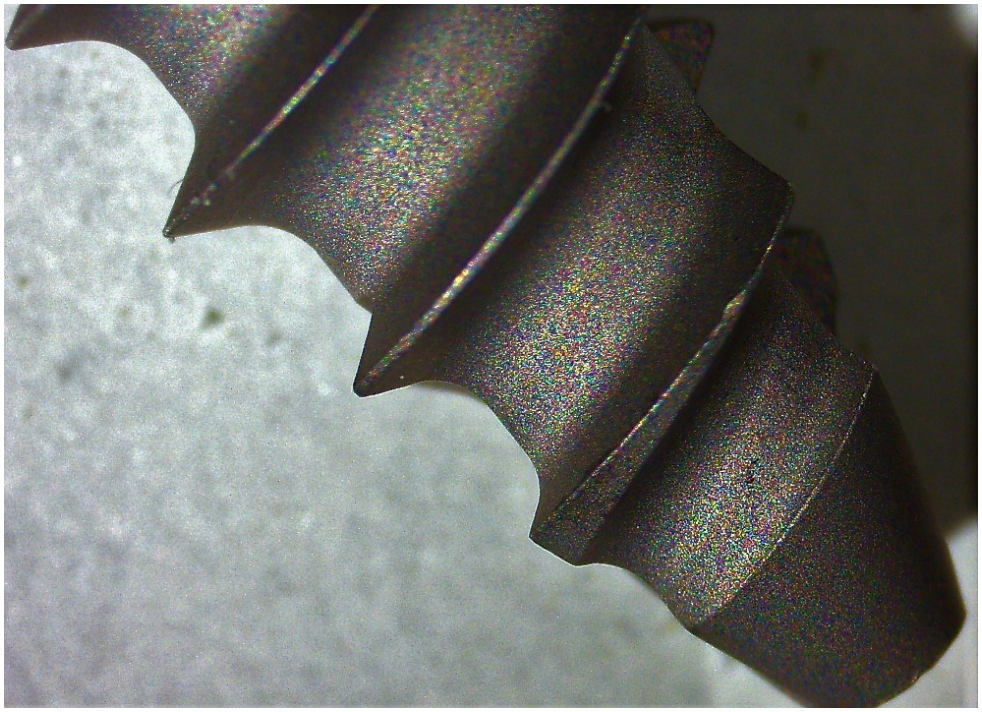

Figure 29 *Surface of a non-treated screw after ultrasonic bath.*

In the tests conducted, solute and solvent were combined in specific proportions and the compound is heated by a thermal plate at a given temperature. The reagents were weighed using the Ohaus STX1202 and AX124 scales, while the compounds were heated using the ARGO LAB M3-D thermal plate. Once the desired temperature is reached, the implant tip is inserted into the compound and left in soaking for a preset time interval keeping the temperature constant. Alternatively, the system was sprinkled with compound, wrapped in aluminum, and heated in direct contact with the thermal plate. Once coated by the process to which they have been subjected and cooled, the implants are washed in deionized water, so as to eliminate excess material, and left to dry at room temperature or by the stove at a temperature of 35 °C. The deionized water was distilled using the PURELAB® flex 3 system and for drying, instead, it was used the UF series memmert stove. Finally, when the surface of the implant is completely dry, it can be inspected under the ZEISS Stemi 508 microscope and photographed using the Axiocam ERc 5s integrated into the microscope. The most promising samples were subjected to IR analysis using PerkinElmer's Spectrum Two spectrometers (Figure 30).

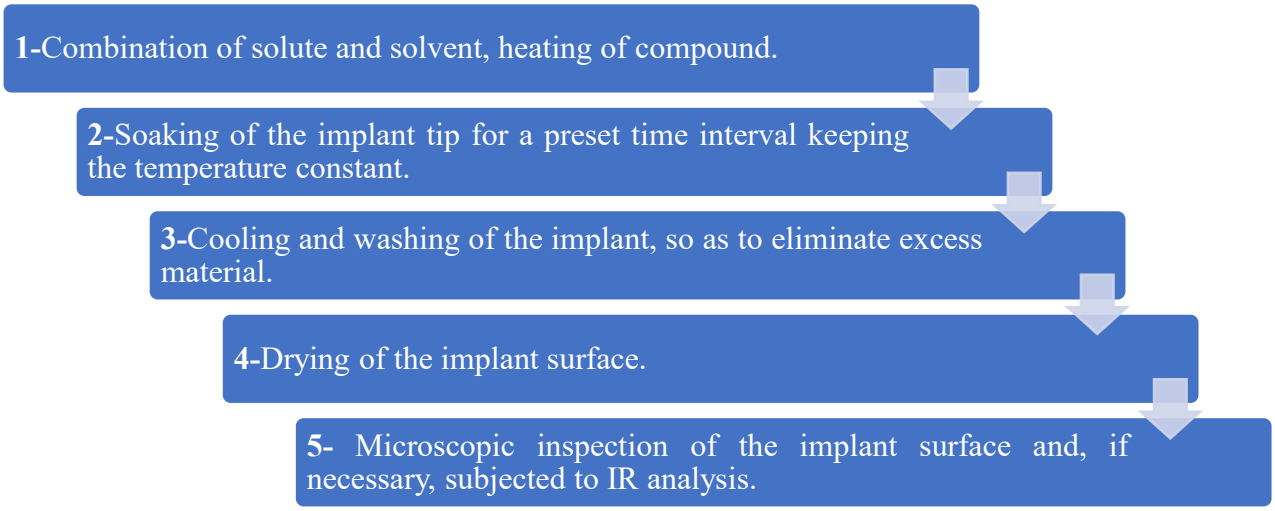

Figure 30 *Schematic representation of passages common to all tests.*

2.3-Tests on bars

The first part of the tests was carried out on cylindrical titanium grade 6 bars about 5 cm long, diameter 0.5 mm, and smooth surface without grooves. For the first set of tests, 1,5 g of bone powder and 1,5 ml of hydrogen peroxide are mixed in a 50 ml beaker at a ratio of 1:1. Two compounds are obtained: a mixture of calcined bone powder and H_2O_2, a mixture of non-calcinated bone powder, and H_2O_2. The bar is soaked for one end in the compound and three tests were carried out for each compound, varying only the temperature by heating to 60° C, 80° C, and 100° C, for a total of 6 tests: B664h, B548m, B079h, B217m, B976h, B435m. The most important conditions are summarized in tables. In the sample code, the letter "m" indicates that the powder used is Matrix, while the letter "h" indicates that the powder used is Hydroxyapatite.

For the second set of tests, a compound shall be used by mixing, in a 50 ml beaker and in a 1:1 ratio, 3 g of bone powder with 3 ml of the solvent containing: 95 % of hydrogen peroxide corresponding to 2,85 ml; 5% of ammonium hydroxide corresponding to 0,15 ml. The compound was made in two versions, in one case the bone powder is calcined, in the other, the bone powder is not calcined. The tests were carried out by varying only the temperature, heating to 60° C, 80° C and 100° C. In addition, another test was carried out at the temperature of 60° C in which the compound consists of 1.5 g of solute and 1.5 ml of solvent (H_2O_2 + NH_4OH). Unlike the previous test at the same temperature, in this case, the drying phase after soaking in the compound is performed on a stove at a temperature of 70° C. In total, the tests were eight: B219h, B066m, B001h, B696m, B167h, B013m, B134h, B653m. Some of these tests were also repeated in subsequent tests on screws (Table 3).

Table 3 *Main details of bar tests.*

Set of tests	***Powder***	***Solute-solvent ratio***	***Solute-solvent amount***	***Treatment temperature (°C)***	***Time of treatment (minutes)***	***Sample code***
1°	Hydroxyapatite	1:1	1,5 g +1,5 ml	60	5	B664h, B548m
				80		B079h, B217m
	Matrix			100		B976h, B435m
2°	Hydroxyapatite		3g + 3ml (2,85ml + 0,15ml)	60		B291h, B066m
				80		B001h, B696m
	Matrix			100		B167h, B013m
				60 + 70 (in stove)		B134h, B653m

2.4-Tests on screws

The tests are performed on grade 4 titanium screws of the company Clover Orthopedics SRL which are usually used in a chest-lumbar stabilization system for the treatment of degenerative, traumatic, or de-formative pathologies. A one molar solution of sodium hydroxide (NaOH) was prepared a priori compared to the first two tests by dissolving 4 g of NaOH in 100 ml of water.

First of all, some tests previously carried out on grade 6 titanium bars were repeated on grade 4 titanium screws. In particular, repeated tests are those involving calcined bone powder and non-calcinated bone powder combined once with hydrogen peroxide and once with hydrogen peroxide and ammonium hydroxide. The conditions under which these tests were carried out are the same as those used for the tests on the bars, however, the tests on the screws were carried out only at the temperature of 80°C and 100°C for a total of eight new tests: S411h, S329m, S515h, S492m, S703h, S076m, S040h, S930m (Table 4).

Table 4 *Main details of bar tests repeated on screws.*

Set of tests	***Powder***	***Solute-solvent ratio***	***Solute-solvent amount***	***Treatment temperature (°C)***	***Time of treatment (minutes)***	***Sample code***
1°	Hydroxyapatite	1:1	3 g +3 ml	80	5	S411h, S329m
	Matrix			100		S515h, S492m
2°	Hydroxyapatite		3g + 3ml (2,85ml + 0,15ml)	80		S703h, S076m
	Matrix			100		S040h, S930m

After the repetition, new tests were performed. In the first test (S579h), in a 50 ml beaker and a 1:1 ratio, 3 g of calcined bone powder are mixed with 3 ml of NaOH solution. Once the compound has been brought to a temperature of 90° C through the thermal plate, the tip of the screw is soaked in the compound and is left there for 10 minutes, keeping the temperature constant.
In the second test (S760m), in a 50 ml beaker and a 1:1 ratio, 6 g of the compound (containing NaOH solution and non-calcinated bone powder) and 6 ml of H_2O_2 are mixed. The mixture (NaOH + non-calcinated bone powder) + H_2O_2 is brought to a temperature of 90° C and the tip of the screw is soaked in the compound (Table 5).

Table 5 *Main details of S579h and S760m.*

Sample code	***Powder***	***Solute-solvent ratio***	***Solute-solvent amount***	***Treatment temperature (°C)***	***Time of treatment (minutes)***
S579h	Hydroxyapatite	1:1	3 g + 3 ml	90	10
S760m	Matrix		6g + 6ml		

2.4.1-2° set of tests

A non-calcinated bone powder treatment was carried out before the second set of tests. Specifically, this powder was soaked in a quantity of ammonia hydroxide (at 37% concentration) equal to twice the volume of powder. The compound is brought and maintained at about 220° C for two hours. Subsequently, the ammonia hydroxide is washed away with dilutions of water and the compound is left to soak overnight in hydrogen peroxide.
In the first test (S133m), 3 g of previously treated non-calcinated bone powder is poured into a 50 ml beaker. The mixture is heated to a temperature of 90° C. At this point, the tip of the screw is soaked and left there for 10 minutes.
In the second test (S359m), in a 50 ml beaker in a 1:1 ratio, 4 g of compound (consisting of 4 g of non-calcinated bone powder and 4 ml of NaOH solution) are mixed with 4 ml of hydrogen peroxide. The resulting mixture is heated to a temperature of 90° C. At this point, the tip of the screw is soaked and left there for 10 minutes (Table 6).

Table 6 *Main details of S133m and S359m.*

Sample code	***Powder***	***Solute-solvent ratio***	***Solute-solvent amount***	***Temperature (°C)***	***Time of treatment (minutes)***
S133m	Matrix ($NH_4OH + H_2O_2$)	-	3 g	90	10
S359m	Matrix	1:1	4g + 4ml		

Four further tests are then carried out using non-calcinated bone powder previously treated with ammonium hydroxide and then with hydrogen peroxide (Table 7):

- In the first (S401m), 30 g of non-calcinated bone powder are heated just over the temperature of 100 °C in a 50 ml beaker. Once reached the temperature, the tip of the screw is soaked in the compound and is left there for 5 minutes keeping the temperature constant.
- In the second (S647m), the screw is covered with bone powder and wrapped in aluminum foil. The wrapped screw is placed in direct contact with the plate heated to a temperature of more than 100 °C for about 5 minutes.
- In the third test (S477m), the screw is covered with bone dust and then wrapped in aluminum foil. The wrapped screw is boiled at a temperature of 100 °C in a beaker containing water for 5 minutes.
- In the fourth test (S642m), 2 g of non-calcinated bone powder are placed in a 5 ml flask and heated to a temperature of 100 °C by thermal plate. Once arrived at temperature, the tip of the screw is inserted in the bottle and left soaked for 10 minutes keeping the temperature constant.

Table 7 *Main details of different tests involving treated-Matrix.*

Sample code	***Powder***	***Compound amount (g)***	***Type of treatment***	***Treatment temperature (°C)***	***Time of treatment (minutes)***
S401m	Matrix ($NH_4OH + H_2O_2$)	30	Boiled in the compound	>100	5
S647m		4	Direct contact		
S477m		4	Boiled in water		
S642m		2	Boiled in the compound	100	10

2.4.2-3° set of tests

In the five tests performed (S876m, S391m, S133m (or S459m), S915m, S206m), the bone powder non-calcinated and treated with NH_4OH and H_2O_2 is diluted in 10 ml of hydrogen peroxide. In the tests, the ratio of solute to solvent is varied, starting from a ratio of 2:10, passing to 4:10, 6:10, 7:10, 8:10. With this solution, 2 ml is inserted in a 5 ml bottle which is then heated on a thermal plate up to the temperature of 100 °C. Once reached the temperature, the tip of the screw is soaked in the solution and left there for 10 minutes keeping the temperature constant. In the last test of this set, the bone powder calcined is diluted in 10 ml of hydrogen peroxide in a ratio of 6:10, the test proceeds as the previous ones (Table 8).

Table 8 *Main details of dilution tests.*

Sample code	***Powder***	***Solute-solvent ratio***	***Solute-solvent amount***	***Treatment temperature (°C)***	***Time of treatment (minutes)***
S876m	Matrix ($NH_4OH + H_2O_2$)	2:10	2g + 10ml	100	10
S391m		4:10	4g + 10ml		
S133m (S459m)		6:10	6g + 10ml		
S915m		7:10	7g + 10ml		
S206m		8:10	8g + 10ml		
S016h	Hydroxyapatite	6:10	6g +10ml		

2.4.3-4° set of tests

In the fourth set of tests, the first three were carried out using non-calcinated bone powder previously treated with NH_4OH and H_2O_2. The powder is mixed with deionized water and 2 ml of this mixture is placed in a 5 ml flask heated to 100 °C. The first two tests (S551m, S869m) are carried out in this way by varying only the solute-solvent ratio which in the first case is 2:1 (2 g of powder and 1 ml of water) while in the second case it is 3:1 (3 g of powder and 1 ml of water). In the third test (S693m), 3 g of powder are placed in a 50 ml beaker and heated at a temperature of 100 °C. In the fourth test (S963h), 2 g of powder mixed with 2 ml of H_2O_2 are placed in a 5 ml flask and heated at a temperature of 100 °C (Table 9).

Table 9 *Main details of S551m, S869m, S693m and S963h.*

Sample code	***Powder***	***Solute-solvent ratio***	***Solute-solvent amount***	***Treatment temperature (°C)***	***Time of treatment (minutes)***
S551m	Matrix ($NH_4OH + H_2O_2$)	2:1	2g + 1ml	100	10
S869m		3:1	3g + 1ml		
S693m		-	3g		
S963h	Hydroxyapatite	1:1	2g + 2 ml		

In the second part of the fourth set of tests, the two versions of bone powder, calcined and non-calcinated, are used. The powder is sieved using the fabric of tights in order to obtain a granule much smaller than 0.5 μm. The screening phase is carried out with three different types of fabric, 20, 30, and 40 deniers, for a total of 6 tests. After the sieving phase, the powder is mixed with hydrogen peroxide in a 2:1 ratio (2 g of solute per 1 ml of solvent). 2 g of the mixture is placed in a 5 ml bottle and heated to a temperature of 100 °C. In all the tests, once the temperature is reached, the tip of the screw is inserted and left in soaking for 10 minutes keeping the temperature constant for a total of six tests: S401m, S961h, S300m, S408h, S056m, S167h (Table 10).

Table 10 *Main details of sieved powder tests.*

Powder	***Solute-solvent ratio***	***Solute-solvent amount***	***Type of fabric***	***Treatment temperature (°C)***	***Time of treatment (minutes)***	***Sample code***
Matrix	2:1	2g + 1ml	20	100	10	S401m, S961h
			30			S300m, S408h
Hydroxyapatite			40			S056m, S167h

2.4.4-5° set of tests

Before this set of tests, the non-calcinated bone powder is sieved with 30 denier fabric tights and then treated first with ammonium hydroxide and then with hydrogen peroxide. Specifically, 25.40 g of bone powder was sieved in 50 ml of NH_4OH for about 30 minutes. After some rinses in water to remove NH_4OH, the powder is soaked in 50 ml of H_2O_2 for about an hour.

In the first test (S439m), the treated powder is mixed with deionized water at a 2:1 ratio (2 g of solute per 1 ml of solvent). 2 ml of this mixture are placed in a 5 ml bottle and heated to a temperature of

100 °C. Once reached the temperature, the tip of the screw is inserted into the bottle and left it soaking for 10 minutes while keeping the temperature constant.
In the second and third tests (S669m, S082h), the screw was sprinkled with a compound in ratio 2:1 hydrogen powder-peroxide, once with the treated non-calcinated bone powder and once with the calcined bone powder. Then the screw soaked with the compound is placed in direct contact with the thermal plate, flows at maximum temperature, for about 2 minutes (Table 11).

Table 11 *Main details of S439m, S669m and S082h.*

Sample code	***Powder***	***Solute-solvent ratio***	***Solute-solvent amount***	***Treatment temperature (°C)***	***Time of treatment (minutes)***
S439m	Matrix ($NH_4OH + H_2O_2$)	2:1	2g + 1ml	100	10
S669m				>100	2
S082h	Hydroxyapatite				

A solution with a concentration of 0,0014 mg/ml NaOH was prepared before proceeding with the second part of the fifth set of tests. To achieve this concentration, 14 mg NaOH was weighed and dissolved in 10 ml H_2O_2 (1,4 mg/ml). 1 ml of this solution was removed and 10 ml of H_2O_2 was added to it, reaching a concentration of 0,14 mg/ml. This last step has been repeated twice before reaching the useful concentration. In addition, the tests were carried out using bone powder sieved with the fabric of 30 denier tights.
In the first three tests (S398h, S656m, S329m), sifted bone powder was combined with NaOH-H_2O_2 solution at a concentration of 0,0014 mg/ml at a ratio of 1:2 (0,5 g powder per 1 ml solution). For each of the two versions of bone powder, calcined and non-calcinated, a compound was prepared which was then heated to a temperature of 100 °C. However, in the third test, the screw was sprinkled with compound (non-calcinated powder) and, instead of being soaked in the mix, it was heated in direct contact with the heat plate, for a few minutes (Table 12).

Table 12 *Main details of NaOH tests on screws.*

Sample code	***Powder***	***Concentration of NaOH in the solvent (mg/ml)***	***Solute-solvent ratio***	***Solute-solvent amount***	***Treatment temperature (°C)***	***Time of treatment (minutes)***
S398h (S249h)	Hydroxyapatite	0,0014	1:2	0,5g + 1ml	100	10
S656m (S928m)	Matrix					
S329m						2

In the following three tests (S380m, S909m, S362m), the non-calcinated and sieved bone powder was combined with NaOH-H_2O_2 solution (ratio 1:2), but the NaOH concentration in the solution varied from a less concentrated solution (0,0014 mg/ml) to a more concentrated one (1,4 mg/ml). The mixture has been heated to a temperature of 100 °C. In the last test (S260m), the non-calcinated and sieved bone powder was combined with the 1:2 ratio solution, but in this case, the solution contains 0,5 ml of NaOH-H_2O_2 solution and 0,5 ml of a solution containing calcium ions (Ca^{2+}). The mixture has been heated to a temperature of 100 °C.

In all the tests, once the temperature is reached, the tip of the screw is inserted and left in soaking for 10 minutes keeping the temperature constant (Table 13).

Table 13 *Main details of S380m, S909m, S362m and S260m.*

Sample code	***Powder***	***Concentration of NaOH in the solvent (mg/ml)***	***Solute-solvent ratio***	***Solute-solvent amount***	***Treatment temperature (°C)***	***Time of treatment (minutes)***
S380m	Matrix	0,014	1:2	0,5g + 1ml	100	10
S909m		0,14				
S362m		1,4				
S260m		0,0014		0,5g + (0,5 + 0,5) ml		

2.5-FT-IR Device

The infrared spectrometer used to analyze the most promising samples is the FT-IR Spectrum Two spectrometer by PerkinElmer®. Such an instrument uses a very low-maintenance optical system able to guarantee accurate and repeatable measurements, day after day, while the tried and tested design of the interferometer guarantees unmatched reliability. Thanks to the robust design and integrated sampling it is possible to carry out analyses of raw materials in warehouse environments all over the world, eliminating the need to send samples for analysis (Table 14) [101].

Table 14 *Main Characteristics of Spectrum Two.*

RELEVANT TECHNICAL DATA OF SPECTRUM TWO	
Detector Type	$LiTaO_3$
Operating range	5 – 45°C
Wavelength range	8300 – 350 cm^{-1}

Advanced electronics, optimized sensitivity, and an exceptional signal-to-noise ratio ensure the constant performance of Spectrum Two. This spectrometer is equipped with a field-proven interferometer (Dynascan™ interferometer) that incorporates a simple, non-critical bearing that provides unmatched longevity and reliability. Environmental protection is provided by the unique humidity shield design (OpticsGuard™ technology), which allows the use of the Spectrum Two in more difficult environments. In addition, the long-lasting desiccant ensures maximum operation of the instrument, regardless of where the analysis takes place. Real-time CO_2 and H_2O absorption is compensated by an advanced digital filtering algorithm called Atmospheric Vapor Compensation™(AVC). Interference is effectively eliminated by these atmospheric components, allowing the laboratory to achieve more consistent results, and eliminating the need for purging of instruments. The accurate calibration of this instrument is ensured by AVI standardization with gas-phase spectra. Compared to conventional calibration methods, the wavenumber and shape of the instrument line are standardized with a higher degree of accuracy. Thanks to this unique standardization it is possible to transfer data precisely between the instruments, whether they are side-by-side or in remote locations [101].

Among the many optional sampling accessories available, the Universal Attenuated Total Reflectance Accessory (UATR) was used to perform samples analysis. It is an internal reflection accessory that

can be used to simplify the analysis of solids, powders, pastes, gels, and liquids. The technique is not destructive [102].

In this technique, the sample is placed over a crystal with a high refractive index. An infrared beam from the instrument is passed into the accessory and up into the crystal. It is then reflected internally into the crystal, and again towards the detector which is housed in the instrument. When the beam is reflected within the crystal, it penetrates the sample of a few microns (Figure 31).

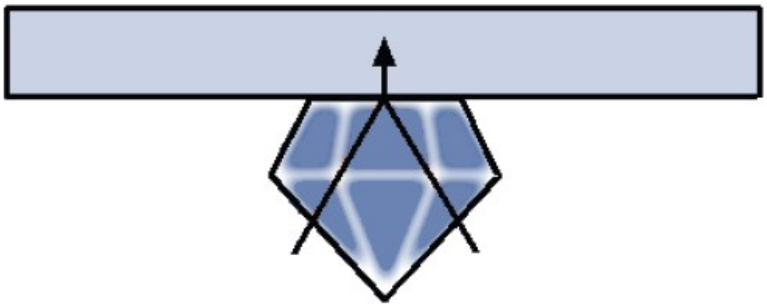

***Figure** 31 Principle of UATR operation* [102].

The UATR may be used to study homogeneous solid samples, solid surfaces, or coatings on solid samples (Figure 32). Good contact is ensured by the use of force on the sample. The Spectrum Two UATR uses a diamond crystal, hard, resistant to strong acids, bases, and high pressures and that does not scratch easily. Despite a reduced sensitivity in the approximate range 1900-2700 cm^{-1}, the diamond-coated UATR has an effective scanning range that corresponds to the entire instrument range [102].

***Figure 32** Spectrum Two FT-IR with Universal ATR Accessory* [103].

There are several features built-in by Spectrum Two that allow infrared analysis to leave the laboratory. Several power options allow you to use Spectrum Two with or without external power. Once powered, quick heating facilitates quick measurement, while optional wireless connectivity allows for portable PC control.

Finally, you can focus on the results through the comprehensive Spectrum 10™ software suite; in fact, this complete FT-IR software package facilitates data collection, processing, and generating results (Figure 33) [101].

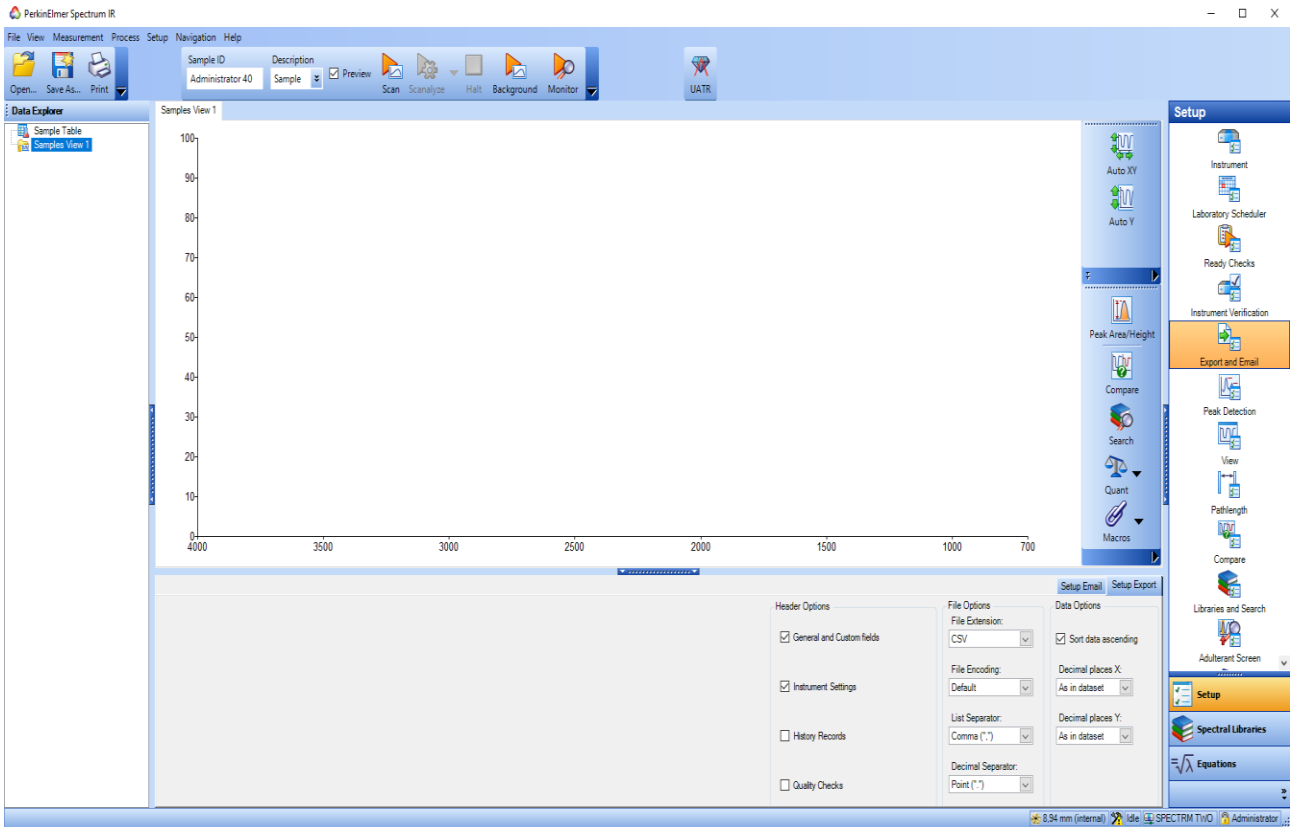

***Figure** 33 Spectrum 10 Software Suite (PerkinElmer).*

2.5.1-Protocol of analysis

The procedure for obtaining the spectra starts by starting the software "PerkinElmer Spectrum IR". Before starting the analysis of a sample, it is necessary to clean the sampling plate of the UATR module and it can be done using a cloth soaked in acetone; for the plate to be completely dry, clean, and ready for the procedure a few seconds are needed.

The first step is to acquire a background scan by clicking on the "Background" button on the Measurement bar. After a brief display of the background spectrum, the Viewing Area is prepared for data collection from the sample. An identifying name is assigned to the single sample by typing it in the space marked with the title "Sample ID". Subsequently, the treated titanium implant is positioned at the diamond crystal present in the UATR module and is stopped momentarily through the spectrometer arm; such arm, indeed, is first placed over the crystal and then the handle is screwed clockwise until the tip of the metal is near the plate. At this point, you can start scanning by clicking on the "Scan" button on the Measurement bar (Figure 34). The software first generates a preview of the spectrum and then, in a few seconds and pressing again "Scan", provides the actual spectrum of the sample. In addition is possible to click “Labels” on the lateral toolbar to assign wave numbers to the major peaks, before printing the spectrum.

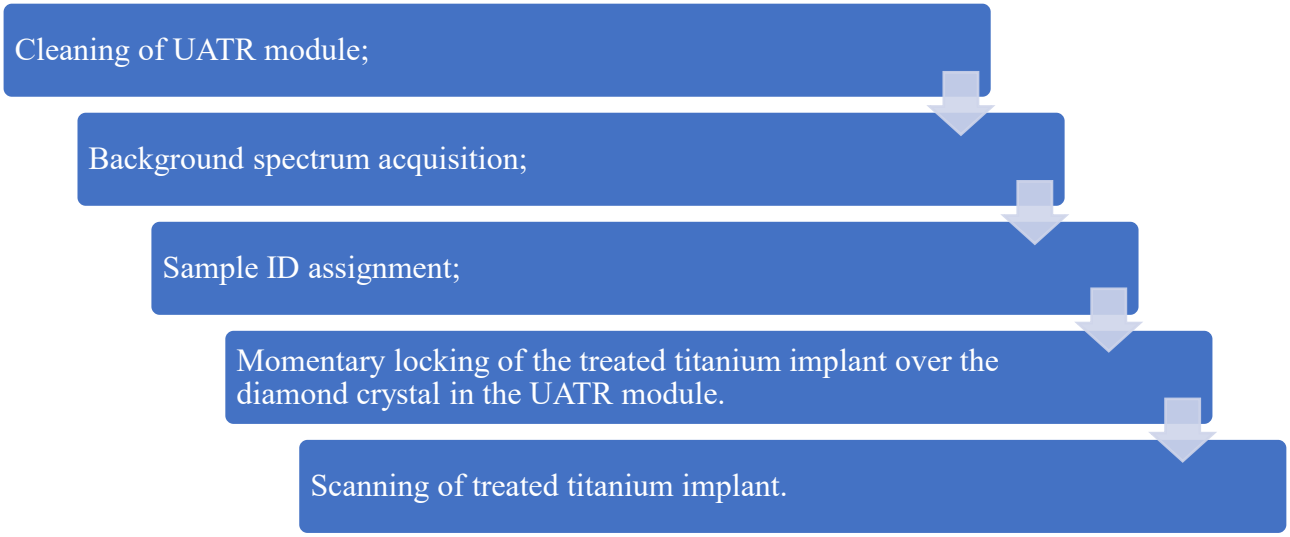

Figure 34 *Schematic representation of the IR-analysis protocol.*

3-RESULTS

The surface of the implants is shown below as a result of the various tests. The photographic results corresponding to each test are presented starting from the bars and passing, then, to the screws. The photographs were taken via the AxioCam ERc 5s camera, integrated into the ZEISS Stemi 508 microscope, and saved to a removable memory from which they were then recovered.

3.1-Bars surface inspection

The photographic results below compare the surface of the bar soaked in the compound, based on Hydroxyapatite or Matrix and hydrogen peroxide, heated at different temperatures. In these images (left column relative to Hydroxyapatite, right column relative to Matrix), one can see an increase in the material bound as the temperature increases (Figure 35-36-37).

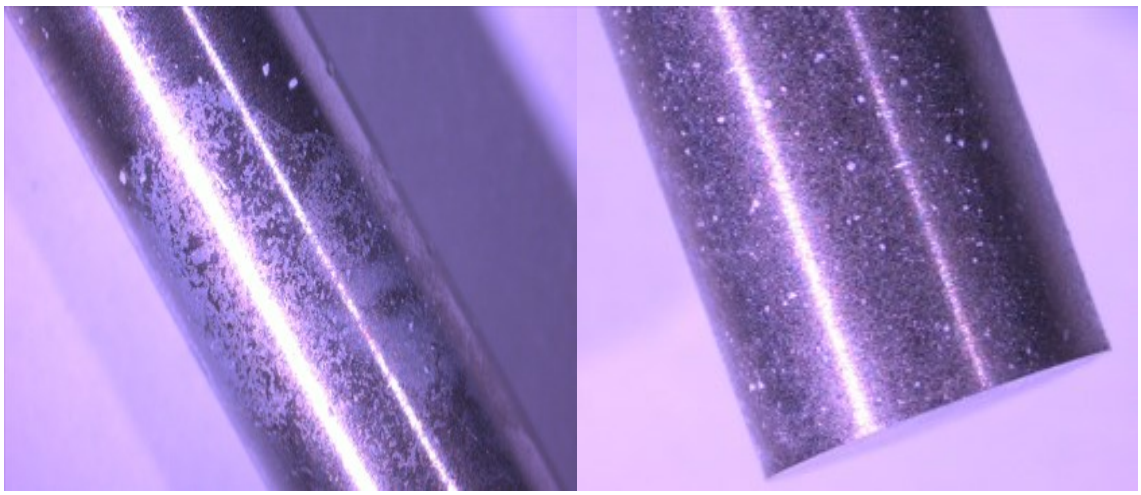

***Figure 35 B664h**: 60°C/soaked in the compound for 5 min. **B548m**: 60°C/soaked in the compound for 5 min.*

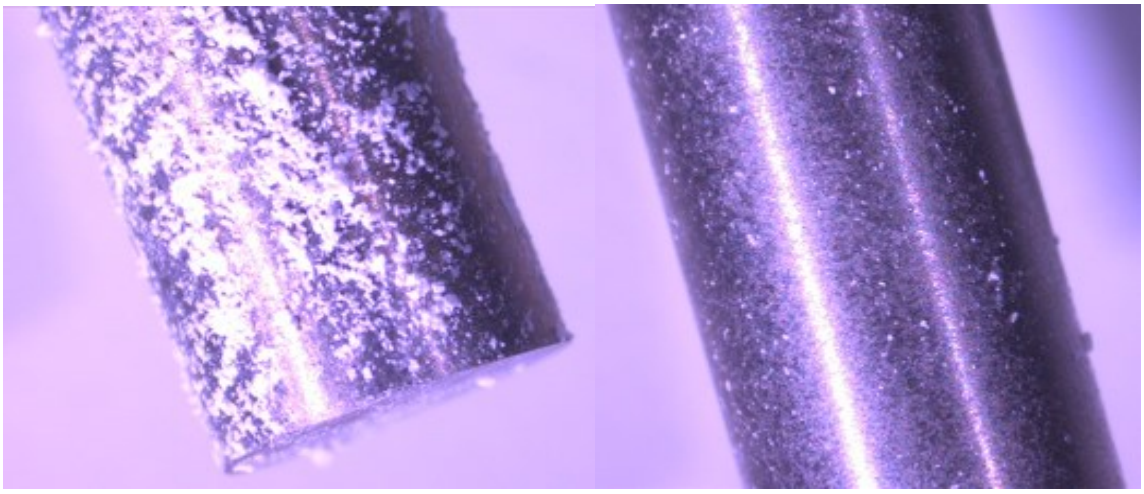

***Figure 36 B079h**: 80°C/soaked in the compound for 5 min. **B217m**: 80°C/soaked in the compound for 5 min.*

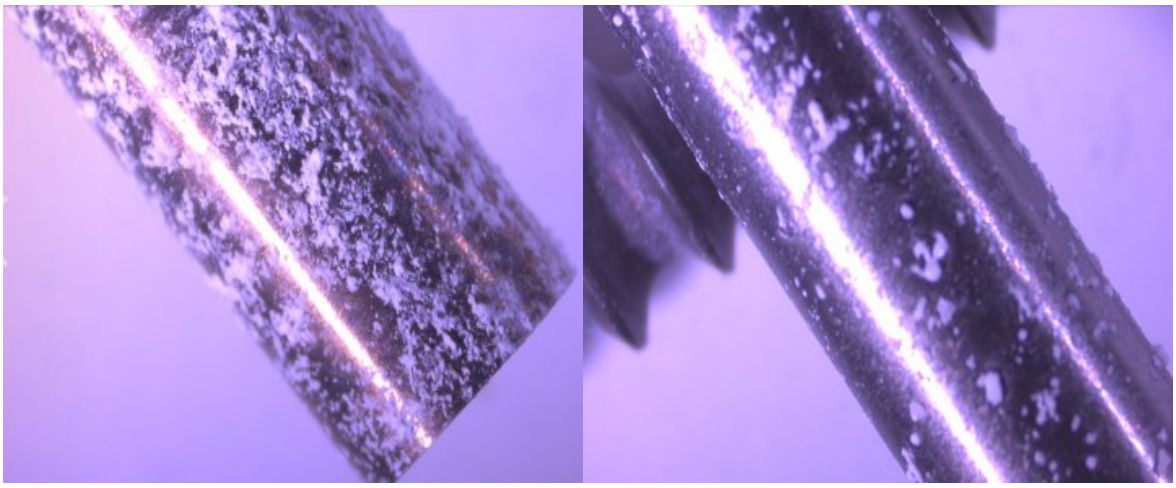

***Figure 37 B976h**: 100°C/soaked in the compound for 5 min. **B435m**: 100°C/soaked in the compound for 5 min.*

The photographic results below compare the surface of the bar soaked in the compound, based on Hydroxyapatite or Matrix and a solution of hydrogen peroxide and ammonium hydroxide, heated at different temperatures. The procedure of the first three tests is the same as the previous ones while in the last one, after the immersion treatment, the bar is dried in an oven at 70°C instead of room temperature. In these images (left column relative to Hydroxyapatite, right column relative to Matrix), one can see an increase in the material bound as the temperature increases. In the last couple of images, it is possible to notice an improvement as regards the Matrix-based covering and a worsening as regards the previous three Hydroxyapatite-based covering (Figure 38-39-40-41).

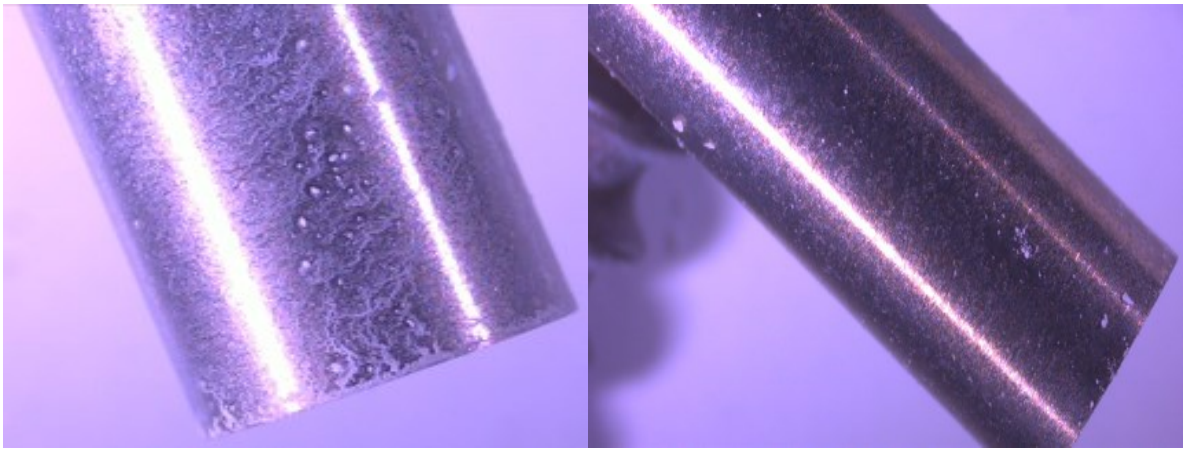

***Figure 38 B291h**: 60°C/soaked in the compound for 5 min. **B066m**: 60°C/soaked in the compound for 5 min.*

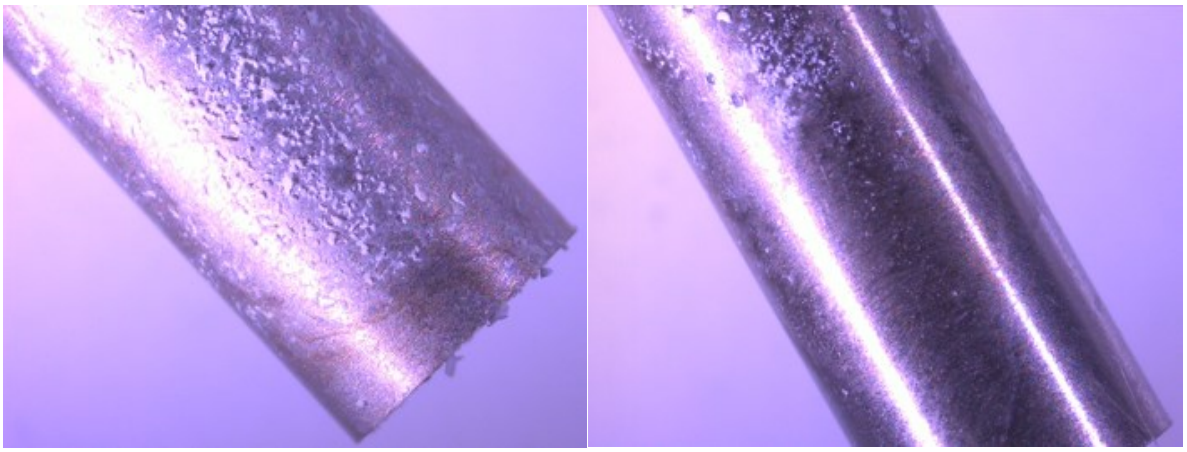

***Figure 39 <u>B001h</u>**: 80°C/soaked in the compound for 5 min. **<u>B696m</u>**: 80°C/soaked in the compound for 5 min.*

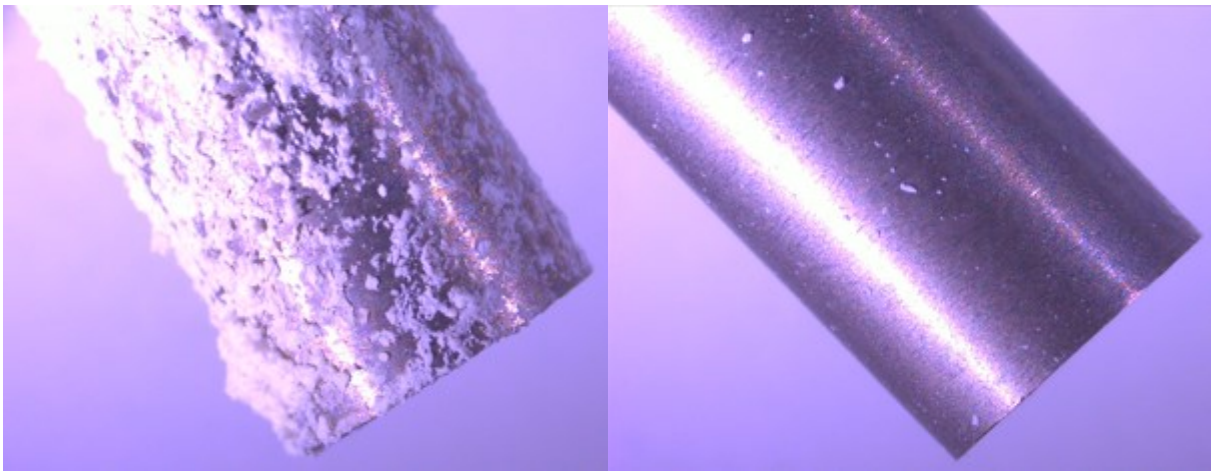

***Figure 40 <u>B167h</u>**: 100°C/soaked in the compound for 5 min. **<u>B013m</u>**: 100°C/soaked in the compound for 5 min.*

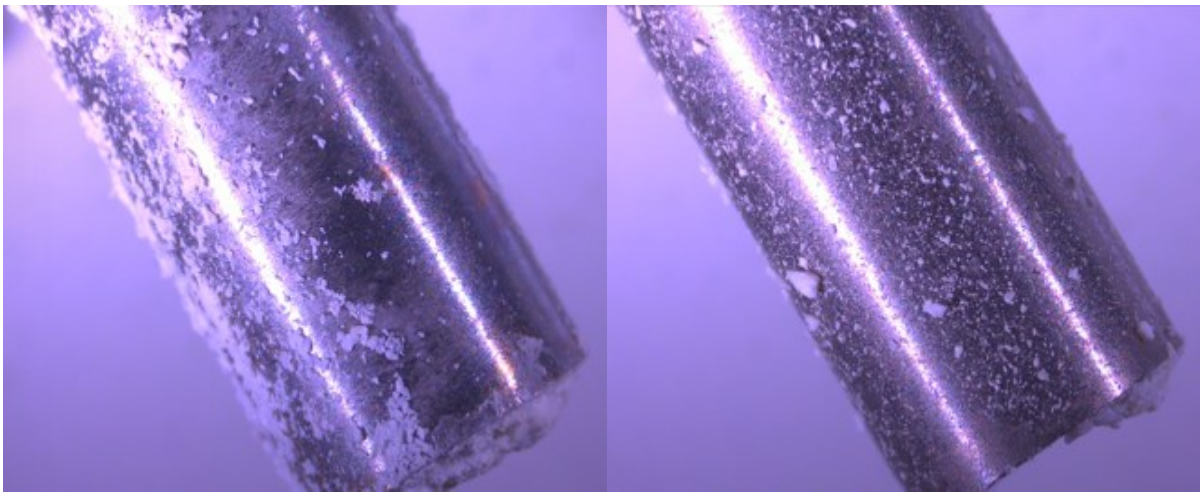

***Figure 41 <u>B134h</u>**: 60°C+70°C in stove/soaked for 5 min. **<u>B653m</u>**: 60°C+70°C in stove/soaked for 5 min.*

3.2-Screws surface inspection

The photographic results below compare the surface of the screw soaked in the compound, based on Hydroxyapatite or Matrix and hydrogen peroxide, heated at different temperatures. It can be seen a slight increase of the material bound as the temperature increases, especially in the case of Hydroxyapatite (left) with respect to that of Matrix (right) (Figure 42-43).

***Figure 42 S411h**: 80°C/soaked for 5 min. **S329m**: 80°C/soaked for 5 min.*

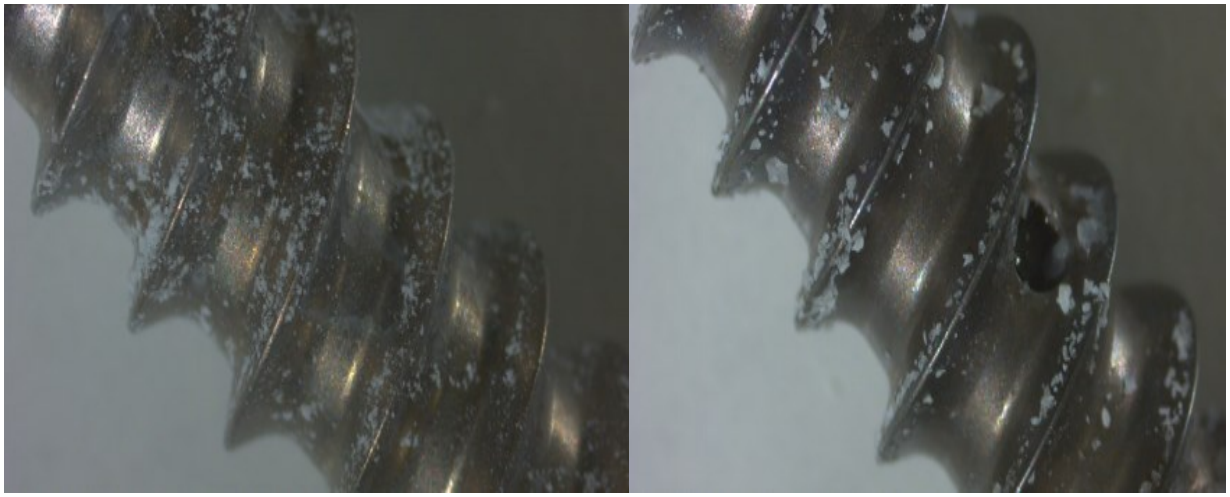

***Figure 43 S515h**: 100°C/soaked for 5 min. **S492m**: 100°C/soaked for 5 min.*

The photographic results below compare the surface of the screw soaked in the compound, based on Hydroxyapatite or Matrix and a solution of hydrogen peroxide and ammonium hydroxide, heated at different temperatures. A greater amount of material left bound to the surface can be seen compared to previous tests where ammonium hydroxide is not present (Figure 44-45).

***Figure 44 <u>S703h</u>**: 80°C/soaked for 5 min. **<u>S076m</u>**: 80°C/soaked for 5 min.*

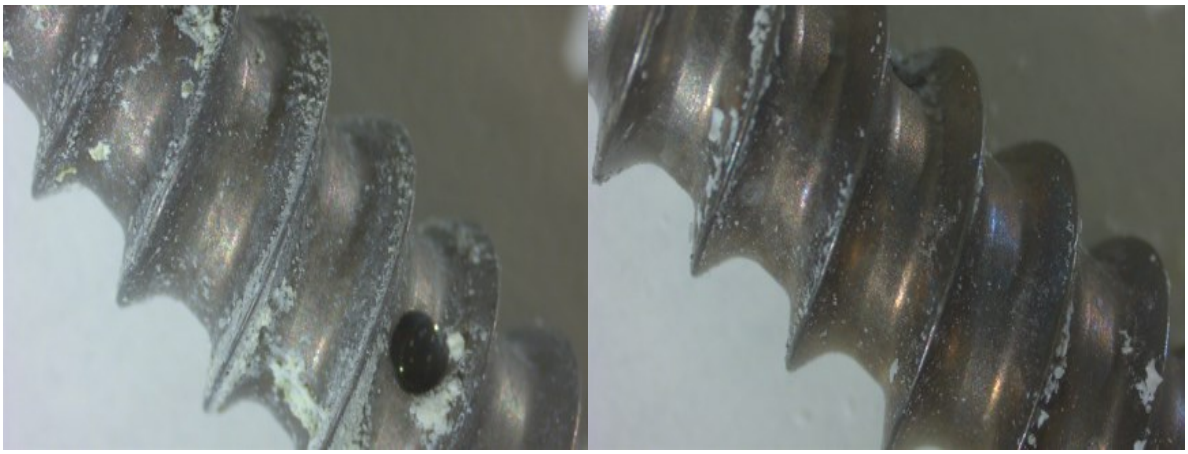

***Figure 45 <u>S040h</u>**: 100°C/soaked for 5 min. **<u>S930m</u>**: 100°C/soaked for 5 min.*

The photographic results below compare the surface of the screw soaked in the compound, heated 90°C. On one side is the compound based on Hydroxyapatite and a solution containing sodium hydroxide (left), on the other is based on Matrix and a solution of hydrogen peroxide and sodium hydroxide (right). The duration of heat treatment is increased but is noted a poor and uneven amount of material in both cases especially for the Matrix (Figure 46).

***Figure 46 <u>S579h</u>**: 90°C/soaked for 10 min. **<u>S760m</u>**: 90°C/soaked for 10 min.*

3.2.1-2°Set of tests inspection

The following photographic results compare the surface of the screw soaked in the compound, heated 90 C. On the one hand, the compound is the matrix treated with ammonium hydroxide and hydrogen peroxide still impregnated with peroxide (left), at the other is based on Matrix and a sodium hydroxide solution subsequently combined with hydrogen peroxide (right). The duration of the heat treatment is unchanged from the last tests there is a clear difference between the amount of bonded material in one case and the other, however, even the best case has a certain uneven coverage (Figure 47).

***Figure 47 S133m**: 90°C/soaked in treated Matrix for 10 min. **S359m**: 90°C/soaked in treated Matrix+H_2O_2 for 10 min.*

The photographic results below compare the screw surface under four different conditions. All involve the treated Matrix, in the first two, the temperature is above 100°C while in the next two the temperature is 100°C. The first two images show granules of different sizes attached to the surface, in the first image on the left the granules are smaller than in the image on the right (Figure 48), while the next two show agglomerates of material attached to the surface (Figure 49).

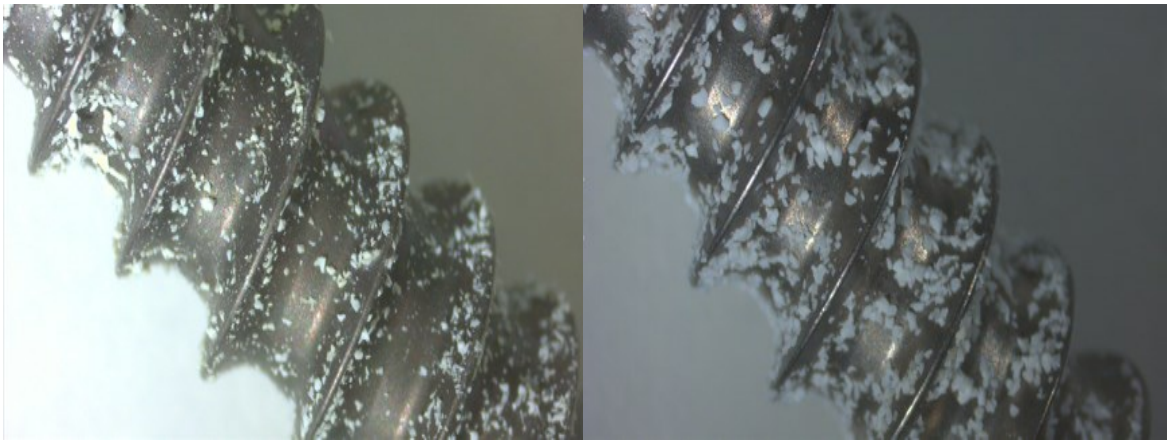

***Figure 48 S401m**: T >100°C/soaked for 5 min. **S647m**: T >100°C/wrapped and heated directly for 5 min.*

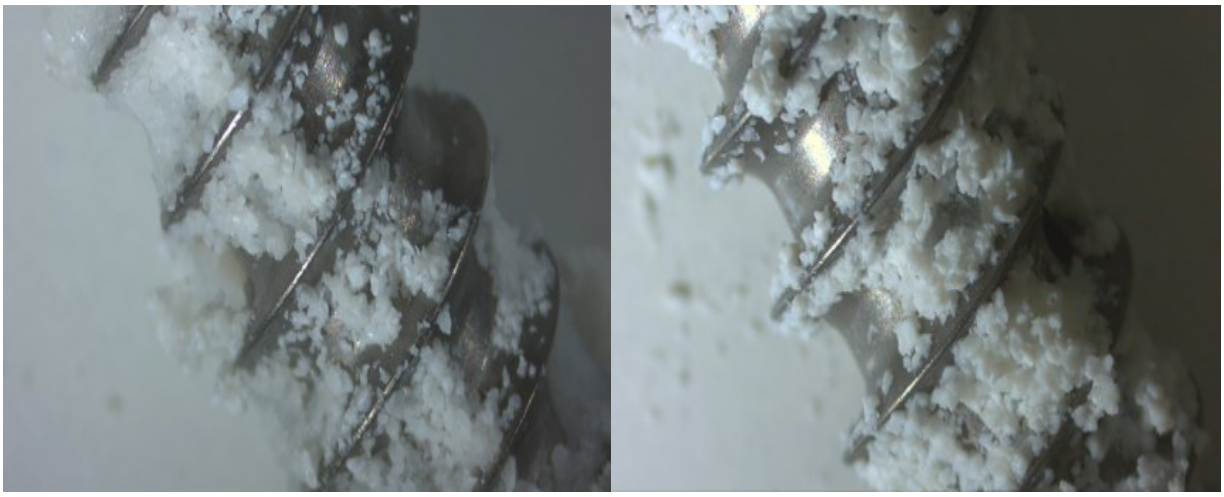

***Figure 49 S477m**: 100°C/wrapped and boiled in water for 5 min. **S642m**: 100°C/soaked for 10 min.*

3.2.2-3°set of tests inspection

The photographic results below compare the surface of the screw soaked in the compound at different solute-solvent ratios. The ratios tested are: 2:10, 4:10, 6:10, 7:10, 8:10 for Matrix, 6:10 for Hydroxyapatite. The screw was immersed in the compound heated at 100°C keeping the treatment time constant (10 minutes). A thin, uniform coating glaze is visible in all images. By increasing the solute portions, the coating appears more visible. The middle images compare the 6:10 case of Matrix (left) and Hydroxyapatite (right) (Figure 50-51-52).

***Figure 50 S876m**: 100°C/ soaked in 2:10 mix for 10 min. **S391m**: 100°C/soaked in 4:10 mix for 10 min.*

***Figure 51 <u>S133m(S459m)</u>**: 100°C/soaked in 6:10 mix for 10 min. **<u>S016h</u>**: 100°C/soaked in 6:10 mix for 10 min.*

***Figure 52 <u>S915m</u>**: 100°C/soaked in 7:10 mix for 10 min. **<u>S206m</u>**: 100°C/soaked in 8:10 mix for 10 min.*

3.2.3-4°Set of tests inspection

The following photographic results compare the surface of the screw immersed in the compound heated to 100 °C. In the first two images varies the solute-solvent ratio, in the first case is 2:1 in the second 3:1. The first three images are related to the Matrix and have little material tied to the surface; the last one (bottom right), instead, is related to Hydroxyapatite and also in this case the coverage obtained is uneven but more visible than the other three (Figure 53-54).

***Figure 53 S551m**: 100°C/soaked in 2:1 mix for 10 min. **S869m**: 100°C/soaked in 3:1 mix for 10 min.*

***Figure 54 S693m**: 100°C/soaked in treated matrix for 10 min. **S963h**: 100°C/soaked in HA+H_2O_2 for 10 min.*

The photographic results below compare the surface of the screw soaked in Hydroxyapatite or Matrix and hydrogen peroxide compound heated to 100°C. The powder is sieved with three different types of tissue, 20, 30, and 40 deniers, while the solute-solvent ratio remains unchanged in the tests (2:1). The images show a more visible coverage in the first two cases for Hydroxyapatite (left) and less in the last one, while for Matrix (right) the coverage is more visible in the last case than in the first two. In all the tests there is no homogeneity of coverage (Figure 55-56-57).

***Figure 55 <u>S961h</u>**: 100°C/20 deniers filter/soaked for 10 min. **<u>S401m</u>**: 100°C/20 deniers filter/soaked for 10 min.*

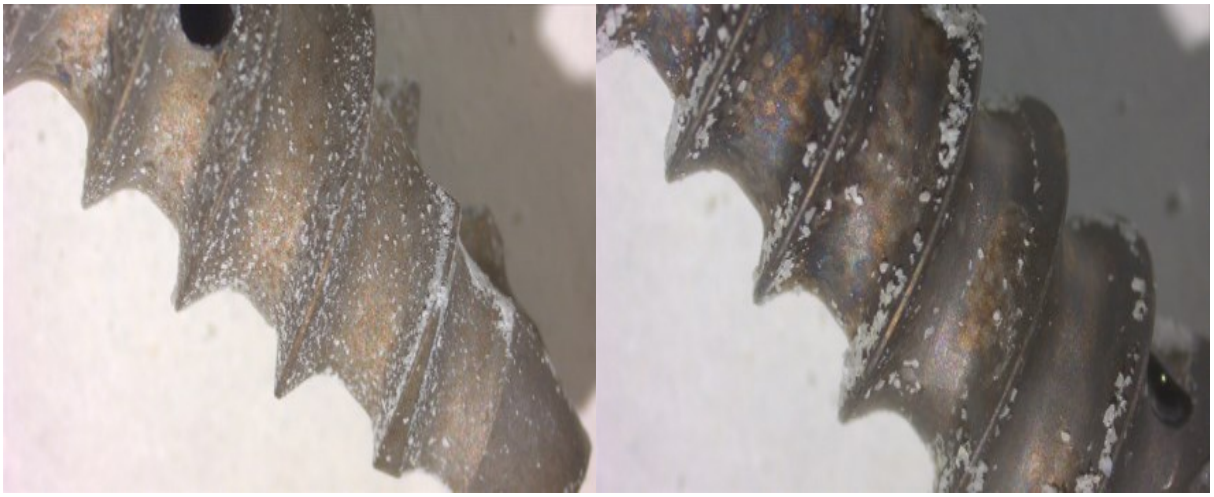

***Figure 56 <u>S408h</u>**: 100°C/30 deniers filter/soaked for 10 min. **<u>S300m</u>**: 100°C/30 deniers filter/soaked for 10 min.*

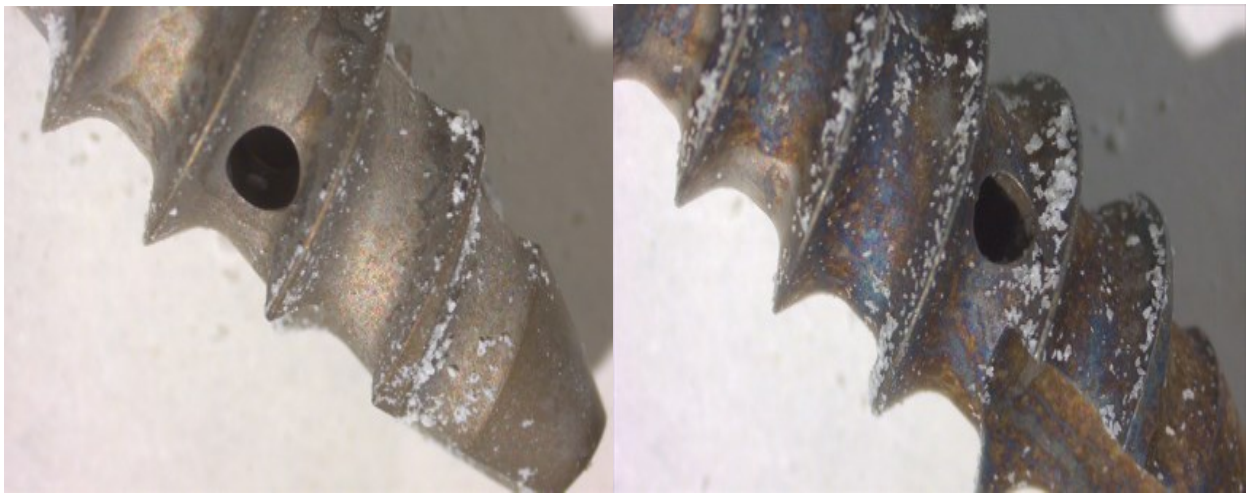

***Figure 57 <u>S167h</u>**: 100°C/40 deniers filter/soaked for 10 min. **<u>S056m</u>**: 100°C/40 deniers filter/soaked for 10 min.*

3.2.4-5°Set of tests inspection

The photographic results below compare the surface of the screw soaked in the heated compound and the one in which the screw is sprinkled with the compound and heated in direct contact with the thermal plate. The first two images are related to Matrix treated with NH_4OH and H_2O_2 (Figure 58-59), the third one is related to Hydroxyapatite (Figure 60). In the images related to Matrix, the material bound is little and inhomogeneous, while in the case of Hydroxyapatite a good amount of material was bound in a rather homogeneous way.

***Figure 58 <u>S439m</u>**: 100°C/soaked in 2:1 mix (1ml of H_2O) for 10 min.*

***Figure 59 <u>S669m</u>**: T >100°C/sprinkled with treated Matrix and heated directly on a thermal plate for 2 min.*

***Figure 60 <u>S082h</u>**: T >100°C/sprinkled with HA+H_2O_2 and heated directly on a thermal plate for 2 min.*

The photographic results below compare the surface of the screw soaked in the heated compound and the one in which the screw is sprinkled with the compound and heated in direct contact with the thermal plate. The first image is relative to Hydroxyapatite (Figure 61), the other two are relative to Matrix (Figure 62-63). The solute-solvent ratio (1:2), the sieving of powders (30 deniers) is unchanged in all three tests, also in all three compounds is present sodium hydroxide. The image related to Hydroxyapatite shows a fairly uniform coverage in which the granules can be distinguished. The images related to the Matrix instead show, especially in the second case, a less uniform coverage but more visible than any previous tests.

***Figure 61 <u>S398h (S249h)</u>**: 100°C/soaked in 1:2 mix (0,5g+1ml of NaOH-H_2O_2) for 10 min.*

***Figure 62 <u>S656m (S928m)</u>**: 100°C/soaked in 1:2 mix (0,5g+1ml of NaOH-H_2O_2) for 10 min.*

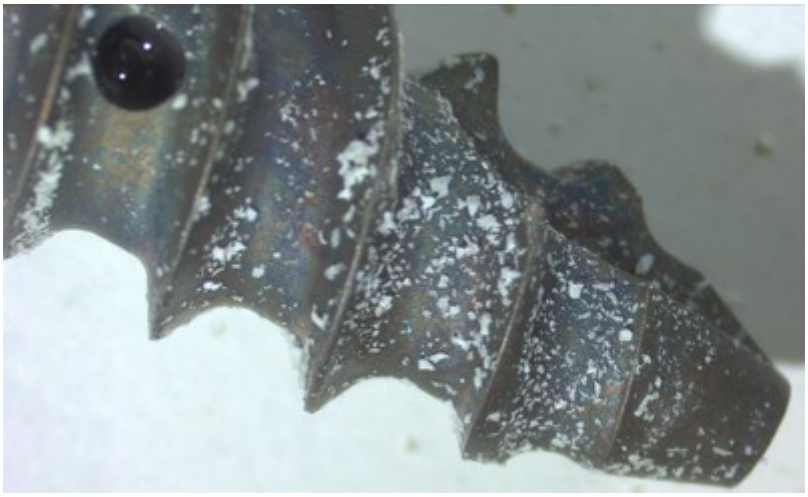

***Figure 63 <u>S329m</u>**: 100°C/sprinkled with 1:2 mix (0,5g+1ml of NaOH-H_2O_2) and heated directly on a thermal plate for 2 min.*

The photographic results below compare the surface of the screw immersed in the compound, based on Matrix (sieved 30 deniers) and a solution of NaOH and H_2O_2, heated to 100°C. In the four tests, the concentration of NaOH in the solution varies, while the solute-solvent ratio (1:2) and the treatment time remain unchanged. The last case differs from the three previous ones for the presence of calcium ions in the solution. The presence of unevenly bound material is visible in the images (Figure 64-65-66-67). Especially in the last two, but partly also in the second one, a thin film of coating can be seen in some areas of the surface.

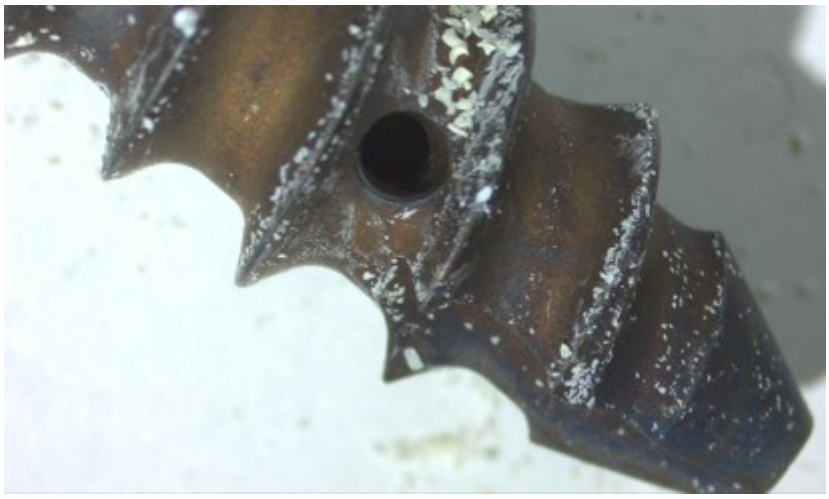

***Figure 64 <u>S380m</u>**: 100°C/ immersed in 1:2 mix (0,5g+1ml of NaOH (0,014 mg/ml)-H_2O_2) for 10 min.*

***Figure 65 <u>S909m</u>**: 100°C/ immersed in 1:2 mix (0,5g+1ml of NaOH (0,14 mg/ml)-H_2O_2) for 10 min.*

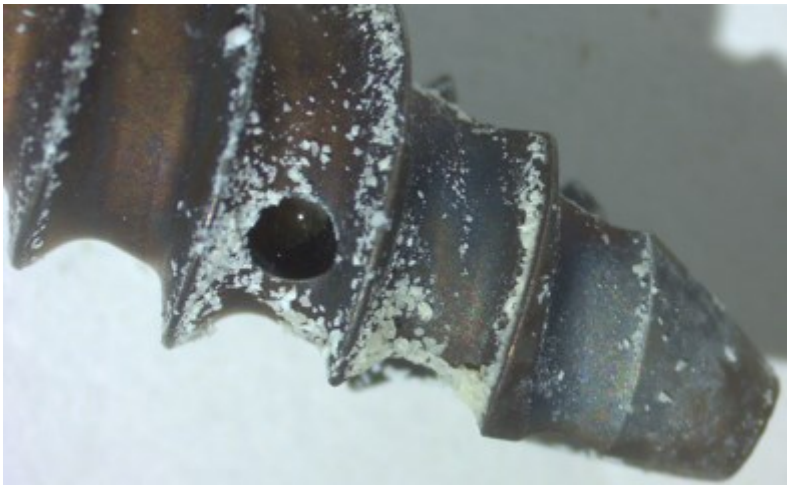

***Figure 66 <u>S362m</u>**: 100°C/ immersed in 1:2 mix (0,5g+1ml of NaOH (1,4 mg/ml)-H_2O_2) for 10 min.*

Figure 67 ***S260m****: 100°C/ immersed in 1:2 mix (0,5g+(0,5ml NaOH (0,0014 mg/ml) +0,5ml of Ca^{2+})) for 10 min.*

3.3-IR-Analysis

The IR analysis was performed only for titanium implants that, on surface inspection under the microscope, showed a visible layer of residual cover after treatment. The IR spectra obtained are shown below; the x-axis shows the wavenumbers of the vibration frequencies, while the y-axis shows the percentage of transmittance.

The graph below shows the IR spectra obtained in the case of the presence of alkaline substance in the coating compound. Specifically, the hydroxyapatite-based coating on the screw, the matrix-based coating formed on the screw, and the substances detached from both screws are compared, respectively (Figure 68).

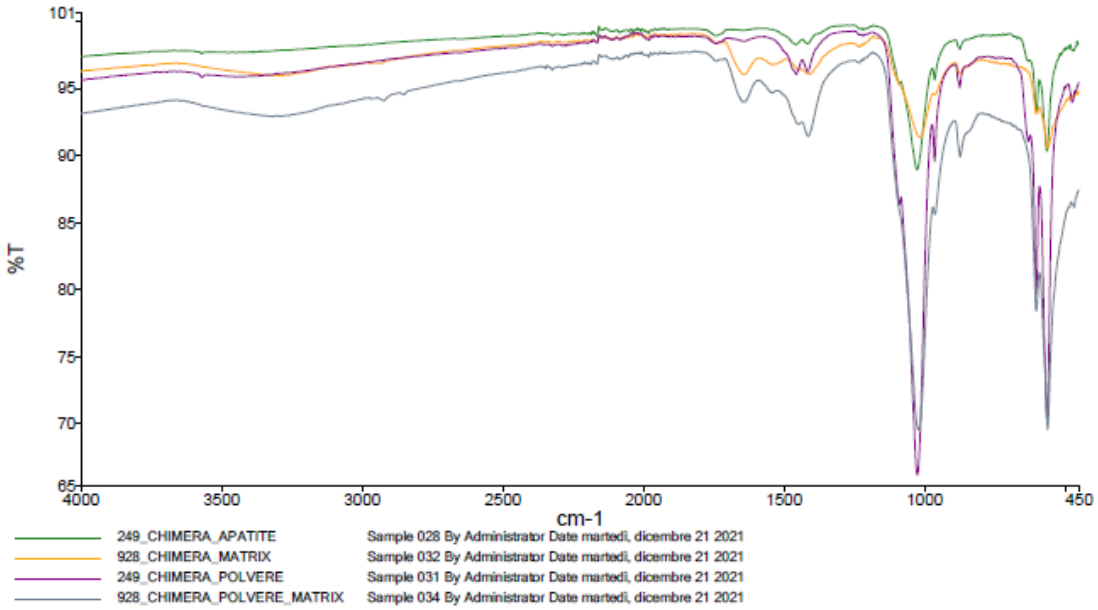

Figure 68 *Comparison between the IR-spectra of the covering and the one of the corresponding detached materials.*

The graph below shows the IR spectra obtained in the case of the presence of alkaline substance in the coating compound. Specifically, the Hydroxyapatite based coating and the Matrix based coating formed on the screw are compared (Figure 69).

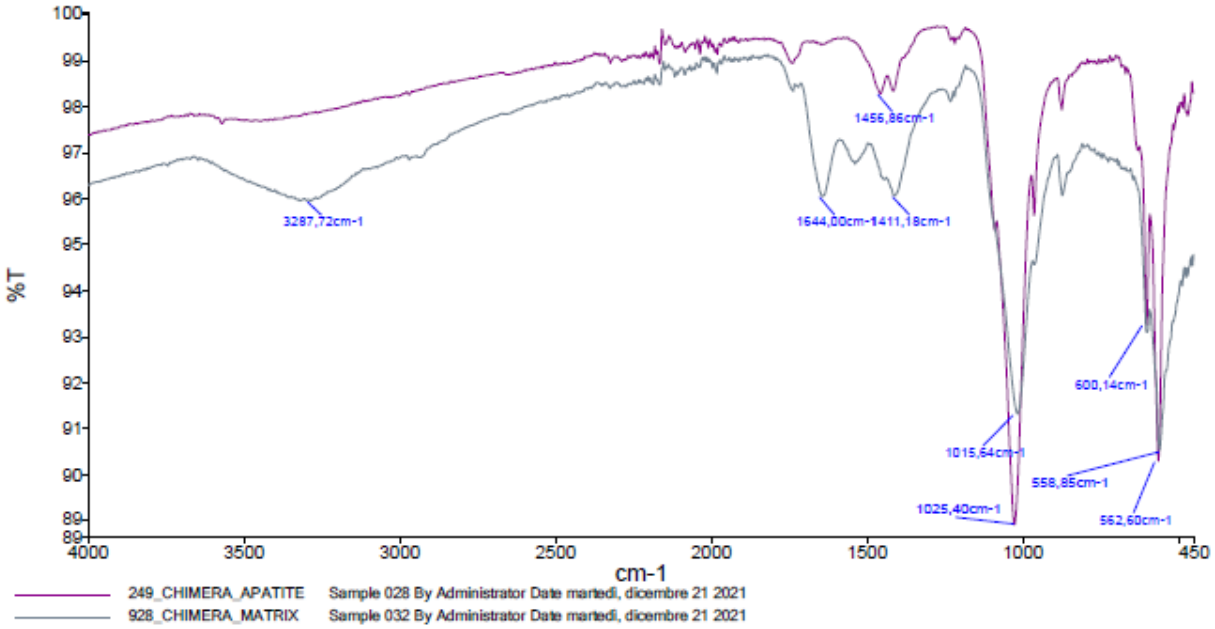

Figure 69 *Comparison between the IR-spectra of the covering obtained by mixing NaOH alkaline solution with the two version of the equine bone powder.*

The graph below shows the IR spectra obtained in the case of dilution of powders in hydrogen peroxide where the ratio of solute to solvent is 6:10. Specifically, the coating based on Hydroxyapatite and the coating based on Matrix formed on the screw are compared (Figure 70).

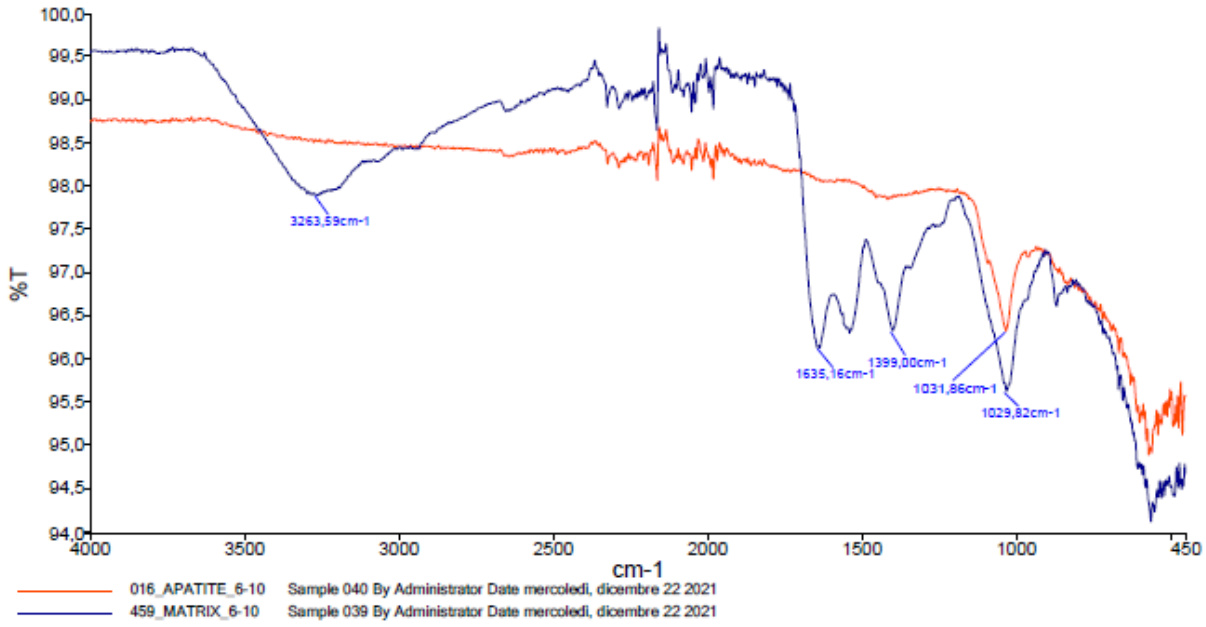

Figure 70 *Comparison between the IR-spectra of the covering obtained by using the diluted solution.*

The graph below shows the comparison between the IR spectra of the coatings based on Hydroxyapatite, obtained in the case of dilution of the powder in hydrogen peroxide and in the case where the alkaline substance is present in the solution (Figure 71).

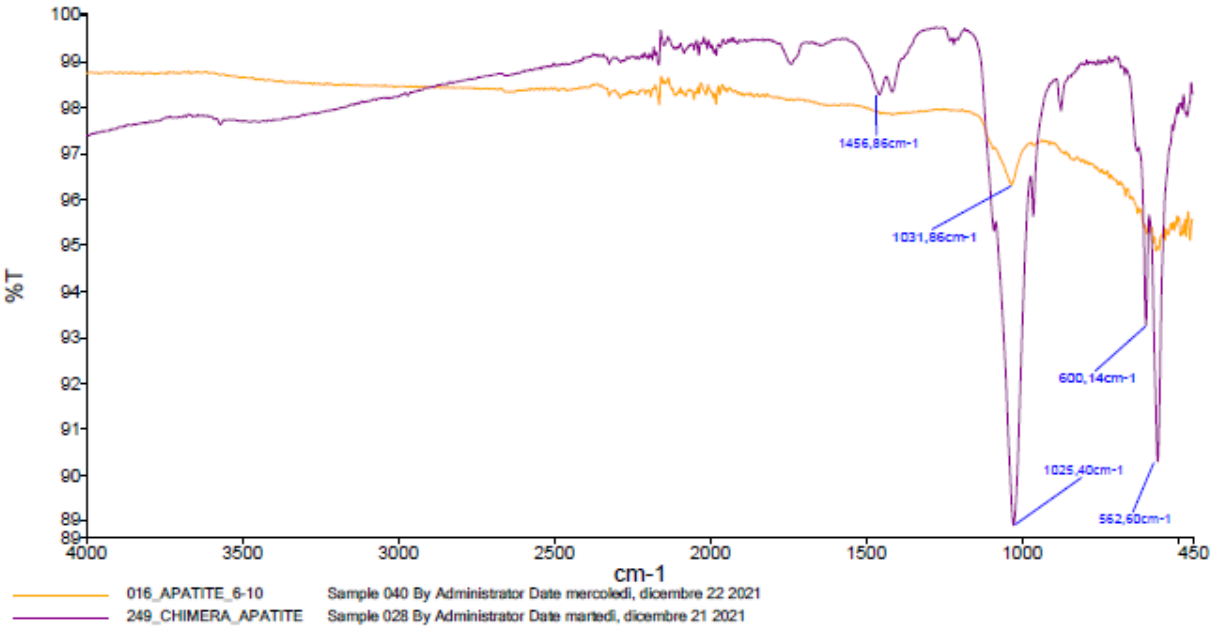

Figure 71 *Comparison between the IR-spectra of the covering obtained by using Hydroxyapatite diluted solution and the one obtained by using the NaOH alkaline solution on Hydroxyapatite.*

The graph below shows the comparison between the IR spectra of the Matrix-based coatings obtained in the case of dilution of the powder in hydrogen peroxide and in the case where the alkaline substance is present in the solution (Figure 72).

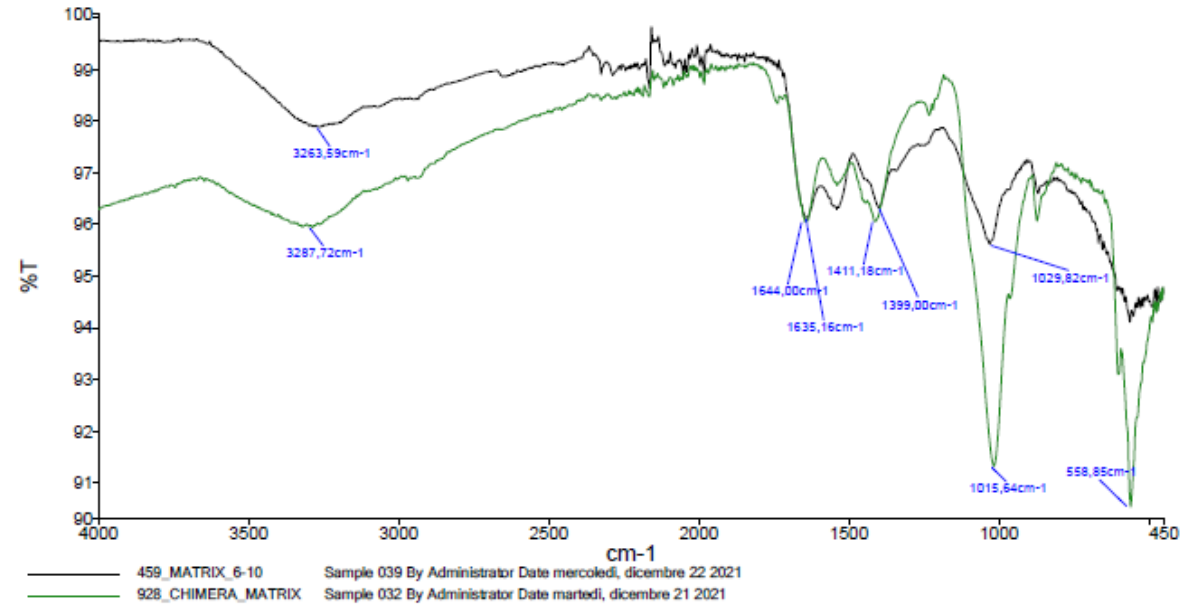

Figure 72 *Comparison between the IR-spectra of the covering obtained by using Matrix diluted solution and the one obtained by using the NaOH alkaline solution on Matrix.*

4-DISCUSSION

Observing all the photographic results obtained in the various tests and reported in the previous section, it is possible to note that in several cases the coverage obtained on the screws is inhomogeneous. Furthermore, with the same treatment, comparing the images of Matrix-based coatings and those of Hydroxyapatite-based coatings, it is evident that Hydroxyapatite binds more easily and more homogeneously than Matrix. In this regard, we can assume, with a minimum margin of error, that the disparity between the coverage based on Hydroxyapatite and that based on Matrix is attributable to a greater presence of collagen in the latter. Probably, the presence of collagen inside the Matrix decreases the possibility of contact between the oxygen atoms of the phosphate groups and those on the titanium surface, making the formation of bonds between the covering compound and the implant more difficult.

The photos below (Figure 73) show some examples of samples for which the covering treatment has produced poor results and in which the material has bonded only in certain points or almost not at all (S579h and S760m). In addition, you can see the disparity between Hydroxyapatite which tends to bind more, and Matrix that instead binds with more difficulty (Figure 74-75)(B167h-B013m and S040h-S930m).

Figure 73 *S579h and S760m.*

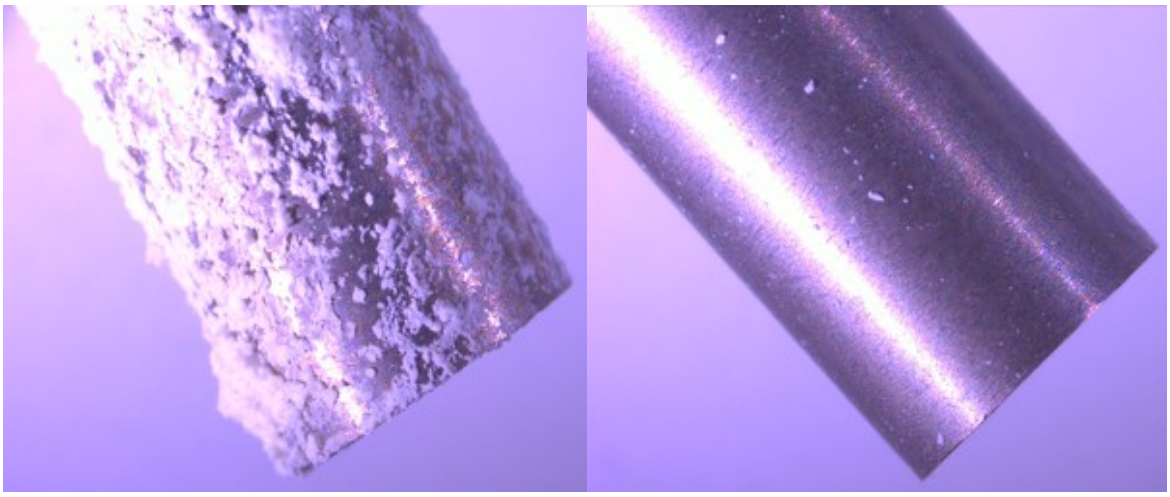

Figure 74 *B167h and B013m.*

Figure 75 *S040h and S930m.*

Notwithstanding these general considerations, two particular occurrences were identified in which the process for coating the surface of the titanium implant proved to be more effective.

The first occurrence is when the Hydroxyapatite and Matrix powders are diluted in hydrogen peroxide creating the respective compound in a 6:10 solute/solvent ratio and a screw is soaked in each of the two mixtures, heated to 100°C, for 10 minutes (Figure 76) (S016h and S133m/S459m).

The second occurrence, instead, is the one in which powders are combined with a solution of hydrogen peroxide and sodium hydroxide, an alkaline substance, where the concentration of such substance (NaOH) in the solution is 0.0014 mg/ml and a screw is soaked in each of the two mixtures, heated at 100°C, for 10 minutes (Figure 77) (S398h/S249h and S656m/S928m).

Figure 76 *S016h and S459m.*

Figure 77 *S249h and S928m.*

In the first case, the dilution effect facilitates the formation of a covalent bond between the powder particles, which are well below 0.5 μm in size, and the titanium surface; it is assumed that the particle size is also below 0.1 μm. This is still related to the fact that smaller particle sizes increase the probability of contact between phosphate groups and the titanium surface.

In the second case, however, the alkaline substance, NaOH, produces a catalytic effect in the reaction, that is, it accelerates and increases the formation of bonds between the solute granules and the titanium surface. Since the samples corresponding to these tests proved to be the most promising to visual inspection by stereomicroscope, they were subjected to IR analysis, by FT-IR spectroscope, in order to verify the presence of the coating and its chemical characteristics on the surface of the implant.

In the spectra obtained, the indicated peaks correspond to the presence of specific functional chemical groups characteristic of the two powders. The functional groups that can be identified by analyzing the Matrix and Hydroxyapatite samples are the following:

- Amide I ($(RCO)NH_2$): 1650-1590 cm^{-1} [104];
- Amide II ($(RCO)_2NH$): 1560-1500 cm^{-1} [104];
- Carbonate (CO_3^{2-}): 1450-1410 cm^{-1} [105];
- Phosphate (PO_4^{3-}): 1100-1000 cm^{-1}/600-400 cm^{-1} [105],[106];
- Hydroxyl (OH): 3600-3200 cm^{-1}/860-820 cm^{-1} [104];

In both test types, dilution, and catalyst effect, observing the spectra of the compared coatings, one based on Matrix and the other based on Hydroxyapatite, it is evident the presence of more pronounced peaks for some functional groups on one type of coating while the same is absent or almost absent on the other. These peaks are more pronounced both with respect to the spectrum to which they belong and with respect to the spectrum obtained with the different powder.

As shown in the following IR spectra, where the Matrix and Hydroxyapatite coatings are compared, first for the dilution effect and then for the catalyst effect, the peaks relative to the characteristic functional groups are highlighted with circles of a different color (Figure 78-79). In particular, the Matrix-based coatings are characterized by more pronounced peaks as regards amide I, amide II, carbonates, and hydroxyls; Hydroxyapatite coatings, on the other hand, are characterized by higher peaks only for phosphates and slightly for carbonates that have not been removed in the calcination process. In the table below are indicated the chemical groups and their corresponding color (Table 15).

Table 15 Functional groups and corresponding color.

Functional chemical group	**Color**
Amide I	
Amide II	
Carbonates	
Phosphates	
Hydroxyls	

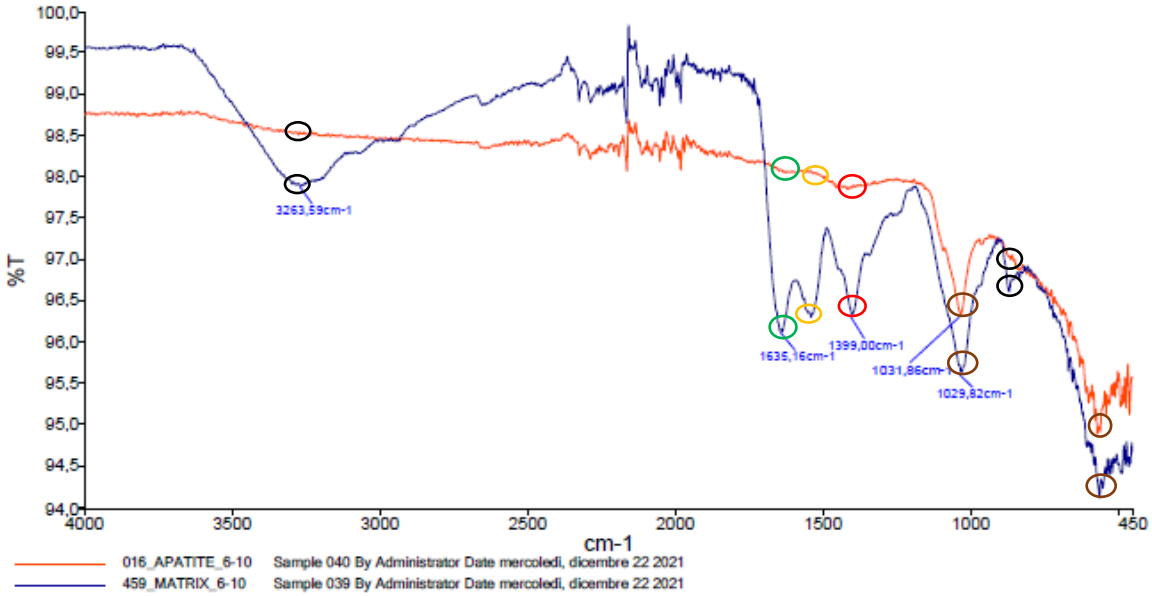

Figure 78 *Comparison of coatings IR spectra in the case of dilution effect with peaks highlighted.*

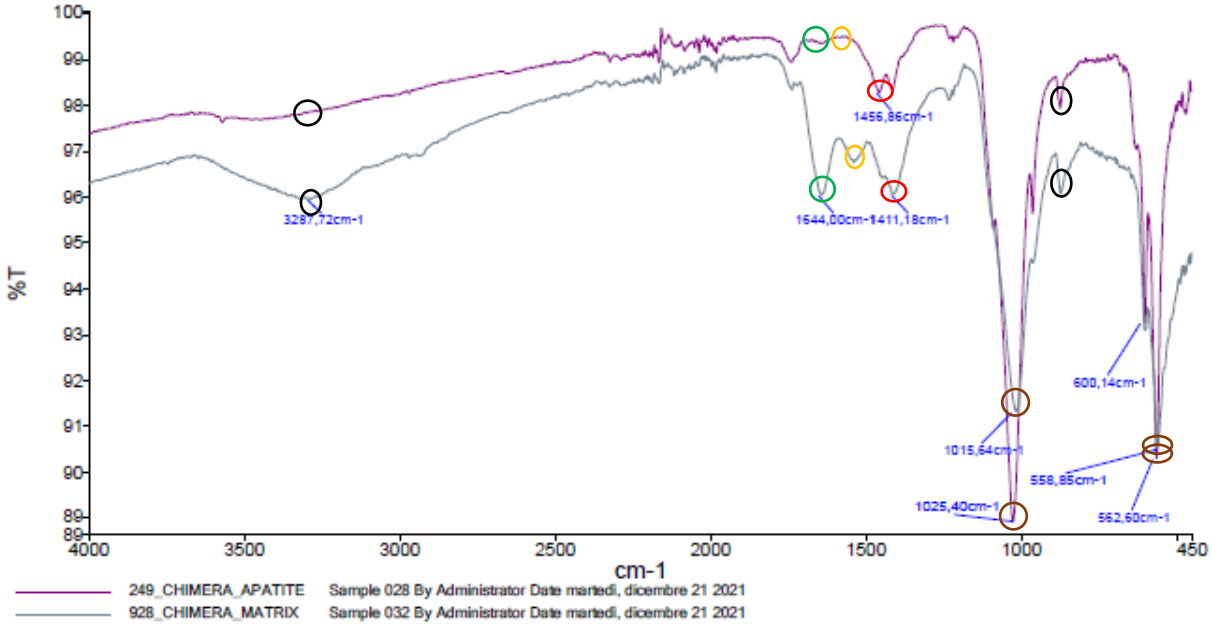

Figure 79 *Comparison of coatings IR spectra in the case of catalyst effect with peaks highlighted.*

The outcome obtained from the IR analysis is consistent with the known chemical properties characterizing the Matrix and Hydroxyapatite powders used, meaning that the coating process operated did not alter the chemical properties of the coating material bonded to the titanium surface.

5-CONCLUSION

The objective initially set and on which the study described in this thesis was focused was achieved on two occasions with respect to all the tests carried out. As you can see from the photographic results, in fact, in many tests the coverage obtained is not homogeneous and also has a poor adherence to the surface of the titanium implant. The tests in which the best and most promising results have been obtained are those in which the powders, Matrix and Hydroxyapatite, have been diluted in hydrogen peroxide at a ratio of 6:10 and those in which they have been combined with the alkaline solution obtained by combining hydrogen peroxide and sodium hydroxide. In such cases, a visual surface inspection of the screw, by stereomicroscope, showed good homogeneity of coverage in both cases and for both powders, although more so in the case of Hydroxyapatite. It has been hypothesized that the reason for this difference between the two powders is due to the rate of collagen present in the Matrix this substance decreases the probability of contact between the phosphate groups and the titanium surface. Consequently, hydroxyapatite binds more easily and homogeneously than the Matrix. What was seen under the microscope was confirmed by the IR analysis of the samples, which highlighted the presence of the coating on the surface of the titanium implant by detecting the presence of the chemical functional groups characteristic of the two powders, namely: amide I and II, hydroxyls and carbonates for the Matrix powder; phosphates and carbonates for the Hydroxyapatite powder. This last consideration is particularly significant as it allows us to conclude that, although the solutions used are different, the covering process developed is capable of producing the coating on the implant while maintaining the chemical properties of the material bonded to its surface.

Overall, therefore, it can be concluded that the presence of bonds is increased by the size of dust particles (obtained by dilution treatments), by the presence of a catalyst element (which accelerates the formation of the bonds between the surface and the coating substance) and that the coating process does not change the chemical properties of the powder used.

6-FUTURE STUDIES

As future studies, starting from the results of this thesis, it is recommended to repeat the tests that gave the most promising results by making improvements and varying some aspects.

Regarding the tests using the dilution effect, where powders are diluted in hydrogen peroxide, it is suggested to use ASTM sieves. These sieves will allow the powders to be sieved down to below 0.5 μm in size and, consequently, will allow an accurate indication of the size of the particles that bind through the process developed.

In the other case, where the catalytic effect of an alkaline substance, i.e., sodium hydroxide, is used, it is suggested to vary the catalyst. By testing other alkaline catalysts and also using alkaline-earth catalysts, it will be possible to see if there can be an improvement in the catalysis of the titanium-dust bonding reaction, either in the case of Hydroxyapatite or in the case of Matrix.

REFERENCES

[1] A. S. Mao and D. J. Mooney, “Regenerative medicine: Current therapies and future directions,” *Proc. Natl. Acad. Sci. U. S. A.*, vol. 112, no. 47, pp. 14452–14459, 2015, doi: 10.1073/pnas.1508520112.

[2] L. C. Zhang and L. Y. Chen, “A Review on Biomedical Titanium Alloys: Recent Progress and Prospect,” *Adv. Eng. Mater.*, vol. 21, no. 4, 2019, doi: 10.1002/adem.201801215.

[3] R. S. Jayesh and V. Dhinakarsamy, “Osseointegration,” *J. Pharm. Bioallied Sci.*, vol. 7, no. April, pp. S226–S229, 2015, doi: 10.4103/0975-7406.155917.

[4] T. A. Petrie, J. E. Raynor, C. D. Reyes, K. L. Burns, D. M. Collard, and A. J. García, “The effect of integrin-specific bioactive coatings on tissue healing and implant osseointegration,” *Biomaterials*, vol. 29, no. 19, pp. 2849–2857, 2008, doi: 10.1016/j.biomaterials.2008.03.036.

[5] M. B. Zaid, R. J. O’Donnell, B. K. Potter, and J. A. Forsberg, “Orthopaedic Osseointegration: State of the Art,” *J. Am. Acad. Orthop. Surg.*, vol. 27, no. 22, pp. E977–E985, 2019, doi: 10.5435/JAAOS-D-19-00016.

[6] W. Jin and P. K. Chu, *Orthopedic implants*, vol. 1–3. Elsevier Inc., 2019.

[7] F. J. García-Sanz, M. B. Mayor, J. L. Arias, J. Pou, B. León, and M. Pérez-Amor, “Hydroxyapatite coatings: A comparative study between plasma-spray and pulsed laser deposition techniques,” *J. Mater. Sci. Mater. Med.*, vol. 8, no. 12, pp. 861–865, 1997, doi: 10.1023/A:1018549720873.

[8] R. Mhanna and A. Hasan, “1 . 2 Clinical Need for Tissue Engineering,” pp. 3–34, 2017, [Online]. Available: https://commons.wikimedia.org/wiki/File:

[9] R. Langer and J. P. Vacanti, “- ARTICLES Tissue Engineering,” *Science (80-.).*, vol. 260, no. May, pp. 920–926, 1993.

[10] M. S. Kim, J. H. Kim, B. H. Min, H. J. Chun, D. K. Han, and H. B. Lee, “Polymeric scaffolds for regenerative medicine,” *Polym. Rev.*, vol. 51, no. 1, pp. 23–52, 2011, doi: 10.1080/15583724.2010.537800.

[11] S. Pina *et al.*, “Regenerative Medicine Applications,” *Materials (Basel).*, vol. 12, no. 11, p. 1824, 2019.

[12] S. C. Marina Torre, Eugenio Carrani and A. C. Alessia Biondi, Mascia Masciocchi, *Riap-Registro Italiano ArtroProtesi Report Annuale 2019*, Prima ediz. Roma, 2019.

[13] K. Ziegler-Graham, E. J. MacKenzie, P. L. Ephraim, T. G. Travison, and R. Brookmeyer, “Estimating the Prevalence of Limb Loss in the United States: 2005 to 2050,” *Arch. Phys. Med. Rehabil.*, vol. 89, no. 3, pp. 422–429, 2008, doi: 10.1016/j.apmr.2007.11.005.

[14] A. Mater and S. Universit, “Analisi strutturale e biomeccanica di protesi da corsa transtibiali e transfemorali,” 2016.

[15] E. Rodríguez *et al.*, “We are IntechOpen , the world ’ s leading publisher of Open Access books Built by scientists , for scientists TOP 1 %,” *Intech*, vol. 32, no. tourism, pp. 137–144, 1989, [Online]. Available: https://www.intechopen.com/books/advanced-biometric-technologies/liveness-detection-in-biometrics.

[16] S. G. Kang, C. H. Park, and S. J. Song, “Stem fixation in revision total knee arthroplasty: Indications, stem dimensions, and fixation methods,” *Knee Surg. Relat. Res.*, vol. 30, no. 3, pp. 187–192, 2018, doi: 10.5792/ksrr.18.019.

[17] B. Szerlip, S. Muh, J. J. Streit, and R. Gobezie, “Humeral Fixation in Shoulder Arthroplasty: Does Stem Geometry Matter?,” *Semin. Arthroplast. JSES*, vol. 23, no. 2, pp. 103–105, 2012, doi: 10.1053/j.sart.2012.03.008.

[18] P. Collin, T. Matsukawa, P. Boileau, U. Brunner, and G. Walch, “Is the humeral stem useful in anatomic total shoulder arthroplasty?,” *Int. Orthop.*, vol. 41, no. 5, pp. 1035–1039, 2017, doi: 10.1007/s00264-016-3371-4.

[19] S. Stenicka *et al.*, “High revision rates of a cementless beta-titanium alloy stem with contamination-free roughened surface in primary total hip arthroplasty,” *J. Clin. Med.*, vol. 9, no. 7, pp. 1–12, 2020, doi: 10.3390/jcm9072138.

[20] T. Reiner *et al.*, “The migration pattern of a cementless hydroxyapatite-coated titanium stem under immediate full weight-bearing—a randomized controlled trial using model-based rsa,” *J. Clin. Med.*, vol. 9, no. 7, pp. 1–10, 2020, doi: 10.3390/jcm9072077.

[21] J. D. Keener, P. N. Chalmers, and K. Yamaguchi, “The humeral implant in shoulder arthroplasty,” *J. Am. Acad. Orthop. Surg.*, vol. 25, no. 6, pp. 427–438, 2017, doi: 10.5435/JAAOS-D-15-00682.

[22] J. T. Kim and J. J. Yoo, “Implant Design in Cementless Hip Arthroplasty,” *Hip Pelvis*, vol. 28, no. 2, p. 65, 2016, doi: 10.5371/hp.2016.28.2.65.

[23] J. Walker, “Skeletal system 1: the anatomy and physiology of bones,” *Nurs. Times [online]*, vol. 116, no. 2, pp. 38–42, 2020, [Online]. Available: https://cdn.ps.emap.com/wp-content/uploads/sites/3/2020/01/200129-Skeletal-system-1-the-anatomy-and-physiology-of-bones.pdf%0Ahttps://www.nursingtimes.net/clinical-archive/orthopaedics/skeletal-system-1-the-anatomy-and-physiology-of-bones-27-01-2020/.

[24] G. Rouhi and M. Amani, “A Brief Introduction Into Orthopaedic Implants : Screws , Plates , and Nails,” *Res. Chapter*, no. january, pp. 1–19, 2012.

[25] Tapscott DC, Wottowa C. Orthopedic Implant Materials. In: StatPearls [Internet]. Treasure Island (FL): StatPearls Publishing;

[26] H. L. Freese, M. G. Volas, and J. R. Wood, "Metallurgy and Technological Properties of Titanium and Titanium Alloys," pp. 25–51, 2001, doi: 10.1007/978-3-642-56486-4_3.

[27] C. L. and M. Peters, *Titanium and Titanium Alloys Edited by*. 2003.

[28] Y. M. Ahmed, K. Salleh, M. Sahari, M. Ishak, and B. A. Khidhir, "Titanium and its Alloy," no. October, 2014.

[29] J. R. Chapman, R. M. Harrington, K. M. Lee, P. A. Anderson, A. F. Tencer, and D. Kowalski, "Factors affecting the pullout strength of cancellous bone screws," *J. Biomech. Eng.*, vol. 118, no. 3, pp. 391–398, 1996, doi: 10.1115/1.2796022.

[30] J. P. Paul and A. Gefen, "Optimizing the biomechanical compatibility of orthopedic screws for bone fracture fixation (multiple letters)," *Med. Eng. Phys.*, vol. 25, no. 5, pp. 435–436, 2003, doi: 10.1016/S1350-4533(03)00025-0.

[31] P. Joshua J. Jacobs, MD, Nadim J. Hallab, PhD, Robert M. Urban, And Markus A. Wimmer, "Wear Particles," *J. Bone Jt. Surg.*, vol. 88-A, pp. 99–102, 2006.

[32] G. Rémond, C. Nockolds, M. Phillips, and C. Roques-Carmes, "Implications of polishing techniques in quantitative x-ray microanalysis," *J. Res. Natl. Inst. Stand. Technol.*, vol. 107, no. 6, pp. 639–662, 2002, doi: 10.6028/jres.107.052.

[33] M. Merola and S. Affatato, "Materials for hip prostheses: A review of wear and loading considerations," *Materials (Basel).*, vol. 12, no. 3, 2019, doi: 10.3390/ma12030495.

[34] M. I. Z. Ridzwan, S. Shuib, A. Y. Hassan, A. A. Shokri, and M. N. Mohammad Ibrahim, "Problem of stress shielding and improvement to the hip implant designs: A review," *J. Med. Sci.*, vol. 7, no. 3, pp. 460–467, 2007, doi: 10.3923/jms.2007.460.467.

[35] F. Lotti, F. Ranieri, G. Vadalà, L. Zollo, and G. Di Pino, "Invasive intraneural interfaces: Foreign body reaction issues," *Front. Neurosci.*, vol. 11, no. SEP, pp. 1–14, 2017, doi: 10.3389/fnins.2017.00497.

[36] A. J. Tande and R. Patel, "Prosthetic joint infection," *Clin. Microbiol. Rev.*, vol. 27, no. 2, pp. 302–345, 2014, doi: 10.1128/CMR.00111-13.

[37] P. Izakovicova, O. Borens, and A. Trampuz, "Periprosthetic joint infection: current concepts and outlook," *EFORT Open Rev.*, vol. 4, no. 7, pp. 482–494, 2019, doi: 10.1302/2058-5241.4.180092.

[38] B. Wan *et al.*, "On fatigue failure prediction of prosthetic devices through XFEM analysis," *Int. J. Fatigue*, vol. 147, no. November 2020, p. 106160, 2021, doi: 10.1016/j.ijfatigue.2021.106160.

[39] I. Naert and M. Quirynen, “A Study of 589 consecutive implants fixed prostheses. Part II: Prosthetic,” *J. Prosthet. Dent.*, pp. 949–956, 1987.

[40] T. D. Taylor, “Prosthodontic problems and limitations associated with osseointegration,” *J. Prosthet. Dent.*, vol. 79, no. 1, pp. 74–78, 1998, doi: 10.1016/S0022-3913(98)70197-0.

[41] N. Assefa and T. Yosief, “Human Anatomy and Physiology (Lectures Notes),” *Ephti*, p. 428, 2003.

[42] P. A. Downey and M. I. Siegel, “Bone biology and the clinical implications for osteoporosis,” *Phys. Ther.*, vol. 86, no. 1, pp. 77–91, 2006, doi: 10.1093/ptj/86.1.77.

[43] T. Albrektsson and C. Johansson, “Osteoinduction, osteoconduction and osseointegration,” *J. Eur. Spine*, vol. 10, pp. 96–101, 2001.

[44] C. M. Abraham, “A Brief Historical Perspective on Dental Implants, Their Surface Coatings and Treatments,” *Open Dent. J.*, vol. 8, no. 1, pp. 50–55, 2014, doi: 10.2174/1874210601408010050.

[45] J. S. Hoellwarth, K. Tetsworth, S. R. Rozbruch, M. B. Handal, A. Coughlan, and M. Al Muderis, “Osseointegration for Amputees,” *JBJS Rev.*, vol. 8, no. 3, pp. e0043–e0043, 2020, doi: 10.2106/jbjs.rvw.19.00043.

[46] Y. Li and R. Brånemark, “Osseointegrierte Prothesen zur Rehabilitation nach Amputation: Das wegweisende schwedische Modell,” *Unfallchirurg*, vol. 120, no. 4, pp. 285–292, 2017, doi: 10.1007/s00113-017-0331-4.

[47] M. Al Muderis, A. Khemka, S. J. Lord, H. Van De Meent, and J. P. M. Frolke, “Safety of osseointegrated implants for transfemoral amputees: A two-center prospective cohort study,” *J. Bone Jt. Surg. - Am. Vol.*, vol. 98, no. 11, pp. 900–909, 2016, doi: 10.2106/JBJS.15.00808.

[48] J. Sullivan, M. Uden, K. P. Robinson, and S. Sooriakumaran, “Erratum: Rehabilitation of the trans-femoral amputee with an osseointegrated prosthesis: The United Kingdom Experience (Prosthetics and Orthotics International (2003) 27 2 (114-120)),” *Prosthet. Orthot. Int.*, vol. 27, no. 3, pp. 114–120, 2003.

[49] A. F. Mavrogenis, R. Dimitriou, J. Parvizi, and G. C. Babis, “Biology of implant osseointegration,” *J. Musculoskelet. Neuronal Interact.*, vol. 9, no. 2, pp. 61–71, 2009.

[50] M. Browne and P. J. Gregson, “Effect of mechanical surface pretreatment on metal ion release,” *Biomaterials*, vol. 21, no. 4, pp. 385–392, 2000, doi: 10.1016/S0142-9612(99)00200-8.

[51] P. J Y and D. E, J, “Red blood cell and platelet interactions with titanium implant surfaces,” *Clin. Oral Implants Res.*, no. 1996, pp. 530–539, 2000.

[52] H. H. Aschoff, R. E. Kennon, J. M. Keggi, and L. E. Rubin, “Transcutaneous, distal femoral,

intramedullary attachment for above-the-knee prostheses: An endo-exo device," *J. Bone Jt. Surg. - Ser. A*, vol. 92, no. SUPPL. 2, pp. 180–186, 2010, doi: 10.2106/JBJS.J.00806.

[53] M. Al Muderis, W. Lu, K. Tetsworth, B. Bosley, and J. J. Li, "Single-stage osseointegrated reconstruction and rehabilitation of lower limb amputees: The Osseointegration Group of Australia Accelerated Protocol-2 (OGAAP-2) for a prospective cohort study," *BMJ Open*, vol. 7, no. 3, pp. 1–4, 2017, doi: 10.1136/bmjopen-2016-013508.

[54] J. P. M. Frölke, R. A. Leijendekkers, and H. van de Meent, "Osseointegrierte Prothese für Patienten nach Amputation: Multidisziplinärer Behandlungsansatz in den Niederlanden," *Unfallchirurg*, vol. 120, no. 4, pp. 293–299, 2017, doi: 10.1007/s00113-016-0302-1.

[55] S. Jönsson, K. Caine-Winterberger, and R. Branemark, "Osseointegration amputation prostheses on the upper limbs: Methods, prosthetics and rehabilitation," *Prosthet. Orthot. Int.*, vol. 35, no. 2, pp. 190–200, 2011, doi: 10.1177/0309364611409003.

[56] A. Thesleff, R. Brånemark, B. Håkansson, and M. Ortiz-Catalan, "Biomechanical Characterisation of Bone-anchored Implant Systems for Amputation Limb Prostheses: A Systematic Review," *Ann. Biomed. Eng.*, vol. 46, no. 3, pp. 377–391, 2018, doi: 10.1007/s10439-017-1976-4.

[57] R. L. McGough, M. A. Goodman, R. L. Randall, J. A. Forsberg, B. K. Potter, and B. Lindsey, "Transkutanes Compress®-Implantat zur Rehabilitation nach Extremitätenamputation," *Unfallchirurg*, vol. 120, no. 4, pp. 300–305, 2017, doi: 10.1007/s00113-017-0339-9.

[58] N. V. Kang, C. Pendegrass, L. Marks, and G. Blunn, "Osseocutaneous Integration of an Intraosseous Transcutaneous Amputation Prosthesis Implant Used for Reconstruction of a Transhumeral Amputee: Case Report," *J. Hand Surg. Am.*, vol. 35, no. 7, pp. 1130–1134, 2010, doi: 10.1016/j.jhsa.2010.03.037.

[59] P. K. Chu, J. Y. Chen, L. P. Wang, and N. Huang, "Plasma-surface modification of biomaterials," *Mater. Sci. Eng. R Reports*, vol. 36, no. 5–6, pp. 143–206, 2002, doi: 10.1016/S0927-796X(02)00004-9.

[60] J. C.E., T. J.M., J. J.C., G. H.I.M. Walenkamp, and P. J., "Modern Orthopaedic Implant Coatings — Their Pro's, Con's and Evaluation Methods," *Mod. Surf. Eng. Treat.*, 2013, doi: 10.5772/55976.

[61] A. Jemat, M. J. Ghazali, M. Razali, and Y. Otsuka, "Surface modifications and their effects on titanium dental implants," *Biomed Res. Int.*, vol. 2015, 2015, doi: 10.1155/2015/791725.

[62] L. Le Guéhennec, A. Soueidan, P. Layrolle, and Y. Amouriq, "Surface treatments of titanium dental implants for rapid osseointegration," *Dent. Mater.*, vol. 23, no. 7, pp. 844–854, 2007, doi: 10.1016/j.dental.2006.06.025.

[63] T. Albrektsson and A. Wennerberg, "On osseointegration in relation to implant surfaces," *Clin. Implant*

Dent. Relat. Res., vol. 21, no. S1, pp. 4–7, 2019, doi: 10.1111/cid.12742.

[64] H. Singh, R. Kumar, C. Prakash, and S. Singh, "HA-based coating by plasma spray techniques on titanium alloy for orthopedic applications," *Mater. Today Proc.*, no. xxxx, 2021, doi: 10.1016/j.matpr.2021.03.165.

[65] B. J. Gill and R. C. Tucker, "Plasma spray coating processes," *Mater. Sci. Technol. (United Kingdom)*, vol. 2, no. 3, pp. 207–213, 1986, doi: 10.1179/mst.1986.2.3.207.

[66] J. Mostaghimi, M. Pasandideh-Fard, and S. Chandra, "Dynamics of Splat Formation in Plasma Spray Coating Process," *Plasma Chem. Plasma Process.*, vol. 22, no. 1, pp. 59–84, 2002, doi: 10.1023/A:1012940515065.

[67] P. L. Fauchais, J. V. R. Heberlein, and M. I. Boulos, *Thermal spray fundamentals: From powder to part*. 2014.

[68] L. Sun, "Thermal Spray Coatings on Orthopedic Devices: When and How the FDA Reviews Your Coatings," *J. Therm. Spray Technol.*, vol. 27, no. 8, pp. 1280–1290, 2018, doi: 10.1007/s11666-018-0759-2.

[69] D. Ke, A. A. Vu, A. Bandyopadhyay, and S. Bose, "Compositionally graded doped hydroxyapatite coating on titanium using laser and plasma spray deposition for bone implants," *Acta Biomater.*, vol. 84, pp. 414–423, 2019, doi: 10.1016/j.actbio.2018.11.041.

[70] M. F. A. Fouda, A. Nemat, A. Gawish, and A. R. Baiuomy, "Does the Coating of Titanium Implants by Hydroxyapatite affect the Elaboration of Free Radicals. An Experimental Study," *Aust. J. Basic Appl. Sci.*, vol. 3, no. 2, pp. 1122–1129, 2009.

[71] Y. Xie, X. Liu, X. Zheng, C. Ding, and P. K. Chu, "Improved stability of plasma-sprayed dicalcium silicate/zirconia composite coating," *Thin Solid Films*, vol. 515, no. 3, pp. 1214–1218, 2006, doi: 10.1016/j.tsf.2006.07.124.

[72] D. Buser, R. K. Schenk, S. Steinemann, J. P. Fiorellini, and C. H. Fox, "Influence of Surface Characteristcs on Bone Integration of Titanium Implants.," *J. Biomed. Mater. Res.*, vol. 25, no. 7, pp. 889–902, 1991.

[73] J. L. Ong, D. L. Carnes, and K. Bessho, "Evaluation of titanium plasma-sprayed and plasma-sprayed hydroxyapatite implants in vivo," *Biomaterials*, vol. 25, no. 19, pp. 4601–4606, 2004, doi: 10.1016/j.biomaterials.2003.11.053.

[74] G. Fernandez de Grado *et al.*, "Bone substitutes: a review of their characteristics, clinical use, and perspectives for large bone defects management," *J. Tissue Eng.*, vol. 9, 2018, doi: 10.1177/2041731418776819.

[75] V. Campana *et al.*, “Bone substitutes in orthopaedic surgery: from basic science to clinical practice,” *J. Mater. Sci. Mater. Med.*, vol. 25, no. 10, pp. 2445–2461, 2014, doi: 10.1007/s10856-014-5240-2.

[76] W. Schlickewei and C. Schlickewei, “The use of bone substitutes in the treatment of bone defects - The clinical view and history,” *Macromol. Symp.*, vol. 253, pp. 10–23, 2007, doi: 10.1002/masy.200750702.

[77] L. S. Pryor *et al.*, “Review of Bone Substitutes,” *Craniomaxillofac. Trauma Reconstr.*, vol. 2, no. 3–4, pp. 151–160, 2009, doi: 10.1055/s-0029-1224777.

[78] W. Wang and K. W. K. Yeung, “Bone grafts and biomaterials substitutes for bone defect repair: A review,” *Bioact. Mater.*, vol. 2, no. 4, pp. 224–247, 2017, doi: 10.1016/j.bioactmat.2017.05.007.

[79] Nasio, “Ulcers At Kenyatta National Hospital (Knh). a Dissertation Submitted in Part Fulfillment for the Degree of Master of Medicine in Surgery , University of,” 2009.

[80] R. Amid, A. Kheiri, L. Kheiri, M. Kadkhodazadeh, and M. Ekhlasmandkermani, “Structural and chemical features of xenograft bone substitutes: A systematic review of in vitro studies,” *Biotechnol. Appl. Biochem.*, vol. 68, no. 6, pp. 1432–1452, 2021, doi: 10.1002/bab.2065.

[81] A. Oryan, S. Alidadi, A. Moshiri, and N. Maffulli, “Bone regenerative medicine: Classic options, novel strategies, and future directions,” *J. Orthop. Surg. Res.*, vol. 9, no. 1, pp. 1–27, 2014, doi: 10.1186/1749-799X-9-18.

[82] A. Okazaki, T. Koshino, T. Saito, and T. Takagi, “Osseous tissue reaction around hydroxyapatite block implanted into proximal metaphysis of tibia of rat with collagen-induced arthritis,” *Biomaterials*, vol. 21, no. 5, pp. 483–487, 2000, doi: 10.1016/S0142-9612(99)00198-2.

[83] R. D. A. Gaasbeek, H. G. Toonen, R. J. Van Heerwaarden, and P. Buma, “Mechanism of bone incorporation of β-TCP bone substitute in open wedge tibial osteotomy in patients,” *Biomaterials*, vol. 26, no. 33, pp. 6713–6719, 2005, doi: 10.1016/j.biomaterials.2005.04.056.

[84] M. Bohner, “Physical and chemical aspects of calcium phosphates used in spinal surgery,” *Eur. Spine J.*, vol. 10, no. SUPPL. 2, pp. 114–121, 2001, doi: 10.1007/s005860100276.

[85] M. J. S. Beuerlein and M. D. McKee, “Calcium sulfates: What is the evidence?,” *J. Orthop. Trauma*, vol. 24, no. SUPPL. 1, pp. 46–51, 2010, doi: 10.1097/BOT.0b013e3181cec48e.

[86] R. M. Urban, T. M. Turner, D. J. Hall, N. Inoue, and S. Gitelis, “Increased bone formation using calcium sulfate-calcium phosphate composite graft,” *Clin. Orthop. Relat. Res.*, vol. 459, no. 459, pp. 110–117, 2007, doi: 10.1097/BLO.0b013e318059b902.

[87] P. N. De Aza, Z. B. Luklinska, C. Santos, F. Guitian, and S. De Aza, “Mechanism of bone-like formation on a bioactive implant in vivo,” *Biomaterials*, vol. 24, no. 8, pp. 1437–1445, 2003, doi:

10.1016/S0142-9612(02)00530-6.

[88] P. Lei *et al.*, “A new method for xenogeneic bone graft deproteinization: Comparative study of radius defects in a rabbit model,” *PLoS One*, vol. 10, no. 12, pp. 1–17, 2015, doi: 10.1371/journal.pone.0146005.

[89] N. Baldini, M. De Sanctis, and M. Ferrari, “Deproteinized bovine bone in periodontal and implant surgery,” *Dent. Mater.*, vol. 27, no. 1, pp. 61–70, 2011, doi: 10.1016/j.dental.2010.10.017.

[90] A. B. Castro-Ceseña, M. P. Snchez-Saavedra, E. E. Novitskaya, P. Y. Chen, G. A. Hirata, and J. McKittrick, “Kinetic characterization of the deproteinization of trabecular and cortical bovine femur bones,” *Mater. Sci. Eng. C*, vol. 33, no. 8, pp. 4958–4964, 2013, doi: 10.1016/j.msec.2013.08.022.

[91] J. Wei *et al.*, “Enhanced Osteogenic Behavior of ADSCs Produced by Deproteinized Antler Cancellous Bone and Evidence for Involvement of ERK Signaling Pathway,” *Tissue Eng. - Part A*, vol. 21, no. 11–12, pp. 1810–1821, 2015, doi: 10.1089/ten.tea.2014.0395.

[92] R. Uklejewski, M. Winiecki, G. Musielak, and R. Tokłowicz, “Effectiveness of various deproteinization processes of bovine cancellous bone evaluated via mechano-biostructural properties of produced osteoconductive biomaterials,” *Biotechnol. Bioprocess Eng.*, vol. 20, no. 2, pp. 259–266, 2015, doi: 10.1007/s12257-013-0510-2.

[93] L. Pedrotti, *Basics of Spectroscopy*. 2008.

[94] P. . C.-P. Sherman Hsu, “Infrared Spectroscopy Chapter 15,” in *Handbook of Instrumental Techniques for Analytical Chemistry*, 2006, pp. 607–613.

[95] B. Stuart, “INFRARED SPECTROSCOPY: Fundamentals and Applications,” 2004, pp. 1–248.

[96] H. Buijs and B. Stuart, “Infrared Spectroscopy,” *Encyclopedia of Chemical Technology*. John Wiley & Sons, pp. 1–17, 2015, doi: 10.1007/978-0-387-26308-3_40.

[97] A. Barth, “Infrared spectroscopy of proteins,” *Biochim. Biophys. Acta - Bioenerg.*, vol. 1767, no. 9, pp. 1073–1101, 2007, doi: 10.1016/j.bbabio.2007.06.004.

[98] B. C. Smith, “Fundamentals of FOURIER TRANSFORM INFRARED SPECTROSCOPY,” Second edi., T. and F. Group, Ed. CRC Press, 2004, pp. 1–198.

[99] C. Institutes and B. Academy, “Bulgarian Chemical,” vol. 43, no. 3, 2011.

[100] N. H. Haneklaus, “Calcination,” *Encycl. Nucl. Energy*, pp. 131–138, 2021, doi: 10.1016/b978-0-12-819725-7.00161-6.

[101] PerkinElmer, “Ir Ready TOGO.” pp. 1–12, 2011.

[102] PerkinElmer, “UNIVERSAL ATR SAMPLING ACCESSORY User’s Guide.” pp. 1–22, 2017.

[103] PerkinElmer, “SPECTRUM TWO FIXED ANGLE SPECULAR REFLECTANCE ACCESSORY User’s Guide.” pp. 1–126, 2015.

[104] L. C. Go, W. Holmes, D. Depan, and R. Hernandez, “Evaluation of extracellular polymeric substances extracted from waste activated sludge as a renewable corrosion inhibitor,” *PeerJ*, vol. 2019, no. 6, 2019, doi: 10.7717/peerj.7193.

[105] H. Kimmel *et al.*, “Bande di assorbimento ir,” *Elem. di Anal. Chim. Strutt.*, vol. 24, no. 1962, pp. 10815–10837, 2000, [Online]. Available: http://as.osa.org/abstract.cfm?URI=as-22-3-201.

[106] A. Priyam, R. K. Das, A. Schultz, and P. P. Singh, “A new method for biological synthesis of agriculturally relevant nanohydroxyapatite with elucidated effects on soil bacteria,” *Sci. Rep.*, vol. 9, no. 1, pp. 1–14, 2019, doi: 10.1038/s41598-019-51514-0.